University of Naples
"Federico II"

Department of Industrial Engineering

Ph.D. in Industrial Engineering

SMART LIGHTING CONTROLS FOR ENERGY EFFICIENCY AND VISUAL COMFORT

Tutor:
Prof.ssa Laura Bellia

Ph.D. Student:
Francesca Fragliasso

Ph.D. cycle: XXXI

Index

Introduction

In the last few decades daylighting has earned again the key role it deserves as a fundamental part of lighting design. As it has been underlined in the recent IES RP-5-13 report [1], the role of electric light is basically to integrate daylight when it is absent or inadequate to guarantee alone visual tasks performing. This means that, despite electric light gives us the possibility to create whatever lighting condition, daylight must be considered the fundamental light source in indoor environments, especially in those spaces where people perform their every-day life activities and remain for most of the day (workplaces, offices, schools, hospitals, etc).

The attention about daylighting themes is driven by two issues, that by now have become crucial in modern building design culture: on one hand the care about themes concerning energy savings and natural energy sources exploitation; on the other hand, the will to improve more and more users' comfort conditions in indoor spaces. About these topics, modern researches have repeatedly highlighted the strict connection between the use of daylight and the reduction of energy consumptions [2-6]; however, daylighting benefits are even more important, if we consider the direct incidence on people wellness. Researches demonstrated that daylight not only influences visual comfort, but it has non-visual effects as well [7]. It is one of the main regulators of the circadian rhythms [8], influences people's mood and has a fundamental role in defining people's alertness state, work performances and productivity [9].

From this perspective, daylighting design becomes again a primary step, not only of lighting design, but also of building design in general, since aspects like building shape or façades configurations obviously affect daylight entering in indoor spaces.

This makes crucial studies about technologies allowing indoor daylighting to be improved, controlling at the same time the correlated risks (glare, overheating): innovative shading systems, smart façades, daylight transportation devices [10].

Moreover, the use of automated systems, able to manage the integration of daylight and electric light, becomes fundamental: these systems reduce electric light usage, increasing energy savings and, at the same time, they allow light to be tailored to people's needs [11]. These devices are commonly known as daylight-linked control systems (DLCSs). They are based on the use of photosensors installed inside or outside the building, that detect incident daylight, send a signal to a controller. The controller, in turn, regulates luminaires light output. The regulation actions goal is to integrate daylight and electric light, in order to maintain average work-plane illuminance levels around the limits indicated by regulations.

The development of such systems has certainly been boosted by the spread of new LED light sources and of related electronic management systems. According to [12], sophisticated lighting controls use is supposed to increase so that, considering all buildings typologies together, the related revenue from their installation is expected to grow at 14.3% compound annual growth rate between 2017 and 2026.

However, the functioning mechanism of these systems is not yet completely clear. Factors affecting their performances are too many (photosensors characteristics and location, adopted control strategy, lighting systems components features [13]) and not easy to control during both the design phase and the commissioning one. Thus, once they have been installed, DLCSs operate differently from the expectations: illuminance levels are too low or too high compared to the required ones [14], luminaires are turned on and off not properly [15], electric light fluctuations are too frequent and annoy users [16].

The predictable consequence is that users, verifying the improper functioning of the automated controls, disable them and all the presumed benefits are unavoidably lost. It must not be forgotten that the effectiveness of DLCSs strictly depend on the users' grade of acceptance. Previous works, indeed, demonstrated how much is important for people to exercise a direct control in the management of the environment they live in [17]. Moreover, studies based on surveys demonstrated that often people prefer manual than automated control [18], and that, when automated systems are installed, they are more satisfied having the possibility to partially override the

automated control [15, 19]. Moreover, the grade of acceptance of automated controls strictly depends on spaces function and it is major when spaces are perceived not belonging to anyone (e.g. atria, corridors or circulating areas) [20, 21].

Thus, it is fundamental to design automated controls guarantying proper lighting conditions, in order to avoid users disable them.

Given these premises, what are the main causes generating difficulties in DLCSs project? How can they be solved?

Currently the pressing problems are the following:

- As it was previously reported, factors affecting DLCSs performances are many, but it is not completely clear what is the specific incidence of each one of them on DLCS global functioning [22];
- It is crucial for designers to be able to simulate DLCSs operating conditions during the different design stages, in order to evaluate benefits connected to their installation. However, despite the development of dynamic daylight simulation methods and the spread of sophisticated calculation software, DLCSs simulation is neither immediate nor reliable. Indeed available calculation tools are not able to account for all the affecting factors [23] and consequently predicted energy savings turned out to be different from those observed in the field [24];
- Even though performing a reliable simulation was possible, the evaluation of the global performance of these systems is not easy. Generally, DLCSs are assessed exclusively depending on energy savings they allow achieving. This is a too simplistic and not reliable assessment method: these systems sometimes, even providing significant savings, operate so that lighting requirements are not fulfilled. So, how is it possible to evaluate this aspect? Currently, common and shared parameters useful to evaluate DLCSs performances do not exist. So, not only it is problematic to evaluate the convenience in installing such systems, but it is also difficult to assess their performance during the operating life [25].

All these problems determine a poor DLCSs design culture: automated lighting controls based on daylight exploitation are often sold as a ready-made product, sometimes integrated in a wider control network (Building Management Systems - BMS) and designers install them without being really aware of all connected design issues.

Given these premises, the goal of the thesis is to try to suggest a design methodology for DLCSs, accounting for the above-mentioned issues. To do that the work is divided in the following sections:

- Analysis of the state of the art, necessary to collect available information about factors affecting DLCSs performances;
- Definition of new performance metrics useful to evaluate DLCSs capability in integrating daylight;
- Analysis of the current available software to simulate DLCSs and of the related limits;
- Development of a calculation tool trying to overcome these limits, allowing a more reliable simulation of DLCSs;
- Implementation of the proposed performance parameters calculation module in the above-mentioned simulation tool;
- Use of the tool and of the proposed parameters to verify the performance of different typologies of DLCSs in a real space.

It must be underlined that the developed tool evaluates DLCSs performances starting from indoor daylight availability data. These data can be inferred from both simulations and field measurements. For the thesis application, measured data were used. For this purpose, a specifically developed monitoring system was set up. An office located in one of the buildings of the University of Naples “Federico II” was used as case study. Daylight irradiance and illuminance measurements were performed during winter and spring, in order to obtain real daylight data referred to work-plane illuminances and photosensors detections. These data were then uploaded in the calculation tool to evaluate the performance of different DLCSs typologies, to verify their seasonal functioning and compare them, to observe the factors affecting their performances and to identify the most suitable control strategies.

Analysis methodology presented in the thesis and part of the results, were published during the PhD course in [13, 22, 25-27].

I. Daylight-linked control systems (DLCSs): functioning and affecting factors

DLCSs are automated control systems, able to manage luminaires based on indoor daylight availability. One or more photosensors detect incident light and send a signal to a controller. The controller, according to the received information, switches on and off or continuously regulates luminaires emitted flux, in order to integrate available daylight by means of electric light and to guarantee lighting requirements at the work-plane. Despite the simplicity of the base concept DLCSs are based on, designing such systems is not an easy task, due to the big quantity of factors affecting their performances. Following paragraphs propose an analysis of these factors. According to [22], the order factors are presented recalls DLCSs design process, starting from daylight availability evaluation and going ahead with the control strategy definition and the lighting system components choice, finally concluding with the commissioning.

I.1. Daylight availability

Considering that the goal of DLCSs is to reduce the use of electric light maximizing that of the natural one, it is clear that their performances depend first and foremost on the daylight availability characterizing the spaces they are installed in. Previous studies focused on this issue and tried to underline how achievable energy savings can vary depending on all those parameters that influence daylight availability: building orientation and location, weather conditions, shading devices typologies and so on.

For example, Roisin et al. [28] calculated energy savings achievable in an office by using the same DLCS, but varying the orientation and the location of the room. They considered three different cities (Brussels - latitude 50° 51' N, longitude 4° 20' E; Athens - latitude 37° 58' N, longitude 23° 42' E and Stockholm - latitude 59° 19' N, longitude 18° 3' E) and the four main orientations. They found that savings ranged from 46%, considering the worst case (Stockholm – north orientation), to 61%, considering the best one (Athens – south orientation.

The effect both of the seasonal changes and of weather conditions was analyzed by Onaygil and Güler [29]. They observed the case of a north-east oriented office in Istanbul (latitude 41° 0' N, longitude 28° 56' E) equipped with a lighting system managed by a dimming DLCS. The researchers found that energy savings were 27% higher in June and July, if compared with those achieved in December. Moreover, they calculated that savings were equal to 35% in presence of clear skies and to 16% in presence of overcast ones.

Not only the global amount of daylight entering a space affects the way a DLCS functions, but also its spatial distribution. This topic was faced by Galasiu et al. [30], who examined the case of an open-space office, equipped with workstations arranged in different rows. Each workstation was lit by a luminaire equipped with an integrated photosensor. In this way it was possible to properly regulate luminaires flux emission depending on the daylight available at the single desk. Researches underlined how the savings can vary in the same room according to the workstation distance from the window. Specifically, they obtained the following results: depending on the considered season, the savings ranged from 17% to 24% in the perimeter workstations, from 9% to 20% in the second row and from 9% to 16% in the most interior one.

Other studies focused on the interactions between lighting control systems and shading devices. Even if this topic deserves a specific treatise, some studies will be cited to give a general idea of the problem.

Lee et al. [31] observed how the variation of venetian blinds tilt angle can determine a change in the ratio of the work-plane illuminance to the photosensor signal, finally modifying the way DLCSs operate. Galasiu et al [32] calculated energy savings achievable by means of simple switching and dimming systems in a space were different typologies of manual and photocontrolled venetian blinds were installed. Researchers found that, in presence of clear sky, the use of shading devices could reduce achievable energy savings from 5% to 45% in dimming system case and from 5% to 80% in switching system one.

The research of a balance between the maximization of energy savings due to daylight use and the necessity to avoid glare and overheating is an ambitious challenge that some researchers have accepted [33-35]. For example, Shen and Tzempelikos [34] developed an advanced integrated thermal and simulation model to evaluate daylighting and energy performances in private offices with automated interior roller shades. The tool was meant to be used during the design process to identify the most suitable technical choices, accounting for both thermal and lighting issues. Moreover, Shen et al. [35] studied the way to integrate the control both of shading devices and lighting controls with that of HVAC systems as well.

I.2. Control strategy definition

The definition of the control strategy consists in establishing the way the control system operates. Basically, DLCSs can be divided in open-loop and closed-loop ones. The former ones are managed by photosensors detecting exclusively daylight. For this reason, they are installed outside the building (on the roof or on the façade) or inside it, but in this latter case they are located and oriented such to detect exclusively daylight, for example, they look toward a window. In closed-loop systems, photosensors are located in the same room where the control is performed, and they detect both daylight and electric light.

DLCSs can be classified also according to the actions actuated by the controller. In this case we have switching systems, stepped systems and dimming ones. In the first case luminaires are simply switched on and off according to the photosensor detections. Stepped systems are similar to the switching ones, but luminaires can be turned on and off reaching different light output levels (generally two or three), for example 50% and 100%. Finally, dimming systems continuously regulate luminaires flux emission, proportionally to the variations of light levels detected by the photosensor. Depending on the combination of the photosensor typology and of the action actuated by the controller, the corresponding control algorithm can be identified. Basic control algorithms (open-loop and closed-loop switching, open-loop and closed-loop stepped and open-loop and closed-loop dimming) are in-depth described in the Appendix.

Control strategy should be properly chosen depending on the specific case. Atif and Galasiu [36] calculated energy savings achieved in two buildings atria: the former equipped with a dimming system and located in Québec City (latitude 46° 48' N, longitude -71° 12' W); the latter equipped with an on-off switching system and situated in Ottawa (latitude 45° 24' N, longitude 75° 41' W). In the former case savings were equal to 46%, in the latter equal to 17%.

Chiogna et al. [37] monitored the functioning of DLCSs installed in two groups of south-exposed lecture rooms, located in Trento (latitude 46° 04' N, longitude 11° 08' E). They found that the use of an on-off switching system, coupled to an occupancy-based one, provides savings equal to about 40%. Integrating occupancy-based control with a dimming DLCS, savings increased till 65%.

However, Li et al. [38] reported that, differently from what would seem obvious, dimming systems are not always more advantageous than switching ones. According to the researchers, indeed, the benefits deriving from a strategy or another depend both on the daylight availability and on the required task illuminance. Switching systems could turn out to be more advantageous if a low task illuminance value is required and daylight levels are generally high [39].

Rubinstein et al. [38] studied experimental results obtained by means of scale models located on the roof of the third floor of Building 90 at Lawrence Berkeley Laboratory (latitude 37° 52′ N, longitude 122° 16′ W). They compared energy savings achievable by adopting different control strategies and they found that the best results were provided by closed-loop dimming systems.

There are two different typologies of closed-loop dimming systems: integral reset and proportional dimming. Some studies compare these two strategies. Mistrick et al. [40] found that integral reset was not suitable for sidelit spaces. This is due to the fact that the system is calibrated exclusively in presence of electric light, neglecting the daylight contribution. On the contrary proportional dimming calibration procedure accounts for the fact that daylight and

electric light determine different ratios of work-plane illuminance to photosensor signal.

Doulos et al. [41] focused on the same issue. They observed that, in a south-oriented office located in Athens (latitude 37° 58' N, longitude 23° 42' E), proportional dimming systems provided savings ranging from 66.91% to 72.82%, whereas integral reset allowed obtaining higher savings, ranging from 70.35% to 76.09%. However, researchers observed that often integral reset operated so to determine illuminance levels at the work-plane lower than those prescribed by regulations, meaning that part of the energy savings were due to an improper system functioning.

Ihm et al. [3] studied the performances of different DLCSs installed in offices located in Chicago (latitude 41° 51' N, longitude -87° 39' W). They found that dimming systems generally provide higher savings compared with stepped ones. However, this difference decreases on windows glazing area increasing.

I.3. Photosensors choice

Characteristics of photosensors affect the functioning of DLCSs. So, it is fundamental to properly choose its characteristics: *"spatial response (the sensitivity in detecting the incident radiation coming from different directions), spectral response (the sensitivity in sensing the incident radiation depending on different wavelengths) and range of response (a limited range of output signal values in which light measurement is accurate"*[22].

All these features, indeed, contribute to define the ratio of the daylight work-plane illuminance, $\bar{E}_{dl}$, to the daylight photosensor signal, S_{dl}. This ratio is at the basis of DLCSs calibration procedures and the more it maintains itself steady over time, the more the performances of the system are good.

Doulos et al. [42] studied the relative spectral responses of five typologies of photosensors and verified that they were broader than the V(λ) function. Moreover, they observed that the related sensitivity peak corresponded to about 540.9 nm to 600.7 nm. The fact that photosensors spectral response does not match the V(λ) reduces the reliability of detections and obviously has an impact on the global functioning of the DLCSs. In another study [43] the researchers quantified this impact in terms of energy savings, analyzing the performance of different photosensors in a room where window glazing was varied in order to modify the spectrum of entering daylight. They observed differences from 0.37% to 5.44% depending on the analyzed case.

The effect of spatial response was studied by Rubinstein et al. [44], who suggested preferring photosensors characterized by high fields of view and to shield them from the direct light of the window. On the contrary Ranasinghe and Mistrick [45] found that the narrower the photosensor field of view is, the better the system functions.

To solve problems connected to the reliability of photosensor detections, manufacturers and researchers proposed different solutions. One of this is the use of luminaires with integrated photosensors. In this way lighting can be managed according to different criteria in different zones of the same room and the lighting conditions sensed by photosensors should be more representative. Management of these systems is not so easy, and several studies have been published in this regard [46-50]. They focused on defining photosensors networks, to integrate DLCS strategy with occupancy-based ones associating occupancy sensors with light ones. Moreover, they propose the idea that in open-space offices, each user occupying a different workstation can auto-calibrate the control of his own lighting. Obviously, this determines other problems. People have different preferences about luminous environment considering both light intensity and color [51]. This could create in open-space offices unpleasant and not uniform global lighting conditions.

Moreover, research suggested installing devices different from the standard photosensors. Some researches proposed to use CCD (Charge-Coupled Device) cameras or CMOS (complementary metal-oxide semiconductor) image sensors [52-54]. These devices are able to measure luminance distribution of the workstations, controlling at the same time lighting and occupancy conditions. However, these systems present limits as well. On one hand it is not easy to identify precise algorithm starting from luminance maps, especially considering that accidental factors, such as the furniture relocation,

could invalidate the calculation model [52]. Moreover, the now available devices are characterized by costs too high to be used in common applications [54].

I.4. Lighting system component characteristics

When a DLCSs is installed, all the components of the lighting system must be compatible. Different studies underlined how lamps and luminaires characteristics affect DLCSs performances, but, at the same time, the control itself can influences them. For example [55] underlined the necessity to set special time delay, when high intensity discharge lamps are used, in order to account for the restrike time. Moreover, the minimum light output, which the luminaires can be dimmed at, is not the same for all lamp technologies [3]. It must also be considered that continuous on-off switching could reduce lamps life. Tetri [56] underlined that considering fluorescent lamps, switching systems affect lamps life more than the dimming ones and that the use of electronic dimming ballasts helps lamps to maintain their nominal life.

A lighting system fundamental component is the ballast, i.e. the device that controls luminaires light output according to the photosensor detections. Each ballast is characterized by a specific dimming response function, i.e. a curve describing the relationship between photosensor signal and the light output. Before LED luminaires spread, dimming ballasts managing fluorescent lamps were based on an analog 0-10 V control protocol [11]. Some studies, underlined that, since there was not a lighting specific standard to define the correspondence between the received analog signal and the light output, starting from the same signal, using different ballasts, the controller could generate different light outputs. For example, Doulos et al. [41], comparing the way to operate of different ballasts, underlined that the same 5 V signal produced a light output varying from 8.90% to 54.89%, in turn corresponding to a relative absorbed power varying from 20.20% to 60.09%. This obviously influenced energy savings, that varied from 66.91% to 72.82% with a proportional system and from 70.35% to 76.09%, considering reset control. A similar study was performed by Roisin et al. [28], who compared the characteristics of analog systems and digital ones and underlined that digital controllers and related sensors were characterized by energy consumptions higher than analog one. For this reason, the use of digital systems turned out to be more advantageous if a single controller and a single photosensor were responsible to manage different luminaires together, whereas in stand-alone applications the analog ones was profitable.

The spread of LED sources, managed by means of digital controls, has boosted the interest towards the dynamic lighting [51]. For these sources the regulation of emitted flux is more stable than for the traditional ones, and as it was demonstrated by previous researches [46, 47] the relationship between luminaires power consumption and dimming level can be assumed to be linear.

However, in some cases LED dimming can determine undesired perceivable chromatic shifts. For these reasons some studies have focused on the research of methods to control changes in spectral power distribution due to light output variations [57, 58]. Moreover, some LED sources, when dimmed, determine visible or invisible flicker, that could be dangerous for people health [59]. This issue was investigated in [60]. Light frequencies responsible to induce biological human response were found and methods to mitigate the biological effects were discussed.

When lighting controls are designed, another important issue to consider is the impact of stand-by energy use. Gentile and Dubois [61] reported that it represents about the 30% of the total lighting energy use, reaching in extreme cases 55% value. They argued that when standby energy use cannot be minimized, in individual offices or similar applications the use of very efficient light sources can be sufficient and reduce the necessity to design complex controls.

Another crucial aspect is the control zones setting. A control zone is an area lit by luminaires all managed in the same way. Li et al [38] deepened this issue, experimenting different strategy of grouping luminaires. The experiment was performed in a classroom equipped with three rows of fluorescent luminaires arranged parallel to the window. The researchers calculated energy savings by varying the way the control was operated and found that energy savings varied from 23.4% to 70.4%. In the most

disadvantageous case only the row nearest to the window was automatically switched on and off, whereas the others were manually controlled. On the contrary, in the most advantageous case, the row nearest to the window were independently and automatically switch on and off, whereas the row farthest from the window was continuously dimmed.

Galasiu et al. [30] studied the possibility to differently control lamps belonging to the same luminaire. They analyzed the case of luminaires installed in an open space office, equipped with three 32 W fluorescent lamps, one upward directed and two downward directed. They observed that, if the uplight was fixed and the downlight was dimmed depending on daylight availability, daily average savings were equal to 32% in spring and summer and equal to 16% in winter. If all the lamps were dimmed, savings became 47% in spring and summer and 24% during winter.

Caicedo et al. [48] studied LED luminaires generating two different and independent optical beams: one wider and the other narrower. The former was used to provide ambient lighting, the latter to obtain task lighting. Luminaires were equipped with both photosensors and occupancy sensors. The narrowest light beam was turned on and off according to people presence absence in the controlled area and the widest was regulated according to the daylight availability.

I.5. Commissioning

Commissioning consists in the setting of the control system and in the check of its operative conditions during the system life cycle. The correct installation and commissioning is fundamental to guarantee the good performances of control systems [62].

The setting of the control is defined calibration. The calibration procedure is different from each control strategy (see the Appendix). However, generally, it consists in defining the ratio of the daylight work-plane illuminance to the daylight photosensor signal ($\bar{E}_{dl}/S_{dl}$), in order to establish luminaires light output necessary to integrate daylight. To do that the critical task location (i.e. the point receiving the smallest quantity of daylight) must be identified; the related work-plane illuminance must be measured together with the photosensor signal; the necessary light output must be set. From the calibration on, the system will work considering that the ratio of the work-plane illuminance to the photosensor signal, despite daylight availability variations, remains constant and equal to that measured at the calibration phase.

However, researches [40, 63] underlined that this is not true and that this ratio continuously changes depending on indoor daylight distribution.

Choi et al. [64] focused on this issue observing the functioning of different photosensors located in an office in Seoul, Korea (latitude 37° 33' N, longitude 126° 58' E). They underlined that the ratio of work-plane illuminance to the photosensor signal strictly depends on sensor location, its aiming angle and sky conditions.

Chiogna et al. [65] deepened this aspect in an office located in Sesto al Reghena, Pordenone, Italy (latitude 45° 57' N, longitude 12° 39' E). They observed that, when outdoor daylight conditions are similar, similar $\bar{E}_{dl}/S_{dl}$ ratio were observed. Consequently, they proposed to implement the control algorithm by means of seasonal correction functions, accounting for the seasonal $\bar{E}_{dl}/S_{dl}$ variations.

Recently Beccali et al. [66] proposed a method based on artificial neural networks to identify the best photosensor location during design and commissioning phase.

During calibration other parameters such as time delays, minimum and maximum light output are set as well.

Littlefair [16] focused on continuous electric light oscillations in switching systems disturbing users and due to frequent outdoor daylight fluctuations. To reduce them he suggested to introduce time delays equal to 30-45 minutes.

A similar study was performed by Li et al. [67] who analyzed different switching techniques: "*daylight-linked time delay (lights can be switched off only if daylight illuminances exceed a specific target value), switching-linked time delay (lights cannot be switched off if a specific time is not elapsed from the last switching-on), solar reset switching (a reset time is set and only when reset time occurs, daylight levels are monitored: if they*

are higher than target value, lights are switched off)"[22]. They found that the daylight-linked time delay was the strategy providing the most significant reduction of switching actions.

Bellia et al. [26] compared the effectiveness of different switching techniques in an office located in Naples (Latitude 40° 51' 22 N, Longitude 14° 14' 47 E). They found that the better performance was guaranteed by means of switching-linked time delay and that solar reset systems turned out to be the worst. Researchers also suggested that "*the problem of the brusque oscillations cannot be avoided unless it is accepted to introduce a time delay for switching on actions as well*" [26]. They underlined that previous researches [19] demonstrated that people sometimes choose illuminances lower than those prescribed by regulations. Consequently, it is possible that users would prefer occasionally low light levels compared to continuous and sudden switching on actions.

II. New parameters to evaluate the capability of DLCSs in integrating daylight

Previous paragraphs demonstrated that the number of factors affecting DLCSs functioning is huge. Consequently, it is fundamental to be able not only to evaluate performance of automated control systems, but also to understand how the different factors influence their operating conditions. As it was mentioned in the Introduction, nowadays DLCSs are exclusively evaluated considering energy savings they produce. The following paragraphs are explaining why this approach is not sufficient and are introducing new parameters useful to evaluate the capability of DLCSs in integrating daylight.

II.1. Today available parameters and their limits

The birth and the spread of dynamic daylight simulations have provided new possibilities in the daylighting research field. Obviously, this has had an impact on the evaluation of the benefits connected to the installation of DLCSs. Indeed, the possibility to accurately know daylight availability variations during time (accounting for weather conditions, daily and seasonal rhythms) should allow the electric light requirement of a specific space to be estimated. Then, starting from the requirement, it should be easy to evaluate what is the electric lighting system most suitable to integrate daylight and fulfill the calculated requirement. Actually, problems connected to lighting systems dynamic modelling are complex and the related evaluations about their performances and the connected benefits are not immediate.

After the introduction of dynamic daylight simulations, the main problem was to find indices able to synthetically describe daylight availability in indoor environments. Software for dynamic calculations upload weather data file and, based on the related information, define sky luminance distribution for each record of the weather data file (generally corresponding to an hour of the year). Finally, accounting for the optical characteristics of architectural surfaces, they evaluate interactions between daylight and space and calculate for each hour of the year illuminance values at specific points belonging to calculation grids set by users [68]. In some cases, thanks to proper interpolation models, results referred to fractions of hour, e.g. half an hour, 5 minutes or 1 minute [69] can be obtained. This provides an enormous amount of data not easy to be managed. Therefore, statistic indices have been introduced to summarize and comment dynamic daylight simulation results such as Daylight Autonomy (DA) [70], Continous Dayligth Autonomy (DA_{con}) [70], Useful Daylight Illuminance (UDI) [71, 72]. These indices are partially useful also to evaluate DLCSs.

DA represents the time percentage of occupied hours of a year during which daylight illuminance at the work-plane is equal or higher than the task illuminance prescribed by regulations [73]. This means that ideally, during these hours, electric lights could be completely off.

DA_{con} accounts for the fact that daylight contribution should be considered even if the corresponding illuminance is lower than the task illuminance prescribed by regulations. So, the DA_{con} is the percentage ratio of the daylight illuminance to the task illuminance. If for example for the 30% of the year, the work-plane is characterized by DA_{con} value of 80%, it means that, ideally, using a dimming control system, luminaires light output could be equal to 20% for the 30% of the year.

UDI gives us similar information. It is the percentage of the occupied hours of a year during which daylight illuminances are comprised in the range 100 lx – 2000 lx. Based on surveys performed in offices, this range is considered useful by people, since it corresponds to light levels neither too dark nor too bright. The useful range can be divided in two further steps $UDI_{supplementary}$ (from 100 lx to the task illuminance) and $UDI_{autonomous}$ (from the task illuminance to 2000 lx. It must be underlined that

the lower limit of this range is general considered equal to 100 lx (300 lx in [74]), whereas authors do not agree about the setting of the upper limit: it is equal to 2000 lx in [72], 2500 lx in [75], 3000 lx in [76], 8000 lx in [74]. Based on UDI definition, to have an idea about the operation range of a daylight-linked control system, it is necessary to evaluate when daylight illuminance is lower than 100 lx or it falls in $UDI_{supplementary}$.

These parameters allow evaluating the daylighting potential of a space and are useful to have a preliminary idea about the convenience to install or not a DLCS. However, they are based exclusively on the space characteristics without considering the features of a real lighting system. For this reason, simulation software have been implemented by means of tools useful to simulate the dynamic functioning of lighting systems, managed by different typologies of automated controls [77, 78] (a focus on available software to simulate control systems is reported in paragraph III.1). This has allowed obtaining annual scheduling related to lighting system absorbed power and, consequently, to evaluate connected energy consumptions. This has provided the possibility to evaluate the performances of control systems according to energy savings provide. Generally, the savings are estimated considering a reference lighting system switched on at 100% for the entire year.

However, achieved energy savings are not a very reliable indicator of DLCSs performances. For example, if two systems characterized by the same technical features are installed in two spaces with different daylight availability, they would provide different savings. This doesn't mean that the system characterized by lower savings works improperly, but only that the two spaces are characterized by a different potential in terms of daylighting. On the other hand, high energy savings could be the consequences of an improper functioning of the system. For example, a DLCS, that is wrongly calibrated, could determine illuminance levels at the work-plane often lower than those prescribed by regulations. This would reduce energy consumptions to the detriment of lighting quality.

Thus, specific parameters are necessary to describe the performance of DLCSs. Considering that their goal is to integrate daylight, DLCSs should be evaluated according to their capability in maintaining proper indoor light levels, complementing daylight and not on the basis of the achieved savings.

In this respect, it is interesting the work by Doulos et al. [79]. They proposed a multi-criteria analysis methodology useful to identify the optimum position and the proper field of view of the photosensors during the design process. To do that, they suggested to consider two additional parameters beyond the achieved energy savings: the correlation between work-plane illuminance and photosensor signal and the lighting adequacy. The former parameter is useful to control the effect of photosensor characteristics on systems performances. On the other hand, the lighting adequacy is defined as: "the percentage for occupied time with total illuminance exceeding design illuminance" [79], where total illuminance is the sum of work-plane daylight and electric light illuminances. This parameter introduces a fundamental concept: an ideal DLCS should be able to perfectly adapt electric light emission to daylight variations, so that the sum of the work-plane daylight illuminance ($\bar{E}_{dl}(t)$) and work-plane electric light illuminance ($\bar{E}_{el}(t)$) should be always equal to the average maintained illuminance prescribed by regulations ($\bar{E}_{task}$). Obviously, this is impossible owning to the real technical characteristics of DLCSs. So, the total illuminance $\bar{E}_{tot}(t)$ determined by the control system can be higher or lower than $\bar{E}_{task}$, depending on the way the system reacts to photosensor detections. The specific goal of the lighting adequacy is to evaluate the time percentage of the observation period during which the system is able to guarantee prescriptions, i.e. it is verified that $\bar{E}_{tot}(t)$ is equal or higher than $\bar{E}_{task}$. The complement to 1 of the light adequacy informs about an improper control system functioning, corresponding to $\bar{E}_{tot}(t)$ values lower than $\bar{E}_{task}$.

A similar analysis approach was proposed by Bonomolo et al. [14], who introduced two indexes: OAR (Over illuminance Avoidance Ratio) and UAR (Under-illuminance Avoidance Ratio). These indexes describe the capability of

the system in reducing over-illuminance and under-illuminance conditions, i.e. in avoiding that $\bar{E}_{tot}(t)$ is higher or lower than $\bar{E}_{task}$ respectively. The more the indices are close to 1, the better the system operates.

Based on the proposals of [14, 79], new parameters have been introduced [25, 27] during the PhD. course. They are: Daylight Integration Adequacy (DIA), Percentage Light Deficit ($LD_{\%}$), Percentage Intrinsic Light Excess ($ILE_{\%}$) and Percentage Light Waste ($LW_{\%}$).

The parameters are based on issues proposed by [14, 79], but introduce a new concept: the intrinsic light excess. They will be fully described in the following paragraph.

II.2. The rationale for the definition of the new parameters

Standards [73] prescribe that electric lighting systems have to guarantee specific values of average maintained illuminances at the work-plane ($\bar{E}_{task}$), different depending on the performed visual task.

Given a period T (for example the number of occupied hours of a space during a month, a season or a year) we can define the Light Requirement, LR, of the work-plane during T, in terms of light exposure as:

$$LR = \bar{E}_{task} \cdot T \qquad \text{[lx·h]} \quad \text{(II.1)}$$

When a room is daylit, daylight can satisfy part of LR, since at each time t, the work-plane receives a certain amount of daylight, corresponding to an average daylight illuminance $\overline{E}_{dl,t}$. Since, daylight availability varies with time, it is possible to define the function $\overline{E}_{dl}(t)$. The integral of this function over T is defined Daylight Exposure, DE.

$$DE = \int_T \overline{E}_{dl}(t)\, dt \qquad \text{[lx·h]} \quad \text{(II.2)}$$

The Light Requirement fulfilled by daylight, LR_{dl} can be evaluated as:

$$LR_{dl} = \int_T \bar{E}^*_{dl}(t)dt \qquad \text{[lx·h]} \quad \text{(II.3)}$$

Where:

$$\bar{E}^*_{dl}(t) = \begin{cases} \overline{E}_{task} & if \quad \bar{E}_{dl}(t) \geq \overline{E}_{task} \\ \bar{E}_{dl,t} & if \quad \bar{E}_{dl}(t) < \overline{E}_{task} \end{cases} \qquad \text{[lx]} \quad \text{(II.4)}$$

The ratio of LR_{dl} to LR is a good indicator of the daylight availability characterizing the analysed space.

A DLCS is supposed to operate so that when $\overline{E}_{dl}(t)$ assumes values higher than $\bar{E}_{task}$ luminaires are off, whereas, when it assumes values lower than $\bar{E}_{task}$, luminaires flux is properly regulated to integrate daylight.

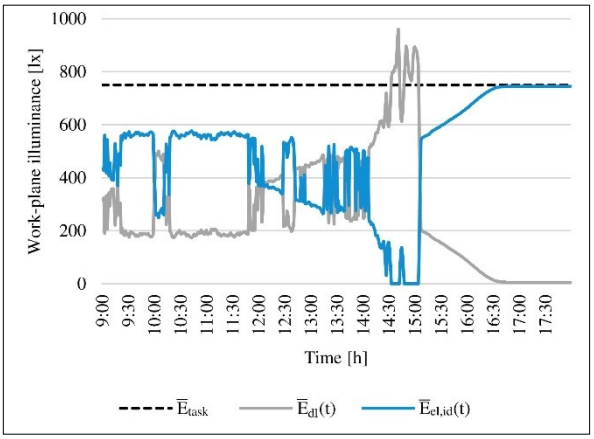

Figure II. 1: Daylight illuminance and ideal electric light illuminance at the work-plane

An ideal and perfectly functioning automated control, based on dimming strategy, at each time t, should determine at the work-plane an electric light illuminance value (let us call it ideal electric light illuminance, $\overline{E}_{el,id,t}$ -see Figure II.1[1]-) so that it is possible to define the function:

$$\bar{E}_{el,id}(t) = \bar{E}_{task} - \bar{E}^*_{dl}(t) \qquad \text{[lx]} \quad \text{(II.5)}$$

[1] All the figures of this section are referred to data measured on the 22nd of December 2017, in the test-room used as case study. Specifically, graphs are related to the west orientation and a task illuminance equal to 750 lx was considered. All the details about the case study are reported in the IV Section.

Obviously, given its technical characteristics, a real control system determines electric light illuminances over time, $\overline{E}_{el}(t)$, different from the ideal ones (see Figure II.2). When $\overline{E}_{el}(t)$ is higher than $\overline{E}_{el,id}(t)$, a light excess occurs. Conversely, when $\overline{E}_{el}(t)$ is lower than $\overline{E}_{el,id}(t)$, prescribed light requirements are not fulfilled and a light deficit arises.

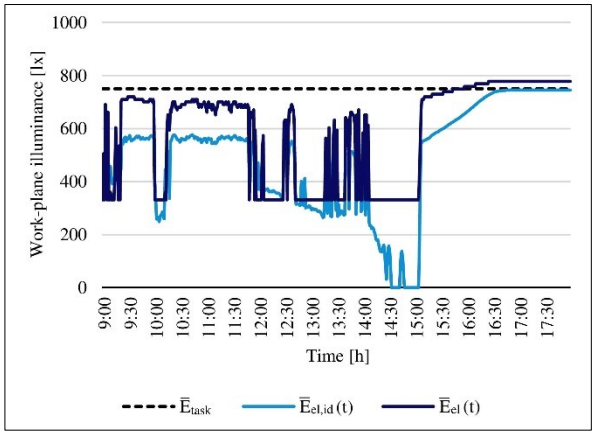

Figure II. 2: Comparison between the ideal electric light illuminance and that provided by a real system

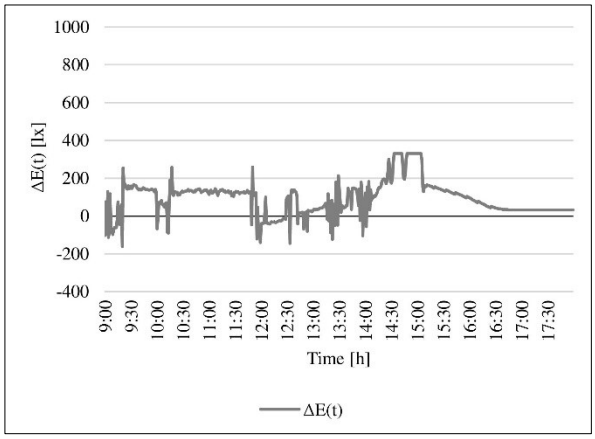

Figure II. 3: ΔE(t) function

The function $\Delta E(t)$, representing at each time t the difference between $\overline{E}_{el}(t)$ and $\overline{E}_{el,id}(t)$, well describe the performance of a DLCS (see Figure II.3).

Shifts of $\overline{E}_{el}(t)$ from $\overline{E}_{el,id}(t)$ can be determined by all the factors described in the Section II. We can divide all these factors in two categories, those that are communal for all design strategies (e.g. daylight availability or photosensors characteristics) and those strictly depending on the adopted control strategy (e.g. number of steps in stepped systems or minimum light output in dimming systems). The two categories of factors determine different effects.

To better understand that, let us consider the case of an open-loop proportional dimming system. It operates so that luminaires light output is continuously regulated according to photosensor detections, varying from a maximum value (δ_{max}) to a minimum one (δ_{min}), without ever being switched completely off (see Figure II.4).

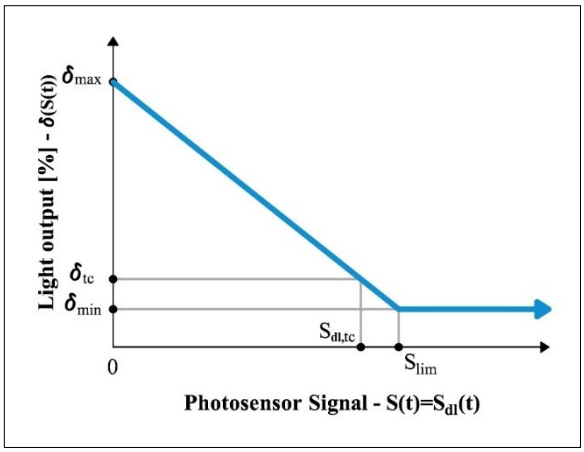

Figure II. 4: Open-loop dimming control algorithm

This system can be calibrated by defining two set points: the former one is set during night, when daylight is absent and luminaires must be turned on at the maximum light output (δ_{max}); the latter is set during day, choosing the daylight photosensor signal, $S_{dl,tc}$, corresponding to a work-plane daylight condition such that, to integrate $\overline{E}_{dl,tc}$ (daylight illuminance at the calibration) the required light output (δ_{tc}) is higher than the minimum one (δ_{min}).

As it was reported in previous paragraphs, the choice of the $S_{dl,tc}$ is crucial in determining system performance.

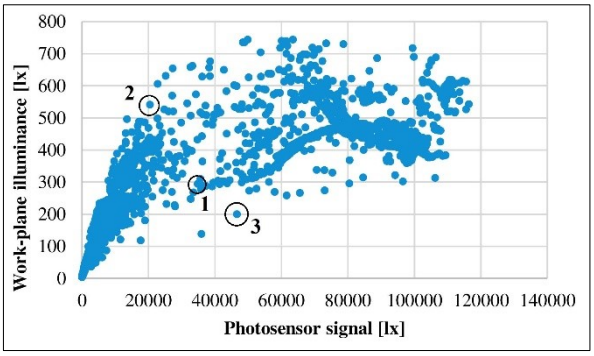

Figure II. 5: Relationship between photosensor signal and daylight work-plane illuminance

This is clear looking at Figure II.5. Let us assume that the above mentioned open-loop system is calibrated based on the couple illuminance-signal identified by the Point 1. When the condition represented by the Point 2 happens, a light excess occurs. Indeed, the photosensor signal in 2 is lower than that characterizing 1, so the system sets a light output higher than δ_{tc}. However, the daylight illuminance at the work-plane corresponding to the point 2 is higher than that registered at the calibration. The opposite happens when the daylight condition represented by the point 3 occurs: in this case a light deficit is produced. Problems connected to the variation of $\overline{E}_{dl}(t)/S_{dl}(t)$ over time can determine both a deficit and an excess. Their effects can be diminished by calibrating the system as properly as possible and adjusting set-points during system life-cycle.

On the other hand, the factors depending on the control strategy always generated an excess. Effects of these factors cannot be avoided unless the strategy itself is changed. Considering the case of the open-loop dimming system, it remains always on at a δ_{min} value, even when daylight is sufficient alone to fulfil light requirements. Obviously, this generates light excesses. For switching systems excesses are even higher, considering that in this case luminaire luminous flux cannot be regulated, but lights are switched on every time the photosensor signal falls down a limit value.

It must be noticed that another cause of light excess is the fact that lighting systems are designed based on maintenance factors, used to account for luminous flux decay over time. So, during the first phases of the systems life cycle, when luminaires are on at 100% the produced illuminance at the work-plane is necessary higher than the task illuminance.

To distinguish light excess due to adopted control strategy from that due to the oscillations of $\overline{E}_{dl}(t)/S_{dl}(t)$ (in turn depending on photosensor characteristics, location, daylight availability and so on), they will be called intrinsic light excess and light waste respectively. The intrinsic light excess also includes the excess due to the use of maintenance factors.

From the $\Delta E(t)$ function two different functions: $\Delta E^{-}(t)$ and $\Delta E^{+}(t)$, can be inferred:

$$\Delta E^{-}(t) = \begin{cases} 0 & \text{if } \Delta E(t) > 0 \\ -\Delta E(t) & \text{if } \Delta E(t) \leq 0 \end{cases} \quad [lx] \quad (II.6)$$

$$\Delta E^{+}(t) = \begin{cases} 0 \text{ if } \Delta E(t) < 0 \\ \Delta E(t) \text{ if } \Delta E(t) \geq 0 \end{cases} \quad [lx] \quad (II.7)$$

$\Delta E^{+}(t)$ in turn, can be seen as the sum of two different functions: $\Delta E^{+}_{intr}(t)$, describing the excess due to the control strategy, and $\Delta E^{+}_{waste}(t)$ describing the excess due to $\overline{E}_{dl}(t)/S_{dl}(t)$ variations.

At this point it is necessary a procedure to calculate $\Delta E^{+}_{intr}(t)$ and $\Delta E^{+}_{waste}(t)$. To evaluate $\Delta E^{+}_{intr}(t)$ we have to neglect excesses due to $\overline{E}_{dl}(t)/S_{dl}(t)$ variations. In order to do that, let us assume that the ratio $\overline{E}_{dl}(t)/S_{dl}(t)$ is constant over time and that it is equal to the calibration ratio.

$$\frac{\overline{\mathrm{E}}_{\mathrm{A,dl}}(\mathrm{t})}{\mathrm{S_{dl}}(\mathrm{t})} = \frac{\overline{\mathrm{E}}_{\mathrm{A,dl,tc}}}{\mathrm{S_{dl,tc}}} \quad (II.8)$$

From the (II.8):

$$\mathrm{S_{dl}}(\mathrm{t}) = \overline{\mathrm{E}}_{\mathrm{A,dl}}(\mathrm{t}) \cdot \frac{\mathrm{S_{dl,tc}}}{\overline{\mathrm{E}}_{\mathrm{A,dl,tc}}} \quad (II.9)$$

At this point, it is possible to simulate the functioning of a reference system (see Figure II.6), i.e. a system with the same characteristics of the analysed one, but operating based on not-real photosensor detections, calculated according to the (II.9).

The reference system determines at the work-plane an electric light illuminance $\overline{E}_{el,ref}(t)$ equal to:

$$\overline{E}_{el,ref}(t) = \delta_{ref}(\mathrm{t}) \cdot \overline{\mathrm{E}}_{\mathrm{el,100\%}} \quad [lx] \quad (II.10)$$

$\delta_{ref}(\mathrm{t})$ is calculated by means of the same equations used to evaluate $\delta(t)$ (they are all reported in the Appendix), but starting from photosensor detections obtained according to the (II.9). $\overline{\mathrm{E}}_{\mathrm{el,100\%}}$ is the electric light illuminance

determined by the system when luminaires are on at 100%.

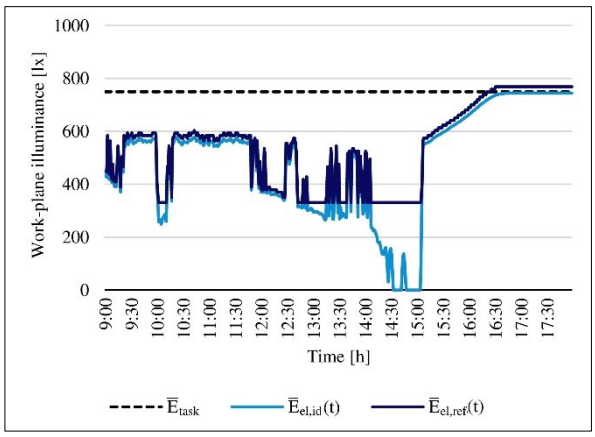

Figure II. 6: Electric light illuminance provided by the reference system.

As it can be seen in Figure II.6., in dimming controls, the reference system functioning is really similar to the ideal one. The $\overline{E}_{el,ref}(t)$ function is slightly higher that the $\overline{E}_{el,id}(t)$ one. This is due to the fact that the provided electric light illuminance in a real system is not perfectly equal to $\overline{E}_{task}$, due to luminaires photometry characteristics. The part were the differences are significant corresponds to the moments of the day when the system could be turned off, but it remains on at minimum light output.

Starting from $\overline{E}_{el,ref}(t)$, it is possible to define the $\Delta E^{+}(t)$ function related to the reference system (see Figure II.7):

$$\Delta E^{+}_{ref}(t) = \overline{E}_{el,ref}(t) - \overline{E}_{A,el,id}(t) \qquad [lx] \quad (II.11)$$

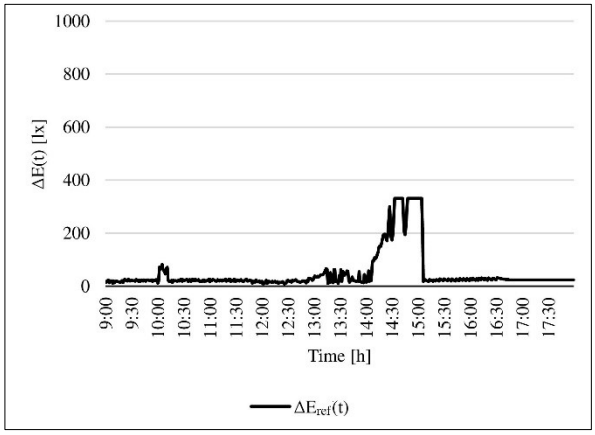

Figure II. 7: ΔE(t) function related to the reference system

Based on the (II.11) we can evaluate $\Delta E^{+}_{intr}(t)$.

$$\Delta E^{+}_{intr}(t) = \begin{cases} \Delta E^{+}_{ref}(t) & if \ \ \Delta E^{+}(t) \geq \Delta E^{+}_{ref}(t) \\ \Delta E^{+}(t) & if \ \ \Delta E^{+}(t) < \Delta E^{+}_{ref}(t) \end{cases} \qquad [lx] \quad (II.12)$$

When $\Delta E^{+}(t)$ is higher than $\Delta E^{+}_{intr}(t)$, the residual excess cannot be due to the control strategy, but it is due to the oscillations of $\overline{E}_{dl}(t)/S_{dl}(t)$. So:

$$\Delta E^{+}_{waste}(t) = \Delta E^{+} - \Delta E^{+}_{intr}(t) \qquad [lx] \quad (II.13)$$

At this point, it is possible to correctly define the light deficit, LD, the Intrinsic Light Excess, ILE, and the Light Waste, LW (see Figure II.8).

$$LD = \int_{T} \Delta E^{-}(t)dt \qquad [lx \cdot h] \quad (II.14)$$

$$ILE = \int_{T} \Delta E^{+}{}_{intr}(t)dt \qquad [lx \cdot h] \quad (II.15)$$

$$LW = \int_{T} \Delta E^{+}{}_{waste}(t)dt \qquad [lx \cdot h] \quad (II.16)$$

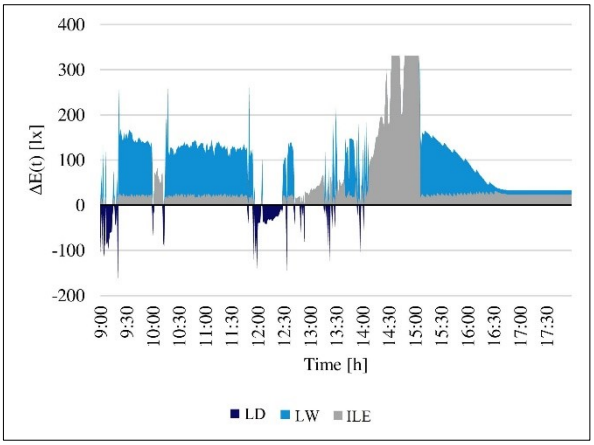

Figure II. 8: LD, LW and ILE

Given these premises it can be said that a DLC can function in four different operating conditions: ideal conditions (when the difference between $\overline{E}_{el}(t)$ and $\overline{E}_{el,id}(t)$ is 0); light deficit, intrinsic light excess and light waste.

Once LD, ILE and LW concepts are described it is possible to finally introduce the new parameters.

Given a period T, DIA (Daylight Integration Adequacy) is the percentage of time during which the control system operates in ideal or intrinsic light excess conditions. To better describe the system functioning DIA^- and DIA^+ can be evaluated. DIA^- is the percentage of time during which the control system operates in light deficit conditions. DIA^+ is the percentage of time during which the control system operates in light waste conditions.

Finally, $LD_{\%}$ (Percentage Light Deficit), $ILE_{\%}$ (Percentage Intrinsic Light Excess) e $LW_{\%}$ (Percentage Light Waste) are respectively:

$$LD_{\%} = \frac{LD}{LR} \cdot 100 \quad [\%] \quad \text{(II.17)}$$

$$ILE_{\%} = \frac{ILE}{LR} \cdot 100 \quad [\%] \quad \text{(II.18)}$$

$$LW_{\%} = \frac{LW}{LR} \cdot 100 \quad [\%] \quad \text{(II.19)}$$

The first three indices give us information about the occurrence during T of the different operating conditions, the others about the quantity of light that is wasted or is lacking. To associate these different data is very important, as a simple example can demonstrate: if two systems have the same DIA^- value, the number of hours during which a deficit occurs is equal. However, if $LD_{\%}$ values are different, as for the system characterized by the higher $LD_{\%}$ value, the differences between $\overline{E}_{el}(t)$ and $\overline{E}_{el,id}(t)$ are on the average more significative compared with the other case. Obviously, a well-functioning system should not only reduce the time percentage during which the functioning is not ideal, but it should also reduce the more is possible the differences between $\overline{E}_{el}(t)$ and $\overline{E}_{el,id}(t)$.

It is important to underline that the proposed parameters have a double value. Indeed, they are meant not only to be used as an evaluation tool during design stage, to identify the technical choices most suitable to the specific cases, but also as a commissioning control tool, to verify systems functioning during operating life.

III. DET: a new tool to evaluate DLCSs performances

The calculation of the parameters described in Paragraph II.1 is not immediate, since it is based on a dynamic approach. Moreover, it assumes that daylight illuminances at the work-plane over time -$\bar{E}_{dl}(t)$- are known, as well as the electric light illuminances determined by the control system -$\bar{E}_{el}(t)$-. If the parameters are used to evaluate an already installed system, these data can be measured. On the contrary, if they are used to estimate systems performances during design process, dynamic daylight simulations are necessary.

Radiance-based software are universally recognised by researchers as the most reliable simulation tools to evaluate daylight availability with a dynamic approach [80]. Thus, they can be used to evaluate $\bar{E}_{dl}(t)$. On the contrary, the simulation of DLCSs is not yet an easy task [22], since, as it was already mentioned in the Introduction, it is pretty difficult to taking into account all the factors affecting DLCSs functioning.

For these reasons, a new tool to evaluate DLCSs performances has been developed (DET- Daylight-linked control systems Evaluation Tool). It accepts as input data daylight availability values obtained by means of dynamic daylight simulation software. Then, based on them, it simulates the functioning of several control system typologies, accounting for different factors neglected by other available software. Specifically, the software is divided in two modules: the simulation module and the evaluation one. The former allows dynamically simulating DLCSs functioning, obtaining $\bar{E}_{el}(t)$ values, the latter calculates Daylight Integration Adequacy (DIA), Percentage Light Deficit ($LD_{\%}$), Percentage Intrinsic Light Excess ($ILE_{\%}$) and Percentage Light Waste ($LW_{\%}$).

In the following paragraphs available simulation software and their limits are described, then DET is presented.

III.1. Today available software and their limits

As it was mentioned in the II.1 Paragraph, the spread of dynamic daylight calculation has deeply changed the way to evaluate daylight.

The most accredited software in this field are those based on Radiance engine [81], specifically Daysim. It is a validated, RADIANCE-based daylighting analysis software, allowing the annual daylight availability in buildings to be modelled [77]. It contains a module to calculate energy savings connected to the use of different DLCSs. Users can divide the work-plane in different zones and define for each zone some control points. For each one of the control zones, users define the control strategy (switching or dimming) and the characteristics of the lighting system: Lighting Power, Standby Power and Ballast Loss Factor [69]. The software calculates daylight illuminances at the control points for each hour or fraction of hour (till 1 minute); evaluates the necessary luminaires light output to reach the required task illuminance at the control point and starting from the light output derives the corresponding power absorbed by the lighting system. Finally, it infers consumptions and related savings based on power. This software most significant problem is that the control is based on the illuminance at the work-plane and not on photosensor detections. Moreover, the calibration procedure is neglected, so the control is simulated as an ideal one able to always perfectly integrate daylight, without determining excesses nor deficits.

The same simulation module is present in DIVA as well. DIVA is a highly optimized daylighting modelling plug-in for Rhinoceros based on Daysim engine [78]. However, the use of DIVA presents an additional problem: it does not allow performing sub-hourly simulations. As it was mentioned in Section 2 brief-time daylight oscillations can strictly affect dynamic daylight simulations functioning [16, 26, 67].

Mistrick developed at Penn State University a modified JAVA GUI for Daysim [77]. This tool can correctly model photosensors location and control algorithm settings, but it presents problems of compatibility with Windows operating system.

Rogers developed an Excel Macro called SPOT (Sensor Placement + Optimization Tool) [70, 82]. It is meant to help designers in defining control strategies, chose photosensors and establish their correct location. The tool contains a database of commercially available photosensors and can correctly model both spatial and spectral photosensor response and the calibration phase of different control typologies (switching, stepped and dimming ones). However, daylight modelling is simplified, and the software allows exclusively evaluating simple spaces characterized by square geometry.

Given that the mentioned software are all based on different calculation models, the use of a software or another, can provide different results in terms of achieved energy savings.

Doulos et al. [23] compared energy savings calculated by means of SPOT, and Daysim, referred to a dimming DLCS. They found that savings obtained with SPOT are 15% higher than those obtained by means of Daysim.

Williams et al. [83] evaluated that generally simulations overestimate actual savings for a percentage equal at least to 10%.

Given the weak points of the available software researches proposed alternative calculation models. Some studies focused their attention on the proposal of quick and simplified methods alternative to dynamic daylight simulations, useful especially in early design stages.

Krarti et al. [84] proposed a method to define energy savings achievable by means of dimming systems starting from the following parameters: the visible transmittance of the window glazing, the ratio of the window area to the daylit floor area, the ratio of the daylit floor area and the total floor area and two coefficients, *a* and *b*, depending on building location and control strategy. The algorithm was then extended by Ihm et al. [3]. They proposed an alternative method to evaluate *a* and *b* coefficients, accounting for the required task illuminance and the specific minimum light output of dimming systems.

Lo Verso et al. [85] developed a tool able to evaluate the electric lighting demand in the early design phases. It is based on two mathematical models, referred to a manual on-off switching and to a dimming DLCS respectively. The models were inferred from results of dynamic daylight simulations studies performed with Daysim and referred to 828 different cases.

A simplified calculation method to evaluate the impact of the use of DLCSs on energy consumptions due to daylight is presented in the European standard EN 15193-1:2017 – Light and Lighting Part I: Energy requirement for lighting [86, 87] as well. It defines the LENI (Lighting Energy Numeric Indicator) representing the annual total energy for electric lighting per square meter in a building and proposes two calculation methods to calculate it: the complete and the rapid one. In the complete one it is proposed a methodology to evaluate the impact of Daylight responsive control systems. It is considered that the time during which the light is on is obtained by multiplying the occupation time of the building by reduction coefficients. One of these coefficients is the F_D, accounting for daylight and being dependent on both the typology of the adopted control strategy and on the available daylight.

In this context, another interesting research field is represented by the use of artificial neural networks to predict the impact of daylighting and DLCSs on building energy consumptions [88-90].

Other studies proposed methods trying to overcome limits of dynamic simulation software. One of the most investigated issue is the way to correctly model the photosensor characteristics, i.e. spectral and spatial responses.

Doulos et al. [42] compared the illuminances detected by means of commercially available photosensors with those obtained by a sensor characterized by a spectral response matching the V(λ) function and they found that the shifts in detections varies in a systematic way. Based on these results, researchers proposed a parameter defined Photosensor Spectral Correction Coefficient (PSCC). It is the ratio of the illuminance registered by the specific photosensor and that measured by the ideal photosensor with a spectral response corresponding to V(λ). The use of PSCC could be used in simulations to obtain more reliable data.

Ehrlich et al. [91, 92] proposed a method to simulate the photosensor detections accounting for their spatial sensitivity starting from two different fisheye images obtained by means of Radiance.

Yoon et al. [93] proposed a method to simulate the spectral sensitivity. It consisted in modelling a

sphere with a diameter of 2.54 cm around the photosensor, assigning a "trans" material in Radiance and in defining a transmission function corresponding to the spectral response of the photosensor.

Other studies focused on lighting systems characteristics simulations.

For example [41, 64] proposed a method to simulate ballast dimming response functions. It consisted in measuring the relationship between control voltage and light output and light output and consumed power. Then best-fit functions describing this relationship were inferred with a regression process. These functions were then used to evaluate absorbed power as a function of the time. Specifically, the calculation phases were the following: daylight illuminances at the work-plane were evaluated by means of Daysim, the electric light requirement and the light output were derived starting from daylight illuminances; finally, from the light output the power was calculated by applying the above-mentioned functions.

Issues connected with the necessity to model the non-linear dimming curve of the luminaires, i.e. the curve relating light output and absorbed power are studied also in [94], where two different energy savings prediction models were verified by using real-time power consumption data.

III.2. DET description

DET is an Excel® macro, that, as it was anticipated in Paragraph III, can simulate the functioning of different DLCSs and evaluate their performances. It is divided in two modules: the simulation tool and the evaluation one. The former module allows dynamically simulating the functioning of several DLCSs typologies, the latter calculates parameters to evaluate DLCSs performances.

Basically, DET consists in a series of screens that users can easily navigate, moving from a section to another. The first screen (see Figure III.1), allows users inserting input parameters.

In more detail, in the A column the following data must be inserted in the specific cells:

- $\overline{E}_{task}$, i.e. the task illuminance indicated by regulations, depending on the visual task performed in the studied environment;
- the time step of the simulation. It can be chosen thanks to a drop-down menu and it can be equal to one hour or one minute;
- the amount of simulated days;
- the number of data per day that were obtained by means of the simulation (for example considering a typical office scheduling, 8, if the simulation was hourly-based and 480 if it is minute-based).

Then, in the columns from C to F, users have to insert results of dynamic daylight simulations:

- date in C column;
- time in D column;
- the values of daylight work-plane illuminances -$\overline{E}_{A,dl}(t)$- in E column;

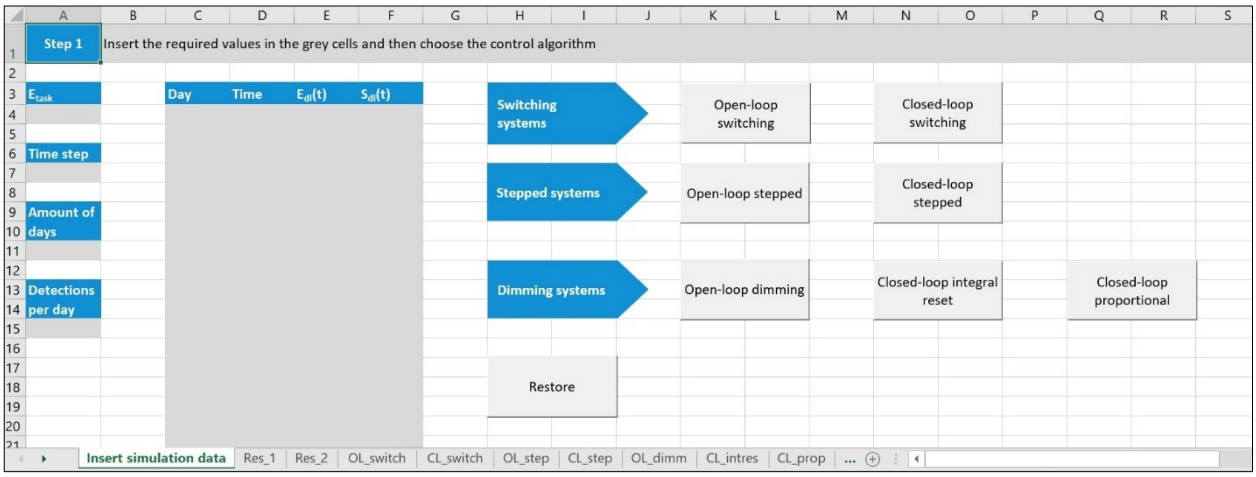

Figure III. 1: DET first screen

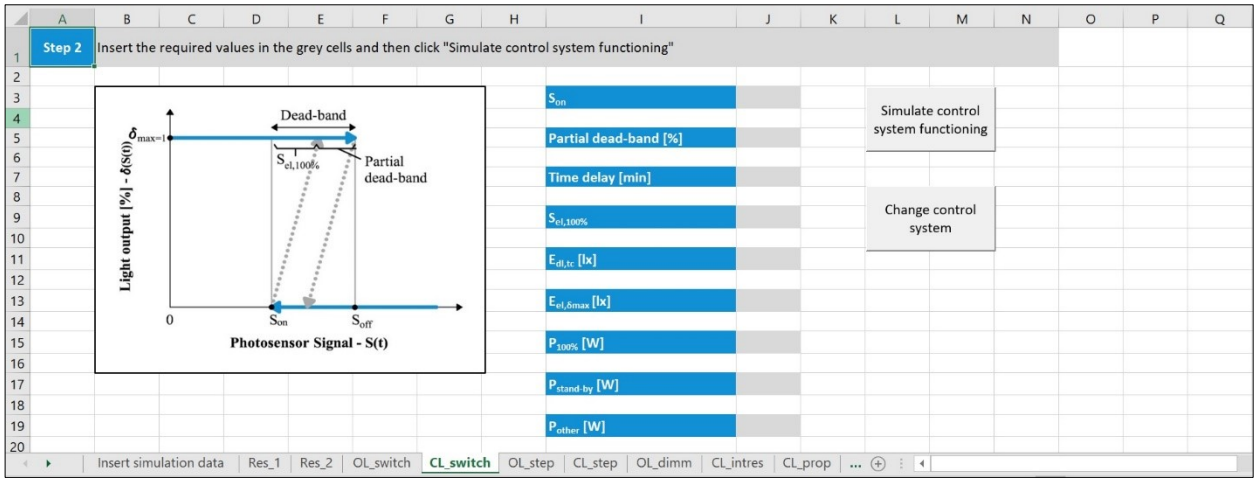

Figure III. 2: Closed-loop switching system screen in DET

- the values of daylight photosensor signal -$S_{dl}(t)$- in F column.

It must be underlined that, even though the software was born to be used together with simulation software, users can also insert measured data of real monitored spaces instead of simulated data, as it will be shown in the next section.

After the input data have been set, users choose the control systems they want to simulate, by clicking on the correspondent button. DET includes open-loop and closed-loop switching systems, open-loop and closed-loop stepped systems, open-loop dimming systems, closed-loop integral reset and proportional dimming systems.

Control buttons activate the screens corresponding to the specific controls (see for example Figure III.2). Here users must set control calibration parameters that are different for each control typology (for example On signal and dead-band for switching systems or maximum and minimum light output for dimming ones) and information about the adopted lighting system such as the electric light illuminance provided at the work-plane when luminaires are 100% on, the absorbed power, the stand-by power and the power absorbed by auxiliary systems like photosensors and controllers. Then, users have to run the simulation by clicking the "*Simulate control system functioning*" button. After few minutes during which calculations are performed, the results page will appear. It will report trends over time of luminaires light output -$\delta(t)$ [%]-, electric light illuminances at the work-plane -$\overline{E}_{A,el}(t)$ [lx]-, total (electric light plus daylight) illuminances at the work-plane -$\overline{E}_{A,tot}(t)$ [lx]- and power absorbed by the lighting system $P(t)$ [W]. The software provides both numerical values and graphs. Moreover, energy consumptions are evaluated and the percentage incidence of consumptions due to luminaires, luminaires in stand-by and other devices are provided.

From the results page the second phase of the analysis can be launched by clicking the "*Performance evaluation*" button. After few minutes, the second page of results will appear. It will contain DIA, DIA^+, DIA^-, $LD_{\%}$, $ILE_{\%}$ and $LW_{\%}$ values. Moreover, trends of work-plane electric light illuminances provided by the real system -$\overline{E}_{el}(t)$-, the ideal one -$\overline{E}_{el,id}(t)$- and the reference one -$\overline{E}_{el,ref}(t)$- (cfr. Paragraph II.2) will be reported. These data represent a useful help to better interpret the performance parameters. Also, in this case both numerical values and graphs are provided.

The following paragraphs contain a more in-depth description of the two calculation modules.

III.2.1 DET simulation module

DET simulation module strong point is the fact that it takes into account different aspects neglected in the other software described in the previous section:

- First of all, being based on output data of dynamic daylight simulations, it can be used also to evaluate DLCSs functioning in spaces characterized by complex geometry;

- Luminaires light output calculation is based on the photosensor signal and not on the work-plane illuminance. So, the control systems simulation accounts for the variation over time of the ratio $\overline{E}_{A,dl}(t)/S_{dl}(t)$;
- For each control system typology, the calibration phase is properly simulated;
- Power, energy consumptions and savings are evaluated considering that there is a linear correspondence between light output and absorbed power (reliable hypothesis for new LED sources [46, 47]). However, the shift between the minimum light output and the minimum absorbed power is considered (i.e. if the minimum light output is 20%, it is not necessarily true that the minimum absorbed power is equal to 20% of the maximum power as well);
- Luminaires stand-by power and power of other devices, such as photosensors and controllers, are considered in the calculation.

The simulation of DLCSs functioning over the observation period consists of the following phases:

- Calculation of the parameters necessary to completely define the control algorithm (for example the Off signal in switching systems or the slope of the curve in proportional systems);
- Calculation of the luminaires light output $\delta(t)$ as a function of the time, depending on the control algorithm, the $S_{dl}(t)$ values and the calibration parameters;
- Calculation of the electric light illuminance at the work-plane as a function of the time, $\overline{E}_{A,el}(t)$. It is evaluated as:

$$\overline{E}_{el}(t) = \delta(t) \cdot \overline{E}_{el,100\%} \quad [\text{lx}] \quad \text{(III.1)}$$

Where $\overline{E}_{A,el,100\%}$ is the average electric light at the work-plane determined by the luminaires when they are turned on at 100% light output.

- Calculation of the total illuminance at the work-plane (daylight plus electric light) as a function of the time, evaluated as:

$$\overline{E}_{tot}(t) = \overline{E}_{dl}(t) + \overline{E}_{el}(t) \quad [\text{lx}] \quad \text{(III.2)}$$

- Calculation of the absorbed power as a function of the time, $P(t)$, considering that:

$$P(t) = P_{luminaires}(t) + P_{other}(t) \quad [\text{W}] \quad \text{(III.3)}$$

Where $P_{luminaires}(t)$ is the power absorbed by the luminaires and $P_{other}(t)$ is the power absorbed by the other lighting system components such as photosensors and controllers.

- Calculation of the energy consumptions starting from the power data;
- Calculation of percentage energy savings considering as reference system a light system with luminaires always on at the full capacity.

Obviously the first two phases are different depending on the considered control strategy. A detailed description about the way controls implemented in DET operate is reported in the Appendix. In the Appendix the equations useful to calculate $\delta(t)$ as a function of $S_{dl}(t)$ are reported for each control typology as well.

As for $P(t)$ calculation, it is possible to assume a linear relationship between luminaires power and their light output, as it is represented in Figure III.3.

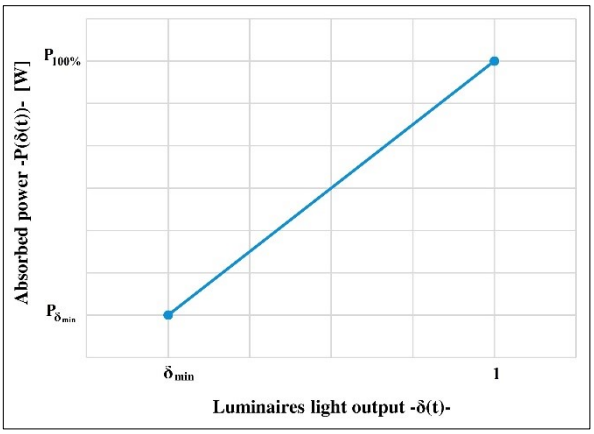

Figure III. 3: Relationship between luminaires light output and absorbed power

Therefore, $P_{luminaires}(t)$ can be calculated as it follows:

$$P_{luminaires}(t) = \begin{cases} m \cdot \delta(t) + q \ \textit{if luminaires are on} \\ P_{stand-by} \ \ \textit{if luminaires are off} \end{cases} \quad [\text{W}] \quad \text{(III.4)}$$

Where $P_{stand-by}$ is the stand-by power of the luminaires and m and q can be calculated as:

$$m = \frac{P_{100\%} - P_{\delta min}}{1 - \delta_{min}} \quad \text{(III.5)}$$

$$q = \frac{P_{\delta min} - \delta_{min} \cdot P_{100\%}}{1 - \delta_{min}} \quad \text{(III.6)}$$

Where δ_{min}, is the minimum light output which the luminaires can be dimmed down at; $P_{100\%}$ is the power absorbed by luminaires when they are turned on at their full capacity (i.e. when $\delta(t)$ is equal to 1) and $P_{\delta min}$ is the power absorbed by luminaires when they are dimmed down at the minimum light output.

III.2.2 DET evaluation module

The evaluation module goal is to calculate performance parameters described in Paragraph II.2. It uses as input data the work-plane daylight illuminance values, the daylight photosensors signals inserted by users and the electric light illuminance values calculated by the simulation module.

First of all, the evaluation module calculates the electric light illuminances provided by the ideal system and by the reference system according to the (II.5) and to the (II.10). Then it infers $\Delta E^{-}(t)$, $\Delta E^{+}_{intr}(t)$, $\Delta E^{+}_{waste}(t)$ functions calculating their values according to the (II.6), the (II.12) and the (II.13) respectively. From these data it infers LD, ILE and LW according to the (II.14), the (II.15) and the (II.16). At this point it has all data necessary to obtain the performance parameters. So, it calculates DIA, DIA^{-} and DIA^{+} according to the definition given in paragraph II.2 and $LD_{\%}$, $ILE_{\%}$ and $LW_{\%}$ according to the (II.17), the (II.18) and the (II.19) respectively.

III.2.3 A worked-out example

A worked-out example is reported to give a better idea of the way DET operates. Specifically, the case of a closed-loop proportional dimming system is presented, using, as input data, measured illuminance values referred to the case study that will be described in the following section (the considered façade configuration is the south-oriented equipped with a balcony window).

Figure III.4 shows DET first screen. In this case the considered $\overline{E}_{task}$ is equal to 750 lx; measurements were performed with a 1-minute time step, so the "*Time-step*" is "*Minute*". On the contrary, if input data were obtained by means of hourly-based simulations, in the drop-down menu, associated to A11, cell the "*Hour*" time step should be chosen. In this application, the analysis is limited to 2 days, and measurements were performed from 9:00 to 18:00, i.e. for 9 hours. So, the "*Amount of days*" is 2 and the "*Detections per day*" are 540 (60 minutes for 9 hours). In an hourly-based simulation, referred to an entire year, the "*Amount of days*" will be 365 and, for example, the "*Detections per day*" would be 10 if the considered time range is 9:00-18:00 as well and both the records corresponding to 9:00 and to 18:00 are inserted. In the column from C to F, the

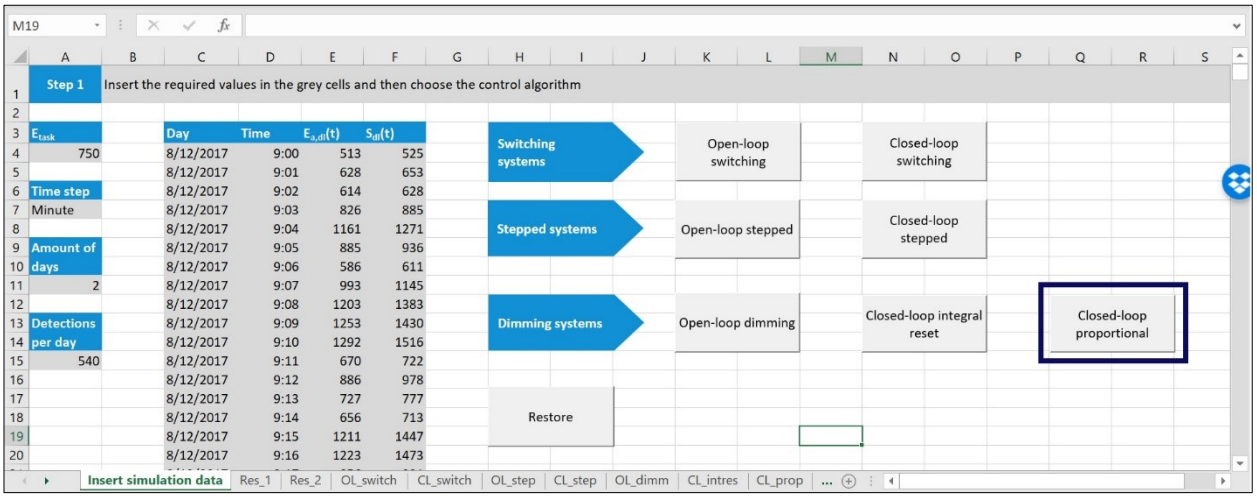

Figure III. 4: DET first screen - Work-out example

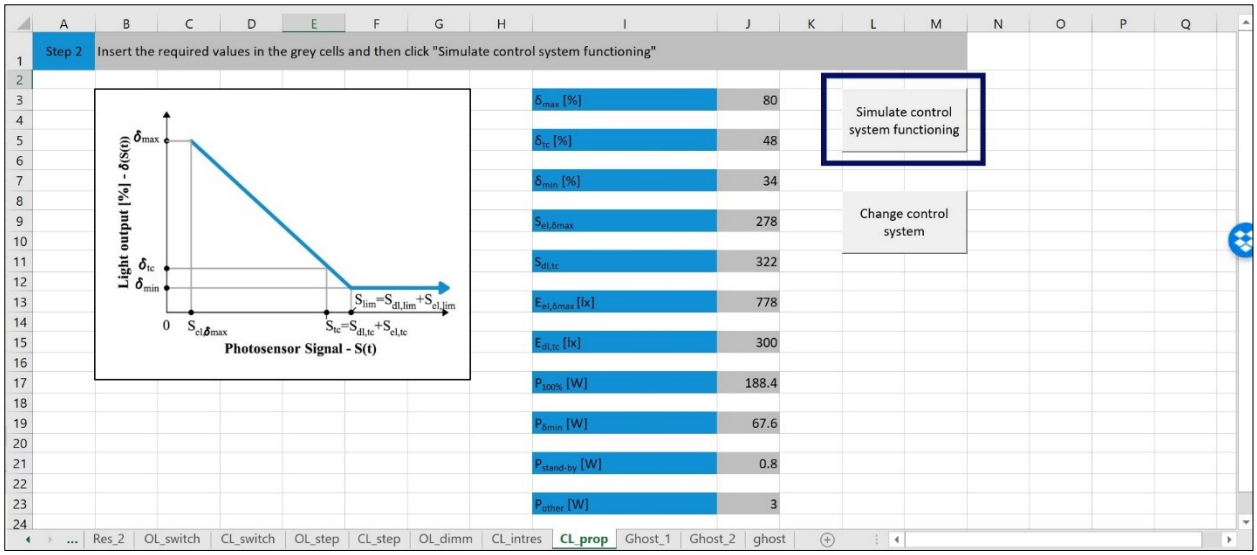

Figure III. 5: DET "Closed-loop proportional dimming screen" – Worked-out example

following data must be set: the "*Day*" (in this case December the 8th and the 9th), the "*Time*" (in this case 9:00, 9:01, 9:02 etc) and the related values of work-plane illuminance -$\overline{E}_{dl}(t)$- and photosensor signal -$S_{dl}(t)$- referred to each considered minute. In the case of hourly based simulations, obviously, the data to insert are the simulations results referred to each hour and evaluated at a calculation point located at the desk (or the average value of illuminances calculated in more points) and at a calculation point located at the photosensor position respectively. Once the data are correctly inserted, the control typology must be chosen: in this case the "*Closed-loop proportional dimming*" button was pressed. At this point the screen represented in Figure III.5 will appear, and calibration parameters must be inserted in the grey cells. The Table III.1 describes for each control system typology the corresponding calibration parameters and explain how to set them when using data obtained by means of dynamic daylight simulations. As for the specific values reported in Figure III.5, they are explained in the following section (see Tables IV.7 and IV.8).

Once calibration parameters are set, the button "*Simulate control system functioning*" must be pressed and the calculation procedure will start. At the end of the calculations, the screen reported in Figure III.6 will appear. In the upper part, data referring to energy consumptions are reported: specifically, the energy consumptions in kWh due to luminaires, luminaires in stand-by and accessories devices. Moreover, the total

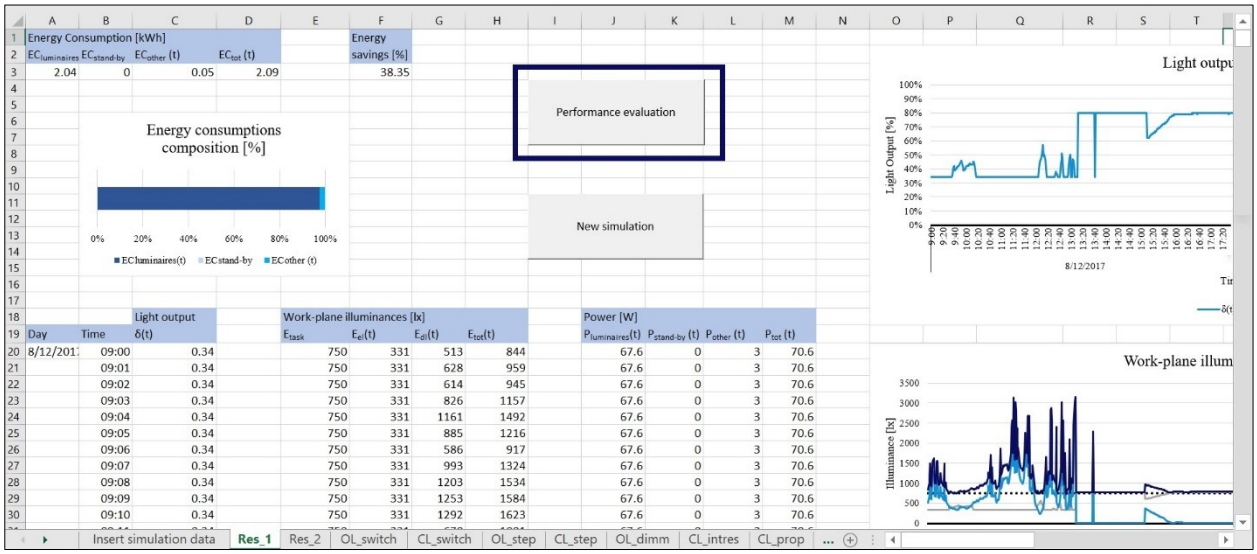

Figure III. 6: DET Simulation results screen – Worked-out example

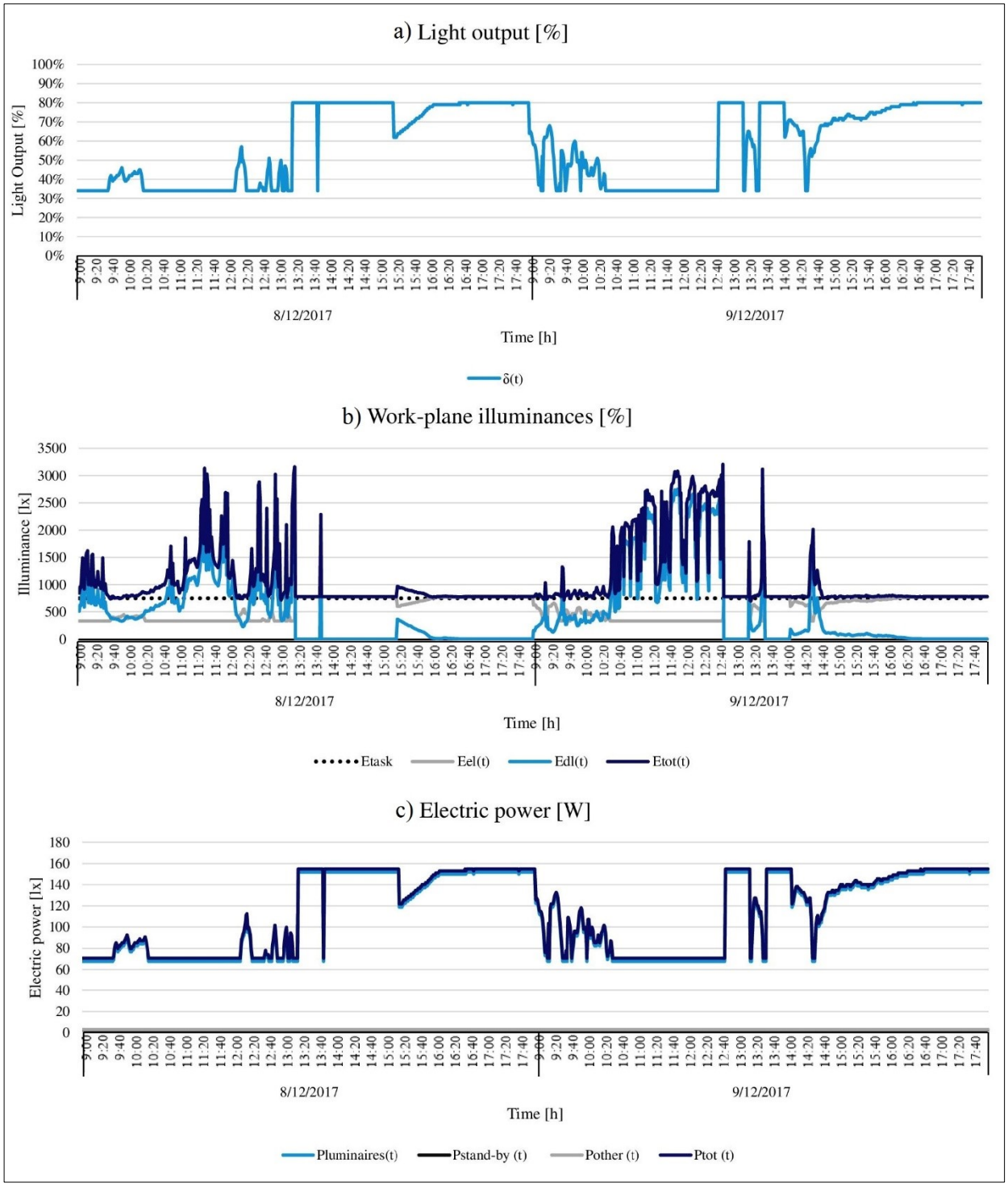

Figure III. 7: Output graphs related to DET simulation module – Worked-out example

consumptions and the savings evaluated referring to an always on lighting systems are indicated in cells D3 and F3. Below the numerical results, a graph reports the percentage incidence of the three rates on the total energy consumptions. In the lower part of the screen, for each day and each minute, the following results are reported: δ, $\overline{E}_{task}$, $\overline{E}_{el}$, $\overline{E}_{dl}$, $\overline{E}_{tot}$, $P_{luminaires}$, $P_{stand-by}$, P_{other} and P_{tot}. The same results are also represented by means of graphs that are not visible in Figure III.6, and so are represented in Figure III.7. In Figure III.7.b, it can be noticed that in this case total illuminances are almost always higher than the task illuminance, so the system rarely works in deficit conditions. Moreover, from Figure III.7.c, it can be inferred that luminaires are never in stand-by, since they cannot be completely turned off. Consequently, the total power is equal to the sum of the power absorbed by luminaires

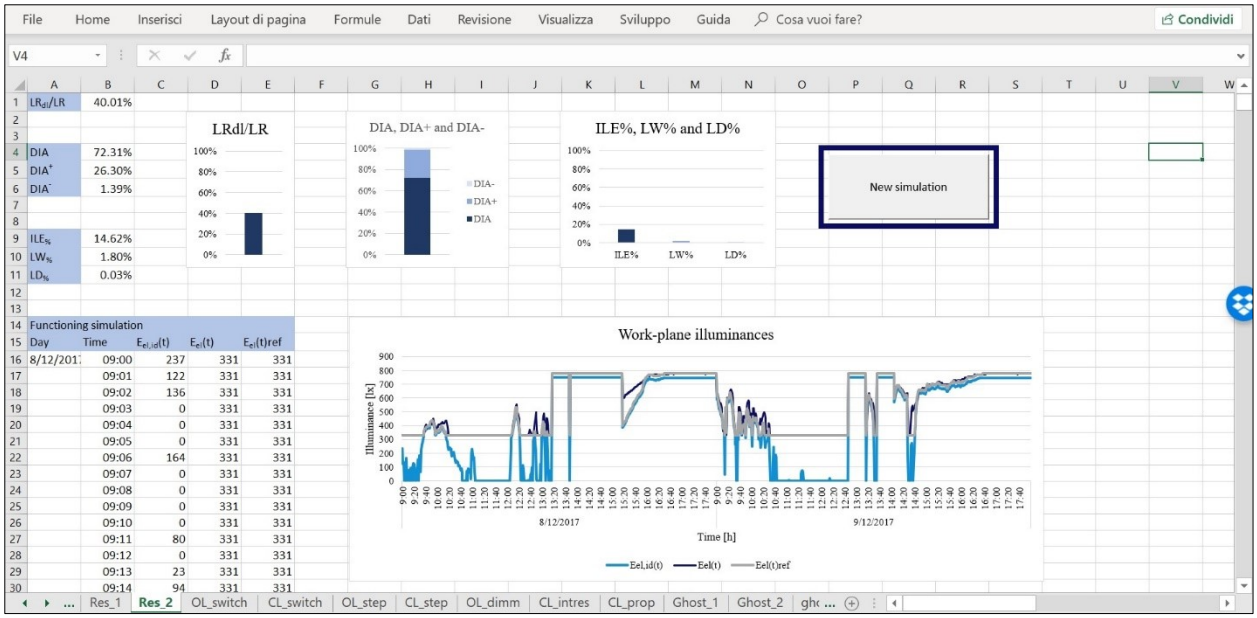

Figure III. 8: DET "Performance evaluation" screen – Worked-out example

(varying with time) and that absorbed by the auxiliary systems (stable on time).

Clicking the "*Performance evaluation button*" (See Figure III.6) the performance parameters are calculated, and the screen reported in Figure III. 8 will appear. In the upper part of the screen numerical values and graphs corresponding to performance parameters are provided. In the lower one for each minute, the following data are reported: $\overline{E}_{el,id}$, $\overline{E}_{el}$ and $\overline{E}_{el,ref}$. They are represented in a graph as well. For this specific application it can be noticed that the reference system trend is only slightly higher than the ideal electric light one, excluding when the system operates at minimum light output (this determines the corresponding ILE% value). The electric light illuminance trend is sometimes higher than the reference one, and this determines the LW% value. As it was previously reported, the deficit is almost 0. By clicking the "New simulation" button, the results will be deleted and the first screen (see Figure III.4) will appear again.

Table III. 1: Calibration parameters related to each DLCS typology implemented in DET

DLCS typology	**Calibration parameter**	**Description**	**How to set it**
Open-loop switching	S_{on}	It is the signal corresponding to the on action and it is set during calibration. It corresponds to the daylight component of the photosensor signal when the work-plane daylight illuminance is just above the task illuminance.	To obtain it users have to select from the results of dynamic simulations all the work-plane illuminances around the task one (e.g. if the task illuminance is 500 lx, consider the range 490lx-510 lx) and the corresponding photosensor signals. Then they have to calculate the average of the obtained photosensor signals and use it as S_{on}.
	Dead-band [%]	Difference between the S_{on} signal and the S_{off}, i.e. the signal corresponding to the off actions.	According to [55] the dead-band extension can range from 10% to 25% of S_{on}.
	Time delay [min]	Time that has to pass after a switching on action before a switching off can occur.	According to [55] the time delay can range from 2 to 30 minutes.
	$\overline{E}_{dl,tc}$ [lx]	Daylight-work-plane illuminance at the calibration time.	It can correspond to the task illuminance.
	$\overline{E}_{el,100\%}$ [lx]	Electric light work-plane illuminance when luminaires are 100% on, without considering the maintenance factor.	It can be calculated with a light calculation software like DIALux.

	$P_{100\%}$ [W]	Power absorbed by all luminaires when they are on at 100%.	It can be inferred from technical data sheet.
	$P_{stand-by}$ [W]	Power absorbed by all luminaires in stand-by conditions.	It can be inferred from technical data sheet.
	P_{other} [W]	Power absorbed by auxiliary devices such as photosensors and controllers.	It can be inferred from technical data sheet.
Closed-loop switching	S_{on}	It is the signal corresponding to the on action and it is set during calibration. It corresponds to the daylight component of the photosensor signal when the work-plane daylight illuminance is just above the task illuminance.	To obtain it users have to select from the results of dynamic simulations all the work-plane illuminances around the task one (e.g. if the task illuminance is 500 lx, consider the range 490lx-510 lx) and the corresponding photosensor signals. Then they have to calculate the average of the obtained photosensor signals and use it as S_{on}.
	Partial dead-band [%]	In closed-loop switching systems the dead-band is the sum of $S_{el,100\%}$ (i.e. the photosensor signal detected when luminaires are 100% on) and a partial dead-band.	The partial dead-band extension can range from 10% to 25% of Son.
	Time delay [min]	Time that has to pass after a switching on action before a switching off can occur.	According to [55] the time delay can range from 2 to 30 minutes.
	$S_{el,100\%}$	Electric light component of the photosensor signal when luminaires are 100% on.	It can be calculated with a light calculation software like DIALux.
	$\overline{E}_{dl,tc}$ [lx]	Daylight-work-plane illuminance at the calibration.	It can correspond to the task illuminance.
	$\overline{E}_{el,100\%}$ [lx]	Electric light work-plane illuminance when luminaires are 100% on, without considering the maintenance factor.	It can be calculated with a light calculation software like DIALux.
	$P_{100\%}$ [W]	Power absorbed by all luminaires when they are on at 100%.	It can be inferred from technical data sheet.
	$P_{stand-by}$ [W]	Power absorbed by all luminaires in stand-by conditions.	It can be inferred from technical data sheet.
	P_{other} [W]	Power absorbed by auxiliary devices such as photosensors and controllers.	It can be inferred from technical data sheet.
Open-loop stepped	S_{up}	It is the signal corresponding to the switching on action at the first light output level and it is set during calibration. It corresponds to the daylight component of the photosensor signal when the work-plane daylight illuminance is just above the task illuminance.	To obtain it users have to select from the results of dynamic simulations all the work-plane illuminances around the task one (e.g. if the task illuminance is 500 lx, consider the range 490lx-510 lx) and the corresponding photosensor signals. Then they have to calculate the average of the obtained photosensor signals and use it as S_{up}.
	δ_{max}	Maximum luminaires light output.	It can be different from 100%. In this case it can be set equal to the maintenance factor value.
	δ_{min}	Minimum luminaires light output.	It can be inferred from literature.
	Number of steps	Number of light output steps.	Chosen by users.
	$\overline{E}_{dl,tc}$ [lx]	Daylight-work-plane illuminance at the calibration time.	It can correspond to the task illuminance.
	$\overline{E}_{el,\delta max}$ [lx]	Electric light work-plane illuminance when luminaires are on at the maximum light output, without considering the maintenance factor.	It can be calculated with a light calculation software like DIALux.

	$P_{100\%}$ [W]	Power absorbed by all luminaires when they are on at 100%.	It can be inferred from technical data sheet.
	$P_{\delta min}$ [W]	Power absorbed by all luminaires when they are on at the minimum light output.	It can be inferred from technical data sheet.
	$P_{stand-by}$ [W]	Power absorbed by all luminaires in stand-by conditions.	It can be inferred from literature.
	P_{other} [W]	Power absorbed by auxiliary devices such as photosensors and controllers.	It can be inferred from technical data sheet.
Closed-loop stepped	$S_{el,\delta max}$	Electric light component of the photosensor signal when luminaires are on at the maximum light output.	It can be calculated with a light calculation software like DIALux.
	δ_{max}	Maximum luminaires light output.	It can be different from 100%. In this case it can be set equal to the maintenance factor value.
	Number of steps	Number of light output steps.	Chosen by users.
	Partial dead-band	In closed-loop stepped systems the dead-band is the sum of $S_{el,\delta max}$ (i.e. the photosensor signal detected when luminaires are on at maximum light output) and a partial dead-band.	The partial dead-band extension can range from 10% to 25% of Son.
	$\overline{E}_{el,\delta max}$ [lx]	Electric light work-plane illuminance when luminaires are on at the maximum light output, without considering the maintenance factor.	It can be calculated with a light calculation software like DIALux.
	δ_{min} [%]	Minimum luminaires light output.	It can be inferred from literature.
	$P_{100\%}$ [W]	Power absorbed by all luminaires when they are on at 100%.	It can be inferred from technical data sheet.
	$P_{\delta min}$ [W]	Power absorbed by all luminaires when they are on at the minimum light output.	It can be inferred from technical data sheet.
	$P_{stand-by}$ [W]	Power absorbed by all luminaires in stand-by conditions.	It can be inferred from literature.
	P_{other} [W]	Power absorbed by auxiliary devices such as photosensors and controllers.	It can be inferred from technical data sheet.
Open-loop dimming	δ_{max} [%]	Maximum luminaires light output.	It can be different from 100%. In this case it can be set equal to the maintenance factor value.
	δ_{tc} [%]	Light output at the calibration.	Chosen by the user, but it must slightly higher than the minimum light output.
	δ_{min} [%]	Minimum luminaires light output.	It can be inferred from literature.
	$S_{dl,tc}$	It is the photosensor signal at calibration detected when the corresponding daylight illuminance is $\overline{E}_{dl,tc}$.	To obtain it users have to select from the results of dynamic simulations all the work-plane illuminances around the $\overline{E}_{dl,tc}$ (e.g. if $\overline{E}_{dl,tc}$is 350 lx, consider the range 340lx-360 lx) and the corresponding photosensor signals. Then they have to calculate the average of the obtained photosensor signals and use it as $S_{dl,tc}$.
	$\overline{E}_{el,\delta max}$ [lx]	Electric light work-plane illuminance when luminaires are on at the maximum light output, without considering the maintenance factor.	It can be calculated with a light calculation software like DIALux.
	$\overline{E}_{dl,tc}$ [lx]	Work-plane daylight illuminance at the calibration. It is such that the electric light output necessary to integrate daylight is slightly higher than the minimum one.	It is such that the electric light output necessary to integrate daylight is slightly higher than the minimum one. For example, if the minimum light output is 20% and the task illuminance is 500 lx, it can be equal to about the 30% of the task illuminance, i.e. 350 lx.

	$P_{100\%}$ [W]	Power absorbed by all luminaires when they are on at 100%.	It can be inferred from technical data sheet.
	$P_{\delta min}$ [W]	Power absorbed by all luminaires when they are on at the minimum light output.	It can be inferred from technical data sheet.
	$P_{stand-by}$ [W]	Power absorbed by all luminaires in stand-by conditions.	It can be inferred from literature.
	P_{other} [W]	Power absorbed by auxiliary devices such as photosensors and controllers.	It can be inferred from technical data sheet.
Closed-loop integral reset	δ_{max} [%]	Maximum luminaires light output.	It can be different from 100%. In this case it can be set equal to the maintenance factor value.
	δ_{min} [%]	Minimum luminaires light output.	It can be inferred from literature.
	$S_{el,\delta max}$	Electric light component of the photosensor signal when luminaires are on at the maximum light output.	It can be calculated with a light calculation software like DIALux.
	$\overline{E}_{el,\delta max}$ [lx]	Electric light work-plane illuminance when luminaires are on at the maximum light output, without considering the maintenance factor.	It can be calculated with a light calculation software like DIALux.
	$P_{100\%}$ [W]	Power absorbed by all luminaires when they are on at 100%.	It can be inferred from technical data sheet.
	$P_{\delta min}$ [W]	Power absorbed by all luminaires when they are on at the minimum light output.	It can be inferred from technical data sheet.
	$P_{stand-by}$ [W]	Power absorbed by all luminaires in stand-by conditions.	It can be inferred from literature.
	P_{other} [W]	Power absorbed by auxiliary devices such as photosensors and controllers.	It can be inferred from technical data sheet.
Closed-loop proportional dimming	δ_{max} [%]	Maximum luminaires light output.	It can be different from 100%. In this case it can be set equal to the maintenance factor value.
	δ_{tc} [%]	Light output at the calibration.	Chosen by the user, but it must slightly higher than the minimum light output.
	δ_{min} [%]	Minimum luminaires light output.	It can be inferred from literature.
	$S_{el,\delta max}$	Electric light component of the photosensor signal when luminaires are on at the maximum light output.	It can be calculated with a light calculation software like DIALux.
	$S_{dl,tc}$	It is the photosensor signal at calibration detected when the corresponding daylight illuminance is $\overline{E}_{dl,tc}$.	To obtain it users have to select from the results of dynamic simulations all the work-plane illuminances around the $\overline{E}_{dl,tc}$ (e.g. if $\overline{E}_{dl,tc}$ is 350 lx, consider the range 340lx-360 lx) and the corresponding photosensor signals. Then they have to calculate the average of the obtained photosensor signals and use it as $S_{dl,tc}$.
	$\overline{E}_{el,\delta max}$ [lx]	Electric light work-plane illuminance when luminaires are on at the maximum light output, without considering the maintenance factor.	It can be calculated with a light calculation software like DIALux.
	$\overline{E}_{dl,tc}$ [lx]	Work-plane daylight illuminance at the calibration. It is such that the electric light output necessary to integrate daylight is slightly higher than the minimum one.	It is such that the electric light output necessary to integrate daylight is slightly higher than the minimum one. For example, if the minimum light output is 20% and the task illuminance is 500 lx, it can be equal to about the 30% of the task illuminance, i.e. 350 lx.
	$P_{100\%}$ [W]	Power absorbed by all luminaires when they are on at 100%.	It can be inferred from technical data sheet.
	$P_{\delta min}$ [W]	Power absorbed by all luminaires when they are on at the minimum light output.	It can be inferred from technical data sheet.

	$P_{stand-by}$ [W]	Power absorbed by all luminaires in stand-by conditions.	It can be inferred from literature.
	P_{other} [W]	Power absorbed by auxiliary devices such as photosensors and controllers.	It can be inferred from technical data sheet.

IV. Case study setting

DET was used to evaluate the performances of different DLCSs related to a specific case study: a square single office situated in one of the buildings of the University of Naples "Federico II" (Latitude 40° 51' 22 N, Longitude 14° 14' 47 E). Even though daylight availability results provided by radiance-based software can be considered reliable, they are unavoidably subjected to errors due to the approximations of the calculation model. For this reason, the evaluation of DLCSs performances is not based on simulated data, but on field measurements. For this purpose, a specific measurement system was set up in the office, to obtain data referred to daylight work-plane and photosensor illuminances over time. Moreover, it provides outdoor irradiance values, in order to characterize weather conditions.

As it was explained in the previous paragraphs, DET needs not only daylight data but also information about the lighting system. Since the office is equipped with obsolete fluorescent luminaires, a new and smart LED system was designed by means of DIALux software [95]. The chosen luminaires were LED ones previously tested in the Photometry and Lighting Laboratory of the Department of Industrial Engineering of the University of Naples "Federico II".

Finally, starting from all the obtained information (referred both to daylight and electric light) the functioning of different control systems was simulated by means of DET. Specifically, the following typologies were analysed: open-loop and closed-loop switching, open-loop and closed-loop stepped and open-loop and closed-loop dimming systems.

Following paragraphs are describing the office used as case study, reporting the setting up of the measurement system, illustrating the luminaires characteristics tested in the Laboratory and presenting the lighting system design. In conclusion, the way all the data have been put together to evaluate the selected DLCSs is explaining and obtained results are showing.

IV.1. Room description

The office is 4 m · 4 m wide, 3 m high and it is located at the top floor of the building (the seventh one). It is sidelit by two French windows: the former facing South and the latter facing West. The west one allows the access to a 1.6 m wide balcony. An overhang of the same size protects the window from the direct radiation. The south French window leads to a big terrace about 7.0 m·12.0 m wide and no shading device protects it. Typical office furniture is located in the office.

Figures IV.1 and IV.2 report measured plan and section and photos of the office.

It was the very double-orientation that drove the choice of the office as case study. Indeed, by using common cardboards, properly attached to the windows frames, it was possible to vary the window to wall ratio and to obtain 4 different façade configurations. They are described in Table IV.1 and shown in Figure IV.3.

In this way different daylighting conditions were evaluated, observing how much daylight availability influences the functioning of control systems.

Table IV. 1: Façade configurations description

Name	Description
SOFW	South orientation with French window
SOSW	South orientation with simple window
WOFW	West orientation with French window
WOSW	West orientation with simple window

IV.2. Setting up of the measurement system

A measurement system was ad hoc set, to obtain data useful to study the DLCSs performances. To do that, the following information were needed: daylight illuminances at the work-plane and photosensor signals for both a closed-loop and an open-loop photosensor. For this purpose, three illuminance meters were located on the desk (see W1, W2 and W3 in Figure IV.1). Another illuminance meter was ceiling-mounted corresponding to the position of a typical closed-loop photosensor (see CL_P in Figure IV.1). Finally, an illuminance meter was located at the

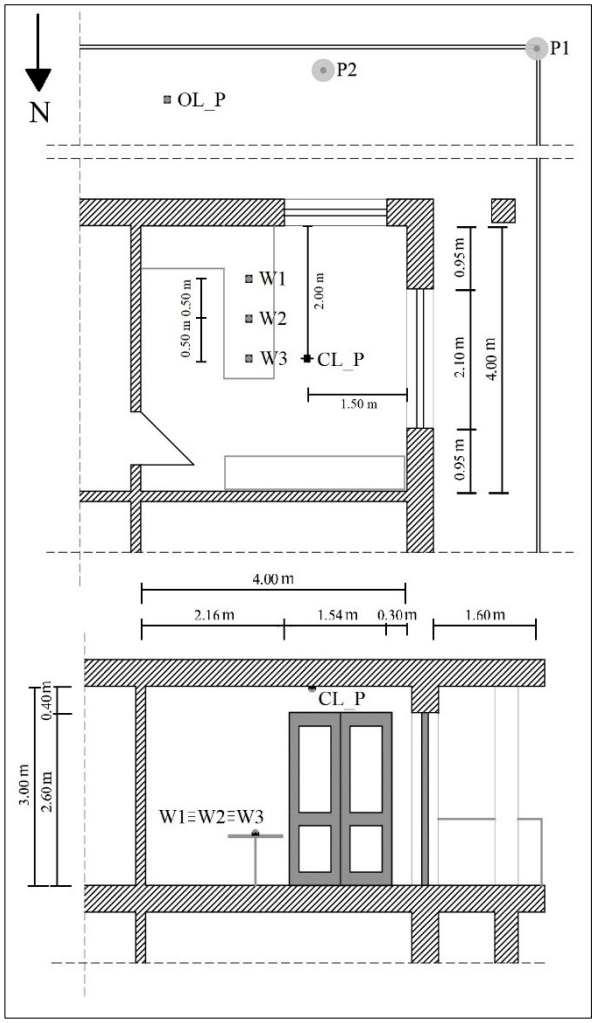

Figure IV. 1: Office measured plan and section

terrace floor to simulate an open-loop photosensor (see OL_P in Figure IV.1). The average value of illuminances at W1, W2 and W3 was assumed as representative of the daylight work-plane illuminances; the illuminances at CL_P and OL_P was assumed as representative of the closed-loop and open-loop daylight photosensor signals.

Beyond illuminances, global and diffuse horizontal irradiance data were acquired by means of two pyranometers, in order to characterize weather conditions. The pyranometers, together with the outdoor illuminance meter were located on the building terrace. Given the building height and the fact that the surrounding buildings are lower, the instruments did not risk being shaded.

The above-mentioned sensors were managed by two different dataloggers acquiring data inside and outside the room respectively. Dataloggers stored daylight data round-the-clock, with a custom-chosen time step. The minimum time step (1 minute) was chosen since suddenly daylight fluctuations strictly affects DLCSs performances [26]. Moreover a 1-minute range can be considered representative of the time response of a photosensor [55].

The considered daily time range for the analysis was 9:00 o' clock-18:00 o' clock (typical office scheduling) considering daylight saving time.

The pyranometer used to measure global horizontal irradiances, $E_{E;global}$, (P1 in Figure IV.1) is a Nesa RSG [96]. It was secured at the balustrade of the terrace.

Figure IV. 2: Photos of the office

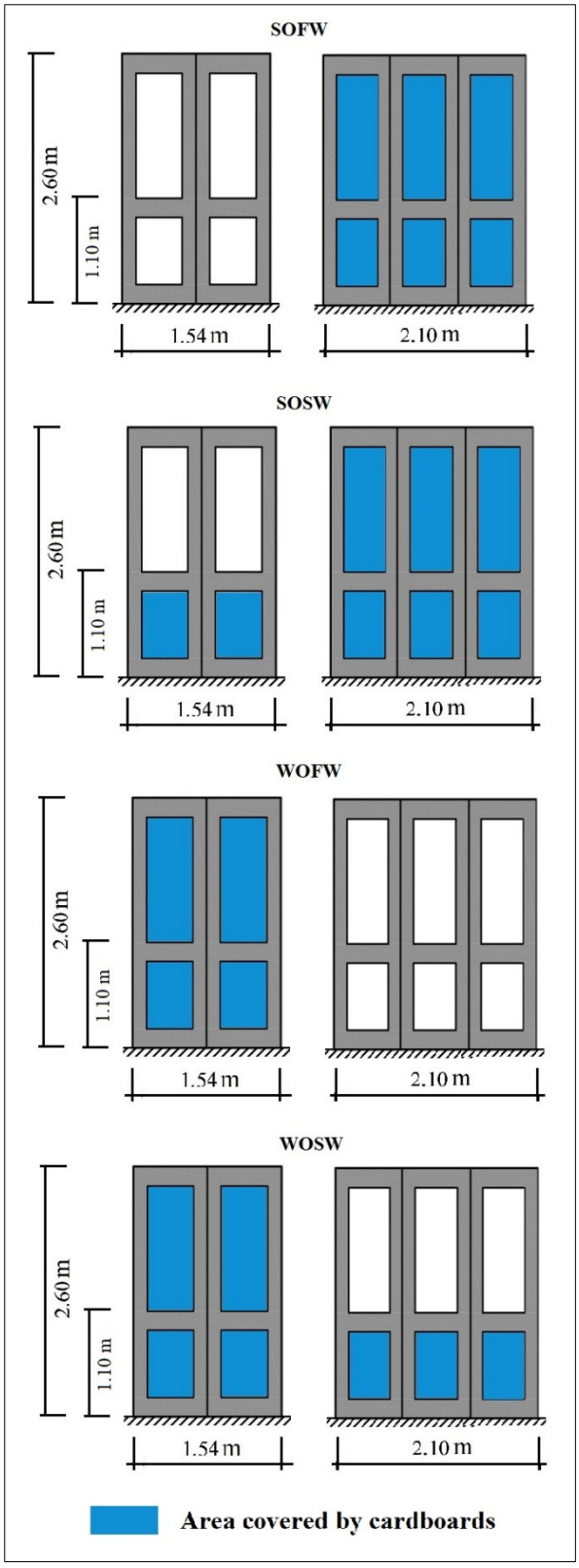

Figure IV. 3: Scheme of façade configurations

The other one (P2 in Figure IV.1) is a Delta Ohm LP PYRA 12 [97], monitoring diffuse irradiance ($E_{E,sky}$). It is installed on a support composed of a pillar and a crossbar connected to four elements: a base, two graduated sliding bars supporting a shadow ring and a rotating arm connected to the actual housing of the pyranometer (see Figure IV.4). The instrument must be positioned considering the following issues: The shadow ring axis must be parallel to the earth's axis (i.e. the rotating arms must have the same direction of solar rays at the solar noon); the goniometer located in correspondence of the rotating arm must be set according to the location latitude; the pyranometer must be perfectly horizontal according to the two spirit levels located in the base and in the pyranometer housing.

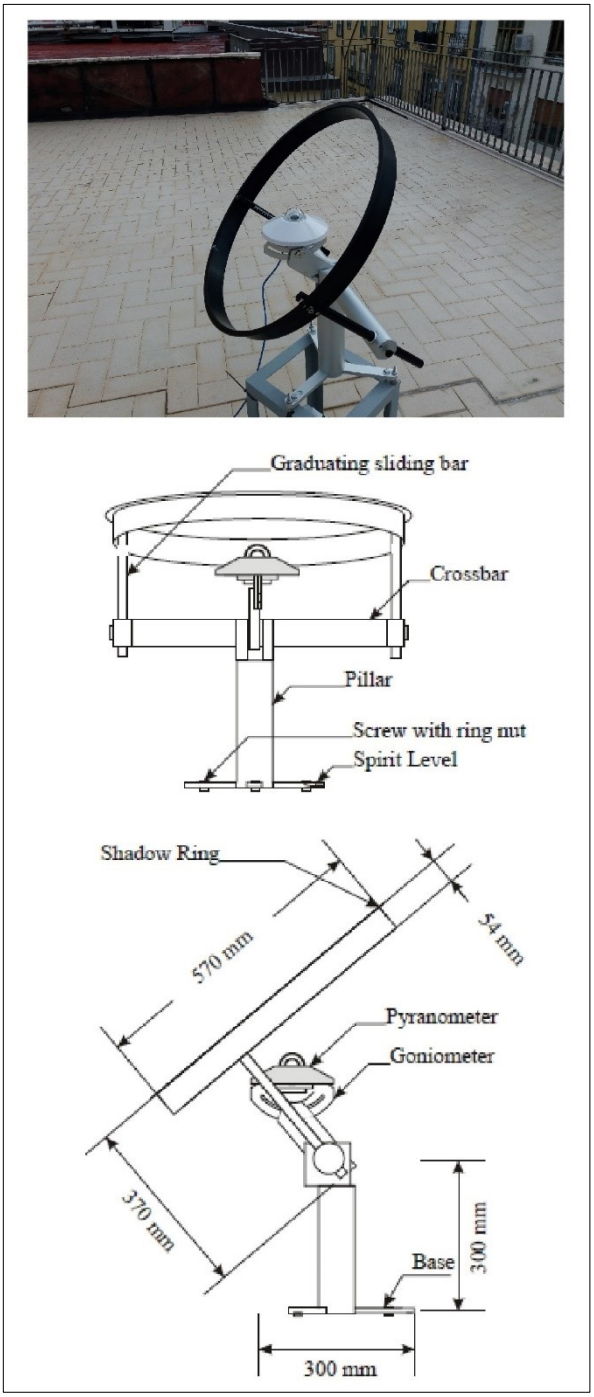

Figure IV. 4: Photo and scheme of the Pyranometer measuring diffuse irradiance

The shadow ring position depends on the location latitude and the sun declination, so it must be periodically adjusted by means of the sliding bars. The proper bars length is provided by the manufacturer, together with the so-called correction factor C. Indeed, the shadow ring intercepts not only the direct radiation, but also a part of the diffuse one, so $E_{E,sky}$ must be evaluated as the product of the measured irradiance $E_{E,sky,measured}$ and C.

$$E_{E,sky} = E_{E,sky,measured} \cdot C \qquad [W/m^2] \qquad (IV.1)$$

Table IV.2 reports sliding bars length and C factor values referred to Naples according to manufactures prescriptions.

Table IV. 2: Sliding bars length and C correction factor referred to Naples

Sun Declination	Bars length [mm]	C Factor
-23	101	1.04
-22	96	1.04
-20	87	1.05
-18	77	1.05
-16	68	1.06
-14	58	1.06
-12	49	1.07
-10	39	1.08
-8	29	1.08
-6	19	1.08
-4	10	1.09
-2	0	1.10
0	10	1.10
+2	20	1.10
+4	30	1.11
+6	39	1.11
+8	49	1.12
+10	59	1.12
+12	69	1.12
+14	78	1.12
+16	88	1.12
+18	97	1.12
+20	107	1.12
+22	116	1.12
+23	121	1.12

Both pyranometers are characterized by the following characteristics: measurement range equal to 0-2000 W/m^2, spectral range equal to 0.3μm to 3μm and field of view equal to 2π sr.

The outdoor illuminance meter (OL_P in Figure IV.1) detects horizontal illuminances and it is secured to the terrace floor. It is a Nesa one [98] and is characterized by a measurement range equal to 0 lx-200000 lx, spectral range corrected according to the V(λ) and a field of view equal to 2πsr.

The 4 illuminance meters installed inside the room (W1, W2, W3 and CL_P) have the same characteristics of that installed outside, except for the measurement range, that is equal to 0 lx-20000 lx.

Table IV. 3: List of the analysis days

Façade configuration	Winter analysis days	Spring analysis days
SOFW	08/12/2017	14/04/2018
	09/12/2017	15/04/2018
	10/12/2017	15/05/2018
	11/12/2017	29/05/2018
	19/12/2017	30/05/2018
	20/12/2017	31/05/2018
SOSW	13/12/2017	17/05/2018
	14/12/2017	18/05/2018
	15/12/2017	19/05/2018
	16/12/2017	20/05/2018
	17/12/2017	26/05/2018
	18/12/2017	37/05/2018
WOFW	22/12/2017	08/06/2017
	23/12/2017	09/06/2017
	24/12/2017	10/06/2017
	25/12/2017	11/06/2017
	26/12/2017	17/06/2017
	27/12/2017	18/06/2017
WOSW	09/01/2018	20/04/2018
	10/01/2018	21/04/2018
	11/01/2018	22/04/2018
	12/01/2018	23/04/2018
	13/01/2018	07/06/2018
	14/01/2018	08/06/2018

Measurements were performed in different periods: during June 2017, from December 2017 to January 2018, from April 2018 to June 2018. This allowed obtaining data referred to both winter and spring, for each façade configuration. Then, 6 analysis days were extracted from the

database for each façade configuration and each season. They are listed in Table IV.3.

IV.3. Luminaires characteristics

As it was previously mentioned, the office lighting system is obsolete, so a new LED system was designed. For this purpose, recessed LED luminaires suitable for office applications and characterized by crystal optic for glare control optimization were chosen (photometry in Figure IV.5).

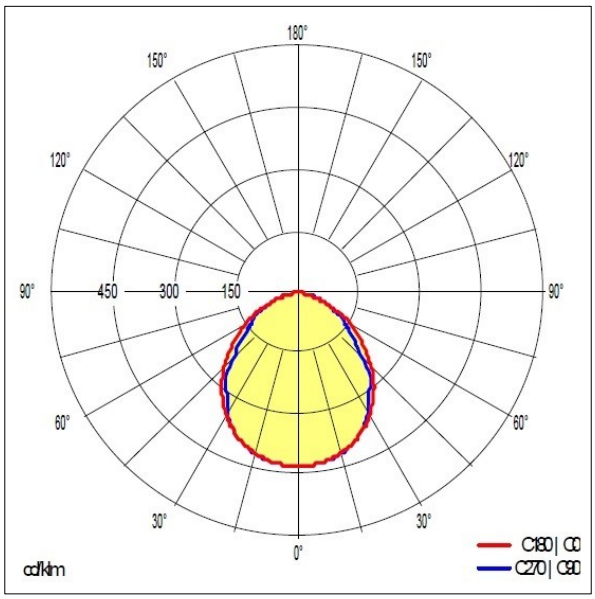

Figure IV. 5: Luminaire photometry

The luminaires characteristics certified by the manufacturer are reported in Table IV.4, but they were tested in the Photometry and Lighting Laboratory of the Department of Industrial Engineering of the University of Naples.

Table IV. 4: Luminaires technical characteristics certified by the manufacturer

Luminous flux	4280 lm
Power	51 W
Stand-by power	0.3 W
Colour Rendering Index (CRI)	>80
Correlated Colour Temperature (CCT)	Varying from 3000 K to 6000 K according to white-tuning technology

The laboratory is an L-shaped environment that can be divided in two different square zones (see Figure IV.6).

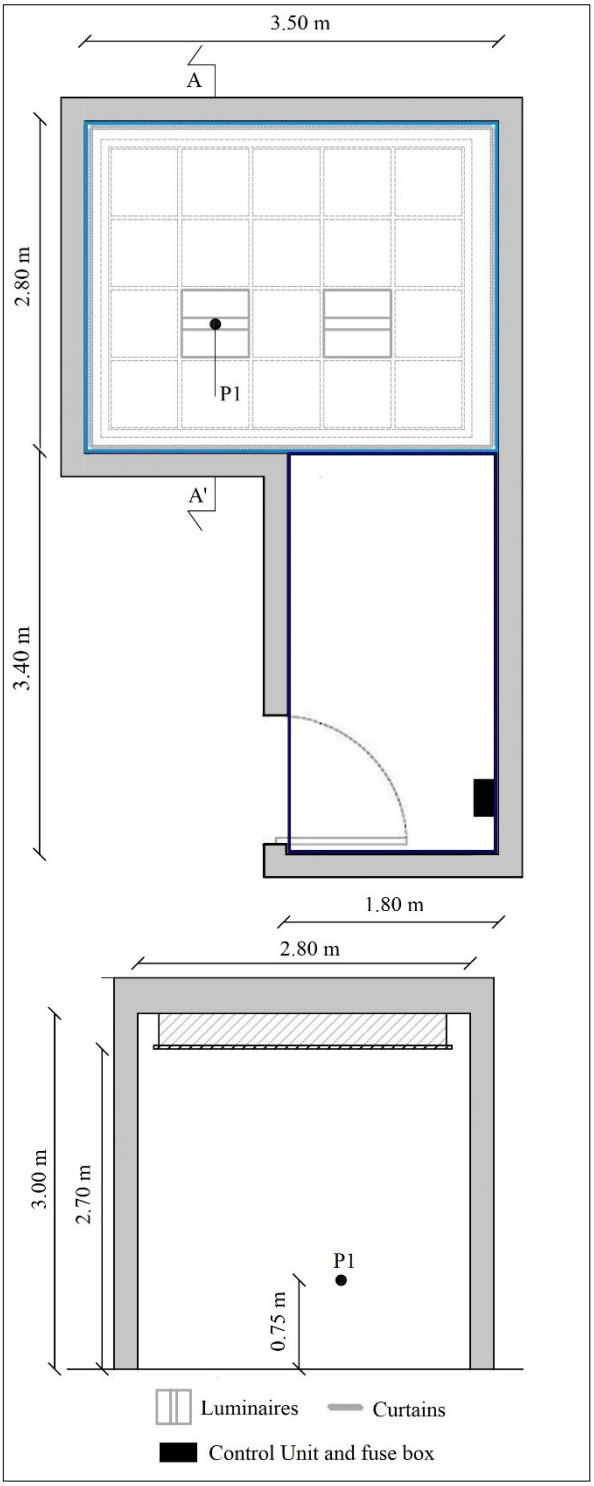

Figure IV. 6: Laboratory plan and A-A' section

In the former zone (highlighted by light blue profile in Figure IV.6) there is a false ceiling where different light sources were installed, among which the LED in question. In the latter zone (highlighted by dark blue profile in Figure IV.6) there is the DALI control unit managing the light sources and the fuse box connected to an electronic power meter. The two zones can be isolated one from each other by means of a white

curtain. Other three curtains of the same material cover the perimeter walls of the former zone (highlighted by light blue profile in Figure IV.6) to make neutral the environment.

As it is reported in Table IV.4 the analysed luminaire CCT can be varied from 3000 K to 6000 K. For this application a 4000 K CCT was considered. So, by means of the control unit, one of the two luminaires was set at 100% light output and at 4000 K CCT, the other was switched off and then measurements were performed.

Spectral power distribution was measured with a Konica Minolta CL-500 A spectroradiometer (see Figure IV.7). The corresponding CCT and CRI values are 4035 K and 86 respectively.

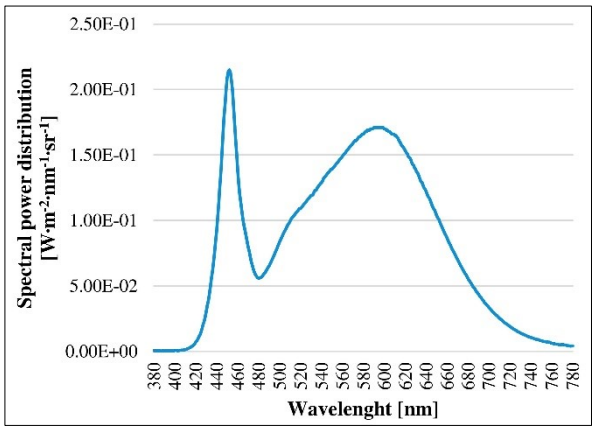

Figure IV. 7: Luminaire spectral power distribution

Moreover, the relationship between the light output set by the control unit $\delta_{c.u.}$ and the work-plane electric light illuminance E_{el} was studied in the test-room.

According to the touch panel of the control unit, the light output can be varied from a minimum value equal to 1% ($\delta_{c.u.min}$) to a maximum value ($\delta_{c.u.max}$) equal to 100%. Illuminance was measured at a distance from the floor equal to 0.75 m at a point corresponding to the projection at the work-plane of the luminaire barycentre (P1 in Figure IV.6) by means of a T10A Konica Minolta illuminance meter. Measurements were performed corresponding to $\delta_{c.u.min}$ and $\delta_{c.u.max}$ and, between these two limit values, for 5% $\delta_{c.u.}$ steps. Moreover, referring to the same light output steps, absorbed power P was measured as well.

Results are reported in Figure IV.8 and IV.9.

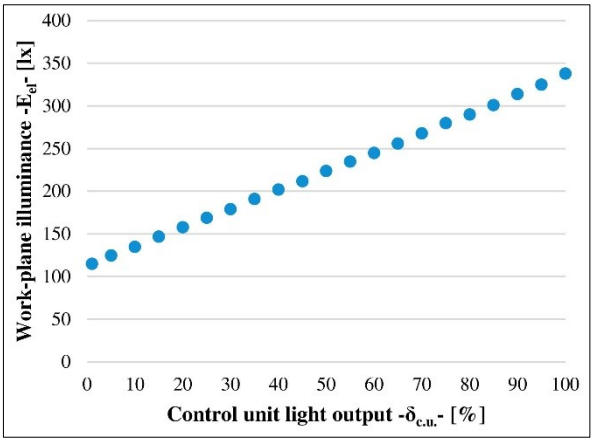

Figure IV. 8: Control unit light output vs Work-plane illuminance

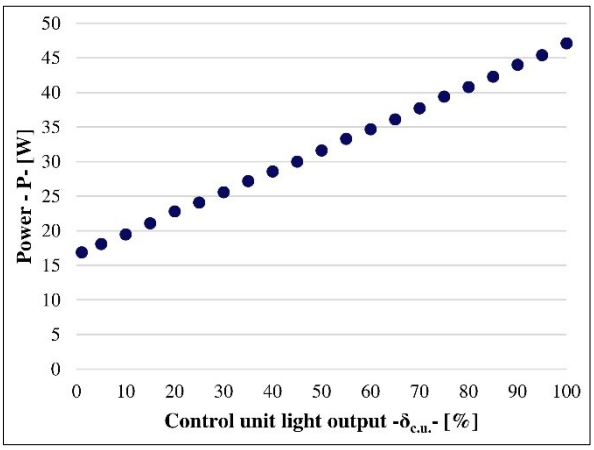

Figure IV. 9: Control unit light output vs Power

The relationship between light output and work-plane illuminance is linear. The illuminance corresponding to $\delta_{c.u.min}$ is equal to 115 lx and that corresponding to $\delta_{c.u.max}$ is equal to 338 lx. This means that, actually, the luminaire can be dimmed down at most at 34% of the total luminous flux. What does this imply from a practical point of view? A simple example can be useful to understand this issue. If an open-loop dimming system must be calibrated (see Figure II.4) the procedure is the following. Daylight illuminance is measured at the work-plane: let us assume that it is equal to 100 lx and that the required task illuminance is equal to 300 lx. According to the performed measurements the remaining 200 lx, necessary to fulfil requirements, can be obtained by means of a light output $\delta_{c.u.}$ equal to 28.6%. This value is very different from the percentage ratio of 200 lx (the electric light requirement) to 338 lx (the maximum produced illuminance) that would be equal to about 59.2%.

In DET the light output δ is always expressed as percentage of the maximum work-plane

illuminance determined by luminaires. This makes the evaluation easier if the system must be simulated during design stage, when it is not possible to verify luminaires characteristics in the field.

The relationship between $\delta_{c.u.}$ and P is linear as well. The measured power is equal to 16.9 W and 47.1 W corresponding to $\delta_{c.u.min}$ and $\delta_{c.u.max}$ values respectively.

Table IV.5 resumes the minimum and maximum values registered, referred to $\delta_{c.u.}$, E_{el}, P and reports the light output δ as calculated in DET.

Table IV. 5: Luminaire measured characteristics

$\delta_{c.u.}$ [%]	E_{el} [lx]	P [W]	δ [%]
1%	115	16.9	34%
100%	338	47.1	100%

Considering DET light output definition, the analysed luminaire can be regulated from a δ_{max} value equal to 100% to a δ_{min} value equal to 34%. Moreover, it can be observed that when the luminous flux is equal to 34% of the total one, the absorbed power is equal to 36% of the power absorbed when the luminaire is on at full capacity

Finally, it was verified that when the luminaire is in stand-by the corresponding power is equal to 0.2 W.

IV.4. Lighting system design

DIALux software was used to design a lighting system equipped with luminaires described in the previous paragraph in the room were daylight measurements were performed (see Figure IV.I and IV.2). The office is generally used for architecture students tutoring and the related visual task according standards [73] is “technical drawing”. For this activity an average illuminance value equal to 750 lx and a uniformity value of 0.7 are prescribed.

To fulfil these requirements, considering a maintenance factor equal to 0.8, four luminaires arranged in two rows are necessary. Figure IV.10 report illuminance iso-lines referred to a calculation surface located at the work-plane height (distance from the floor equal to 0.75 m), with sides distant from the room perimeter walls 0.50 m.

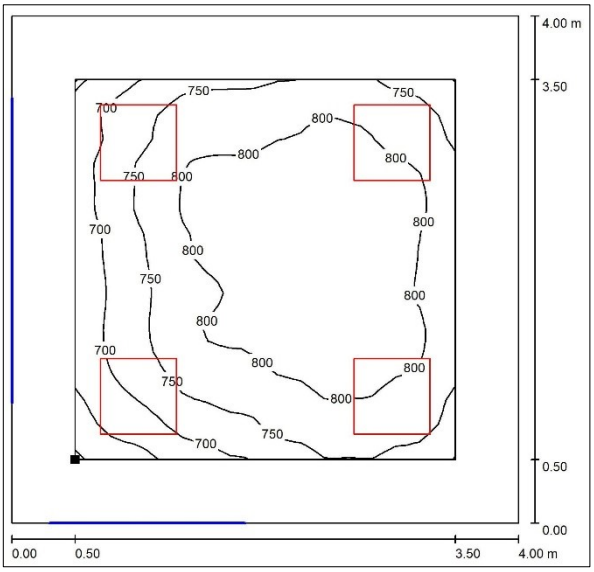

Figure IV. 10:Illuminance iso-lines

The luminaires so arranged determine at the calculation surface an average illuminance equal to 771 lx and a uniformity value equal to 0.78. Considering in detail the desk surface, the average illuminance is equal to 778 lx and the related uniformity 0.85.

DIALux was used to calculate the electric light illuminance at the closed-loop photosensor as well: it is equal to 284 lx.

IV.5. Definition of the calculation parameters to set in DET

According to what was explained in section III, DET needs three different typologies of data to function:

- Daylight data referred to work-plane illuminances and photosensor signals over time -$\bar{E}_{dl}(t)$ and $S_{dl}(t)$-;
- Data referred to the lighting system;
- Calibration data, different depending on the considered control algorithm.

As for daylight data they were acquired by means of field measurements. Specifically, it was assumed that at each time t, $\bar{E}_{dl,t}$ coincides with the average value of illuminances measured at W1, W2 and W3 (see Figure IV.1), whereas $S_{dl,t}$ coincides with the illuminance measured at CL_P and OL_P (see Figure IV.1) for the closed-loop and the open-loop photosensor respectively. For

this reason, it is considered that photosensor signal unit of measurement is lx.

From the analysis of measured data, it was verified that sometimes indoor daylight levels turned out to be too high, so they could create discomfort. As it was previously mentioned, according to the UDI definition [71], a comfort illuminance range exists. Daylight illuminances comprised in this range are considered neither too high nor too low, but adequate to perform office visual tasks. Based on this premise, and considering the definition of the UDI given in [76], it was assumed that discomfort risks occur if daylight illuminances are higher than 3000 lx.

Table IV. 6: Time ranges during which shading device is active

Façade conf.	Season	Day	Time range	Minutes shading is active
SOFW	Winter	08/12	13:17-13:46 13:48-15:17	120
		09/12	12:46-13/15 13:35-14:04	60
		10/12	13:51-14:20 14:24-14:53	60
		11/12	13:46-14:15	30
		19/12	13:31-15:30	120
		20/12	13.34-14:03 14:17-14:46	60
SOSW	Winter	17/12	13:30-15:29	30
		18/12	13:30-14:29 14:35-15:04	90
WOFW	Spring	08/06	17:47-18:00	14
		09/06	17:48-18:00	13
		10/06	17:47-18:00	14
		11/06	17:50-18:00	11
		18/06	17:51-18:00	10
WOSW	Spring	20/04	17:00-17:30 17:32-18:00	59
		21/04	17:02-18:00	59
		22/04	17:02-18:00	59
		23/04	17:03-18:00	58
		07/06	17:54-18:00	7
		08/06	17:32-18:00	29

It was supposed that when illuminance levels are higher than 3000 lx, users activate a shading device and leave it closed for 30 minutes, then daylight levels are checked again, and the shading is opened or closed according to illuminance values. When the shading device is active, measured value of daylight illuminance and photosensor signal are substituted with the 0 value, so that DET considers that luminaires must be turned on at the full capacity, irrespective of the adopted control strategy. The time ranges during which shading device is active are indicated in Table IV.6.

Table IV. 7: DET lighting system parameters

Parameter	Symbol	Value	Source
Minimum light output for dimming system	δ_{min}	34%	Laboratory measures
Maximum light output for dimming system	δ_{max}	80%	It depends on the assumed maintenance factor
Electric light photosensor signal when luminaires are on at full capacity	$S_{el,100\%}$	355 lx	Calculated by means of DIALux
Electric light photosensor signal when luminaires are on at δ_{max}	$S_{el,\delta max}$	284 lx	Calculated by means of DIALux
Electric light illuminance when luminaires are on at full capacity	$\bar{E}_{el,100\%}$	973 lx	Calculated by means of DIALux
Electric light illuminance when luminaires are on at δ_{max}	$\bar{E}_{el,\delta max}$	778 lx	Calculated by means of DIALux
Power absorbed when luminaires are on at full capacity	$P_{100\%}$	188.4 W	Laboratory measures
Power absorbed when luminaires are on at δ_{min}	$P_{\delta min}$	67.6 W	Laboratory measures
Luminaires stand-by power	$P_{stand-by}$	0.8 W	Laboratory measures
Power absorbed by auxiliary components (controller plus photosensor)	P_{other}	3 W	Previous study [28]

Table IV.7 reports data referred to the lighting system. In the last column it is specified how the information is obtained. As it can be inferred from the table, a light output maximum value δ_{max}

corresponding to 80% is indicated. For dimmable systems (stepped and dimming ones) it is considered to associate lumen maintenance control strategy to the daylight-based one. This means that, at the beginning of life cycle, it is possible to set a maximum light output lower than 100%, since the system is oversized due to the adoption of maintenance factors, used to prevent luminous flux decay during time. The possibility to reduce the luminaires flux emission at the beginning of the lighting system operating life is considered in the [86] as well. The strategy is defined Constant Light Output (CLO).

On the contrary, for switching systems, the maximum light output is necessarily equal to 100%. DLCSs performances were evaluated in DET considering that the lighting system is at the beginning of its life cycle. Consequently, it is assumed that the average electric light illuminance at the desk is equal to 973 lx and not to 778 lx. Analogously, $S_{el,100\%}$ is equal to 355 lx instead of 284 lx.

As for calibration parameters, they are different depending on the considered control system. A focus about this issue can be found in the Appendix.

For open-loop and closed-loop switching systems and closed-loop stepped systems dead-bands and partial dead-bands equal to 20% of the switching on signal are set according to [55].

Both for open-loop and closed-loop switching system a time delay equal to 30 min was considered according to [55].

Both for closed-loop and open-loop stepped systems, two different light output steps were considered: 80% and 40%, since the system cannot be dimmed under 34%.

Finally, for switching systems, dimming systems and open-loop stepped systems, the daylight photosensor signal at the calibration phase has to be defined. The following procedure was used to define it. For switching and stepped system, it was considered that calibration happens when daylight work-plane illuminance is equal to about the task-illuminance [11]. The data characterized by similar daylight conditions (daylight illuminance ranging from 750 lx to 780 lx) were extracted from the database. Then the average values of the corresponding photosensor signals were assumed to be the daylight photosensor signals at the calibration. For dimming systems, the procedure is similar, but the considered daylight condition is different. Daylight illuminances ranging from 300 lx to 330 lx were selected. Indeed in this case, to integrate daylight and fulfil regulation requirements, 450 lx-420 lx would be needed, corresponding to a light output equal about to 46%-43%, i.e. slightly higher than the minimum light output (34%) according to [11].

The procedure was repeated for each configuration, season and photosensor. Results are reported in Table IV.8.

Table IV. 8: Daylight Photosensor signals at calibration

Façade conf.	**Season**	**Photo-sensor**	**Signal for switching and stepped controls [lx]**	**Signal for dimming controls [lx]**
SOFW	Winter	OL_P	21771	8208
		CL_P	671	322
	Spring	OL_P	36182	12659
		CL_P	841	320
SOSW	Winter	OL_P	53368	12264
		CL_P	765	297
	Spring	OL_P	80450	32175
		CL_P	1088	436
WOFW	Winter	OL_P	56059	30777
		CL_P	811	331
	Spring	OL_P	83311	107497
		CL_P	1047	364
WOSW	Winter	OL_P	49135	81102
		CL_P	553	370
	Spring	OL_P	68207	100131
		CL_P	867	324

It must be underlined that, both for daylight and electric light, photosensor illuminance is used instead of photosensor signal, since for measurements a common illuminance meter was used and in DIALux is not possible to simulate spectral and spatial response of photosensors.

V. Case study results

Following paragraphs report results referred to the case study. Specifically, the analysis is divided in two parts. In the former, results of daylight measurements will be commented, in the latter, data referred to the performance of simulated control systems will be shown and discussed.

V.1. Daylight measurements results

Figures from V.2 to V.9 report results of the daylight measurements referred to each façade configuration. The first four (V.2-V.5) are related to the winter and the others (V.6-V.9) to the spring. Three different graphs are reported in each figure. The first one (indicated with the *a* letter) represents the sky ratio values, that are useful to define the weather conditions. According to [99] the sky ratio can be calculated as:

$$SR = \frac{E_{E,sky}}{E_{E,global}} \quad [W/m^2] \qquad (V.1)$$

Where $E_{E,sky}$ is the diffuse horizontal irradiance, and $E_{E,global}$ is the global horizontal irradiance. The sky can be classified as clear, when SR<=0.3, partly cloudy when 0.3<SR<0.8 and overcast when SR>=0.8. The second graph (indicated with the *b* letter) represents the outdoor horizontal illuminance, corresponding to the illuminance at the open-loop photosensor, OL_P. Finally, in the last graph (indicated with the *c* letter) indoor illuminances at the work-plane and at the CL_P photosensor are reported. It must be underlined that the vertical axis maximum value varies in order to make the data easier to read. Specifically, it is equal to 140000 lx for outdoor measurements, 3500 lx for indoor ones, and 14000 lx for indoor ones when the direct radiation hits the work-plane.

Let us start the analysis from the winter measurements referred to the two south oriented façade configurations. Considering SOFW (see Figure V.2-a), the first four monitored days are all mostly characterized by overcast sky conditions, whereas for the 5th day the sky ratios are generally lower than 0.3. Finally, during the last day, sky conditions are generally partly cloudy. Excluding the clear day, SR values are very fluctuating and never stable. Weather conditions of the measurement days referred to the SOSW configuration are the following (see Figure V.3-a): the first four days are really overcast and characterized by SR very high, whereas the last two days are almost clear and sky ratios are lower than 0.3, assuming an oscillating trend only between 14:00 and 15:00. Illuminance trends at OL_P give a clear idea of the outdoor daylight availability. The first thing that can be noticed is that, even if for both SOFW and SOSW the first four days are overcast, the sky cover conditions are very different. In the first case (SOFW) the illuminance trends are really fluctuating, reaching peaks of 100000 lx, i.e. values comparable to which characterizing clear days. On the contrary, for SOSW the SRs are so high and the clouds cover so thick, that outdoor illuminance levels are often lower than 10000 (see 13/01 and 15/01 in V.3-b Figure). Observing the OL_P trends during clear days (19/12 in Figure V.2-b 17/12 and 18/12 in Figure V.3-b), it can be noticed that around 15:00 daylight availability suddenly decreases: due to the low solar altitude, the sun is shaded by the San Martino hill. It must be underlined that, given this reason, from 15:00 on, the sky ratios are not reliable since the measured $E_{E,sky}$ and $E_{E,global}$ assumes very similar values. Considering the work-plane illuminances and the SOFW configuration (Figure V.2-c), excluding the clear day, the trends are really oscillating, well matching the outdoor ones and ranging peaks higher than 12000 lx in the time range 13:30-15:00, due to the incidence of the direct radiation. As for SOSW (Figure V.3-c), work-plane illuminances are always lower than 2000 lx on the first four days and on the clear ones peaks higher than 120000 are observed in the time range 13:30-15:00 as well. Clear days allow daylight availability to be compared for the two façade configurations. Indeed 19/12 outdoor illuminance trend (Figure V.2-b) is really similar to those characterizing 17/12 and 18/12 (Figure V.3-b). The corresponding work-plane illuminances are comparable as well. It can be observed that at noon, when outdoor illuminances are around

100000 lx, indoor work-plane illuminance is equal to about 2000 lx in SOFW (Figure V.2-c) and to 1800 lx in SOSW (Figure V.3-c). So, the glazing area reduction does not determine a brusque reduction of indoor daylight availability. Regarding CL_P photosensor (Figures V.2-c and V.3-c), for both configurations, illuminance trends are really fluctuating as well. Obviously, the sensor is never hit by direct radiation, so in the time range 13:30-15:00, its illuminance values are generally really lower than work-plane ones. The ratio of the work-plane illuminance to the CL_P illuminance is not stable. Sometimes CL_P illuminances are higher than work-plane ones, sometimes they are lower. It must be noticed that, when sky is clear, but the direct radiation does not hit the work-plane, CL_P illuminances are very high, compared to the work-plane ones. This is probably due to the fact that the CL_P sees a portion of the floor, reached by direct radiations and consequently characterized by very high luminance values.

The sky ratios evaluation related to winter measurements and west orientation allows making the following observations. As for the WOFW (Figure V.4-a) the 1st and the 4th days are characterized by very fluctuating sky conditions with SR values ranging from 0.2 to 1. The 23/12 and the 24/12 are substantially clear days, even if SR is characterized by suddenly increases around 11:00, 12:00 and 15:00 on 23/12. Finally, on 26/12 and 27/12 sky is mostly overcast. Considering WOSW (Figure V.5-a), we can observe that only the 13/01 is a clear day, whereas 9/01 and 12/01 are overcast ones. On 10/01, 11/01 and 14/01 SR values oscillates a lot, assuming values generally corresponding to overcast and partly cloudy skies. Obviously as for OL_P illuminance trends, the same observations previously done are valid in this case as well, since measurements are performed close in time. On the other hand, indoor illuminance trends are completely different. It must be underlined that, given the west orientation, and the fact that the sun is covered by the hill from 15:00 on, exclusively diffuse daylight enters the room. This determines illuminance values to be really low (lower than 1000 lx) at both the work-plane and the photosensor, for both WOFW (see Figure V.4-c) and WOSW (see Figure V.5-c). However, the sudden and strong daylight fluctuations are perceivable in the room as well. The ratio of the work-plane illuminance to the photosensor signal is not constant and varies a lot over time. Moreover, also in this case, the glazed area reduction does not significantly reduce the indoor daylight availability (compare for example 24/12 in Figure V.4-c with 13/01 in Figure V.5-c).

Figures V.6 and V.7 are referred to spring measurements and SOFW and SOSW façade configurations. During measurements related to SOFW (see Figure V.6-a), weather conditions were really instable. On the first three days sky is predominantly overcast, but SR values are sometimes comprised in the range 0.6-0.8 corresponding to partly cloudy sky cover. The 4th day is characterized by fluctuating, but lower SR values, so the sky is predominantly partly cloudy, whereas during the last two days the sky is predominantly clear, with SR increases registered at the end of the 30/05 and at the beginning of the 31/05. As for SOSW (see Figure V.7-a), excluding the last day, during which SRs oscillate a lot, all the analysed day are mostly clear excepting for some partly cloudy small periods. Compared to winter measurements related to the same façade configurations it must be underlined that, thanks to the high solar altitude, direct radiation cannot reach the work-plane. Consequently, for both SOSW (see Figure V.6-c) and SOSW (see Figure V.7-c), daylight illuminances are often higher than the task one, but do not achieve the disturbing limit value of 3000 lx. Also for spring measurements, when the day is pretty clear, the CL_P illuminance trends is higher than the work-plane one.

Finally, as for spring measurements referred to west orientation, the weather conditions are the following. Both for WOFW (see Figure V.8-a) and WOSW (see Figure V.9-a) sky is mostly clear with some slight oscillations in SRs, assuming values corresponding to partly cloudy sky cover. The only one exception is the 07/06 (see Figure V.9-a), during which sky ratios are very fluctuating and assume values corresponding to overcast and partly cloudy skies. For these façade configurations, the work-plane illuminance assumes the following trends. In the first part of the day, they are generally comprised in the range 500 lx-1000 lx and start to decrease after 10:00 because the incidence of the radiation reflected from the frontal building is reduced. Then illuminances start to increase again around 14:00

and achieve very high levels with peaks until 14000 lx after 17:00, due to direct radiation incidence. The CL_P trend matches the work-plane one pretty well.

Daylight availability data are summarized in Figure V.1.

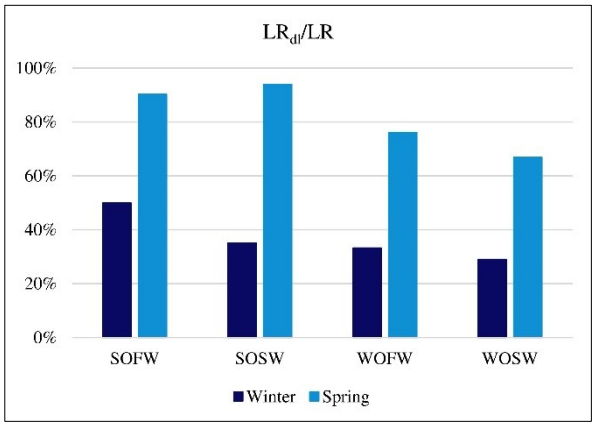

Figure V. 1: LR_{dl}/LR ratios referred to all configurations

It reports the ratio of the light requirement fulfilled by daylight, LR_{dl}, to the electric light requirement, LR. To obtain the graph, measured data were corrected according to Table IV.6, in order to account for the presence of an ideal shading system. As the previous analyses have demonstrated, the shading device is necessary exclusively during winter for south orientations between about 13:30 and 15:00, and during spring for west orientations after 17:00. As it can be inferred from Figure V.1, obviously in spring the daylight availability is higher than in winter. For example, considering SOSW, an ideal DLCS could satisfy the 93.96% of the electric light requirement. Moreover, generally the reduction of the glazed surface determines a slight reduction of the daylight availability as well. The entity of this reduction depends on the orientation and on the season. The only exception is observed in spring for the south orientation. Indeed, SOSW is characterized by a higher value of LR_{dl}/LR ratio than SOFW. This is due to the fact that, during measurements related to SOSW sky was predominantly clear (see Figure V.7-a). For west orientation, considering spring, the difference between WOFW and WOSW is due not only to the glazed area reduction, but also to the major use of the shading device (see Table IV.6). On the contrary, considering winter, the difference in LR_{dl}/LR ratio is not really significant. Finally, the 14.82% difference in LR_{dl}/LR ratio for south orientation in winter, is due to the fact that, even if for SOFW the operability range of the shading device is wider than SOSW (see Table IV.6), SOSW is characterized by worse sky conditions compared to SOFW (compare V.2-b and V.3-c).

To conclude the daylight analysis, the relationship between the photosensor signal and the work-plane illuminance for each configuration and photosensor during winter and spring was observed. Results are reported in Figures V.10 and V.11 analyse respectively. In each graph data are classified based on the sky typology (clear, overcast and partly cloudy). The analysis is limited exclusively to work-plane illuminances lower that the task-one, i.e. corresponding to the control operability range. R^2 values calculated considering all the three series together (clear, overcast and partly cloudy) are reported in Table V.1.

Table V. 1 : R^2 values calculated without differentiating data based on the sky typology

Season	Façade conf.	CL_P	OL_P
Winter	SOFW	0.89	0.77
	SOSW	0.88	0.78
	WOFW	0.93	0.72
	WOSW	0.88	0.59
Spring	SOFW	0.75	0.57
	SOSW	0.47	0.38
	WOFW	0.81	0.05
	WOSW	0.63	0.05

Considering winter, it can be observed that the CL_P maintains a good correlation with R^2 values always higher than 0.87. The reduction of the glazed area determines only slight R^2 reductions. As for the OL_P correlations are obviously worse, since the photosensor is outdoor located. However, excluding the WOSW (Figure V.10-h) R^2 is always higher than 0.7. A completely different situation can be observed for spring measurements. In this case R^2 values are very lower than those observed for winter and sometimes it is not possible to recognize any correlation. As for the CL_P the worst case is the SOSW (Figure V.11-b – R^2=0.47), whereas for the OL_P the best case is SOFW (Figure V.11-e), but the R^2 is low anyway (0.57).

Excluding the two south orientations in winter, for which it can be observed that most of the data correspond to overcast skies, for the other cases, it can be noticed that depending on weather conditions, data dispersion is different. For this reason, the correlations between photosensor signal and work-plane illuminance was studied, considering the three series of data in turn: clear, overcast and partly cloudy. For each series, the least squares straight line, describing data correlations, was identified by calculating the slope and the intercept, *m* and *q*. They are reported in Tables from V.2 to V.5. Even if some of the obtained results should be integrated, since the observed sample is not very huge, the tables underline that, depending on façade configuration and orientation, photosensor typology and sky conditions, the *m* and *q* obtained values are very different, demonstrating that the E_{dl}/S_{dl} ratio is very unstable.

To give an idea of the related effects on DLCSs functioning, a simple observation can be done. During its operating life, the photosensor estimates the work-plane illuminance based on the calibration ratio and then calculates the required electric light as a consequence of this evaluation.

Based on this premise, the work-plane illuminance corresponding to a photosensor signal equal to 300 lx was estimated considering that the relationship between the photosensor signal and the work-plane illuminance can be evaluated by using *m* and *q*. Then, based on the assessed illuminance, the corresponding electric light integration was evaluated as a percentage of the task illuminance (i.e. 750 lx). Results are reported in the last two columns of Tables from V.2 to V.5. Considering for example the case of WOSW in spring with the OL_P (see Table V.5), for which the quantity of clear, overcast and partly cloudy data is comparable (so the observed samples are more reliable), it can be noticed that, if the system is calibrated in clear, overcast o partly cloudy conditions, the work-plane illuminance estimated by the photosensor, when it detects a signal equal to 300 lx, would be 242 lx, 225 lx and 107 lx respectively. This means that the control would calculate that the needed electric light to integrate daylight would be 68%, 70% or 86% of the maximum flux. This obviously would determine different lighting conditions and different energy consumptions.

Table V. 2 : Effect of E_{dl}/S_{dl} variations on DLCSs functioning – CL_P Winter

Façade conf	Sky Condition	m	q	Estimated Work-Plane illuminance [lx]	Estimated needed electric light [%]
SOFW	Clear	1.35	-0.61	403	0.46
	Overc.	0.95	38.01	324	0.57
	Part. cl.	0.78	2.25	236	0.69
SOSW	Clear	0.88	-0.22	264	0.65
	Overc.	1.26	19.02	396	0.47
	Part. cl.	1.16	1.26	350	0.53
WOFW	Clear	0.70	6.69	217	0.71
	Overc.	0.96	23.62	311	0.59
	Part. cl.	0.69	72.39	279	0.63
WOSW	Clear	0.68	47.71	251	0.67
	Overc.	1.11	32.37	367	0.51
	Part. cl.	0.93	52.31	330	0.56

Table V. 3 : Effect of E_{dl}/S_{dl} variations on DLCSs functioning – OL_P Winter

Façade conf	Sky Condition	m	q	Estimated Work-Plane illuminance [lx]	Estimated needed electric light [%]
SOFW	Clear	0.07	0.17	20	0.97
	Overc.	0.03	90.71	99	0.87
	Part. cl.	0.02	4.66	11	0.99
SOSW	Clear	0.05	0.23	16	0.98
	Overc.	0.03	63.99	72	0.90
	Part. cl.	0.03	4.26	12	0.98
WOFW	Clear	0.00	165.79	167	0.78
	Overc.	0.01	114.18	116	0.85
	Part. cl.	0.00	240.51	242	0.68
WOSW	Clear	0.00	90.19	91	0.88
	Overc.	0.01	120.71	122	0.84
	Part. cl.	0.00	181.04	182	0.76

Table V. 4 : Effect of E_{dl}/S_{dl} variations on DLCSs functioning – CL_P Spring

Façade conf	Sky Condition	m	q	Estimated Work-Plane illuminance [lx]	Estimated needed electric light [%]
SOFW	Clear	0.15	558.79	602	0.20
	Overc.	0.85	95.16	350	0.53
	Part. cl.	0.58	207.51	382	0.49
SOSW	Clear	0.30	348.38	439	0.41
	Overc.	0.66	275.43	472	0.37
	Part. cl.	0.41	354.07	477	0.36
WOFW	Clear	0.54	156.08	317	0.58
	Overc.	1.05	3.95	319	0.57
	Part. cl.	0.83	13.87	262	0.65
WOSW	Clear	0.67	68.42	271	0.64
	Overc.	1.15	59.10	405	0.46
	Part. cl.	0.79	52.26	289	0.61

Table V. 5 : Effect of E_{dl}/S_{dl} variations on DLCSs functioning – OL_P Spring

Façade conf	Sky Condition	m	q	Estimated Work-Plane illuminance [lx]	Estimated needed electric light [%]
SOFW	Clear	0.00	638.29	639	0.15
	Overc.	0.02	150.81	156	0.79
	Part. cl.	0.01	281.33	285	0.62
SOSW	Clear	0.00	357.58	359	0.52
	Overc.	0.01	298.93	302	0.60
	Part. cl.	0.01	389.40	391	0.48
WOFW	Clear	0.00	642.25	642	0.14
	Overc.	0.01	36.60	41	0.95
	Part. cl.	0.01	101.40	103	0.86
WOSW	Clear	0.00	241.39	242	0.68
	Overc.	0.01	223.17	225	0.70
	Part. cl.	0.01	105.05	107	0.86

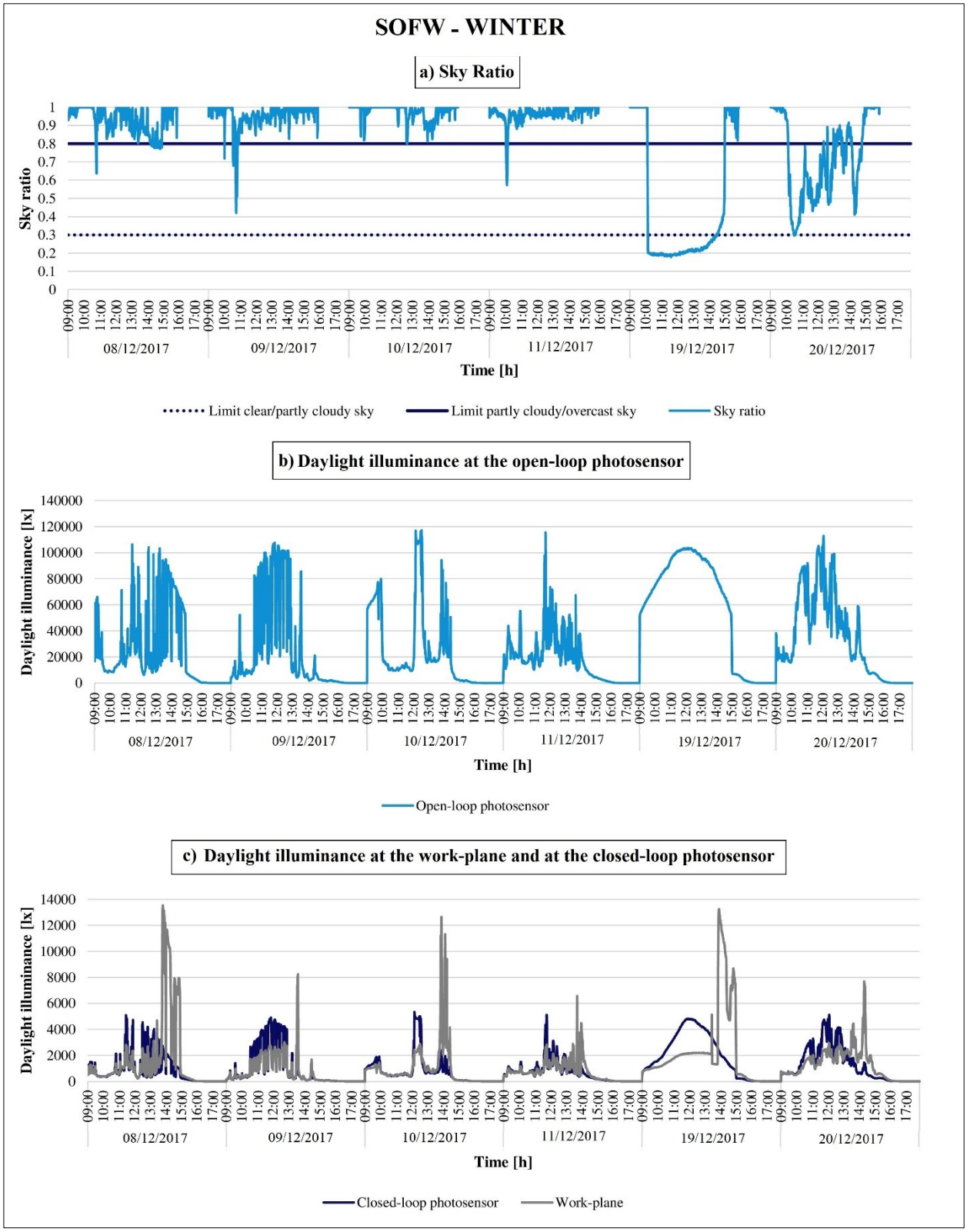

Figure V. 2: Winter daylight measurements referred to SOFW configuration

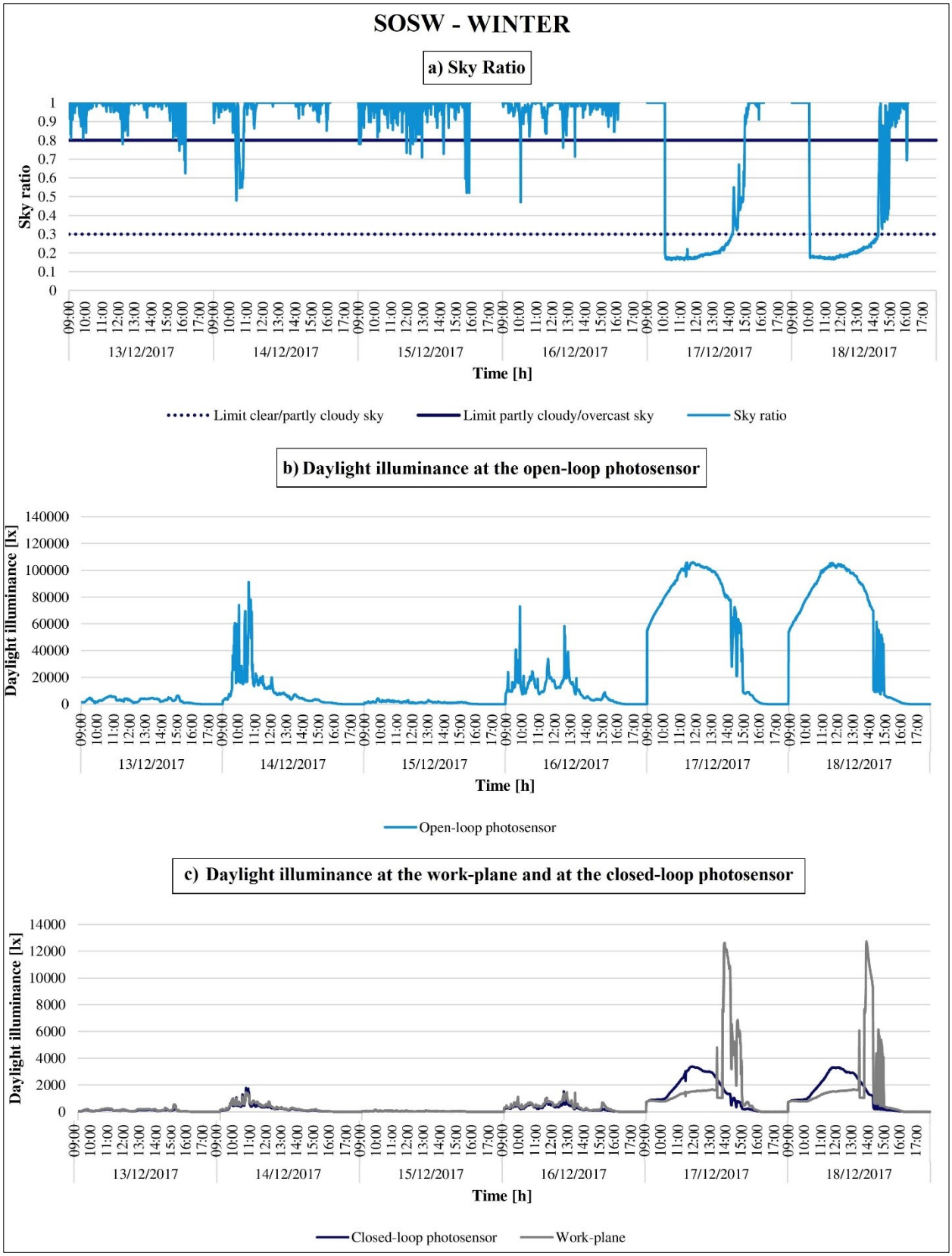

Figure V. 3: Winter daylight measurements referred to SOSW configuration

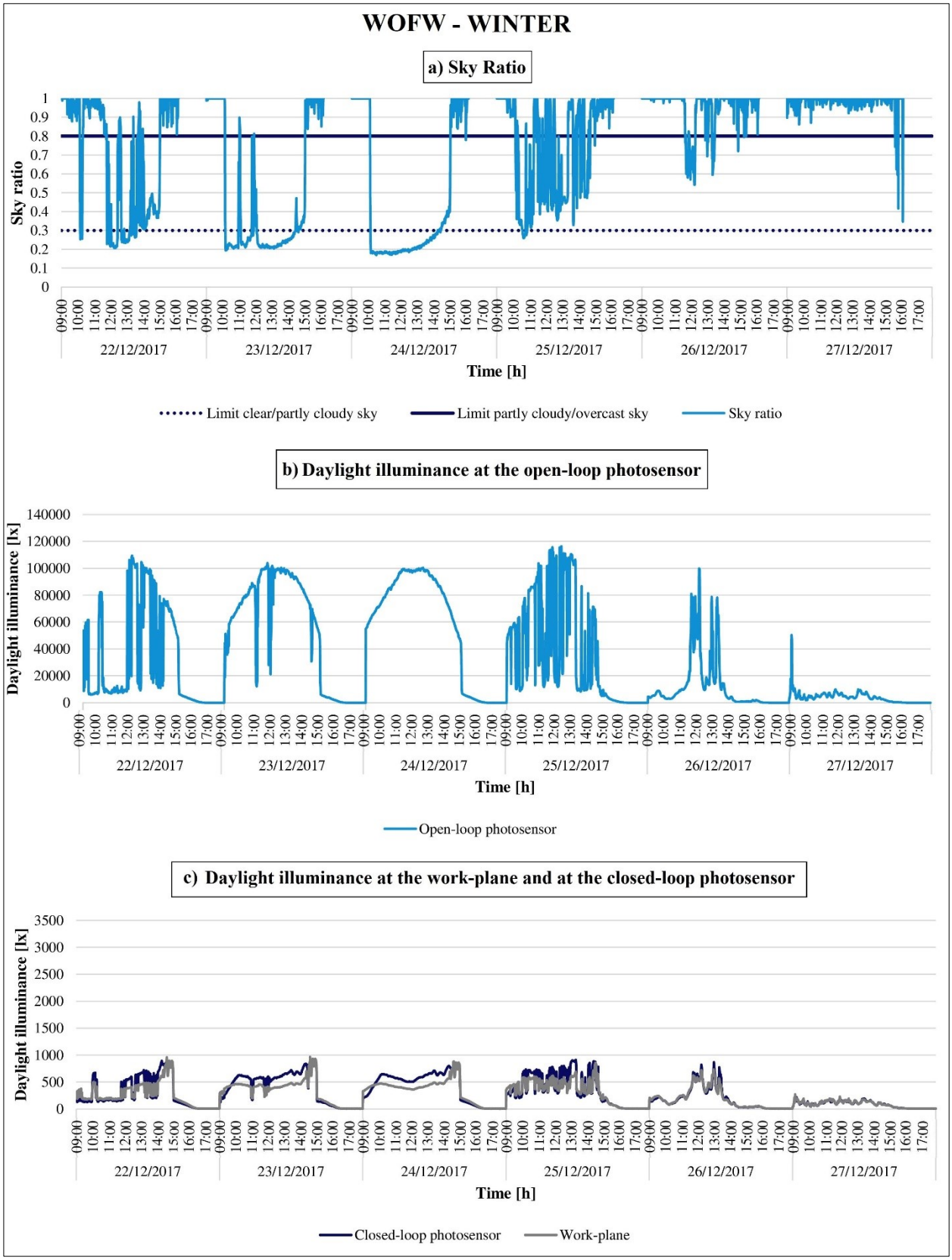

Figure V. 4: Winter daylight measurements referred to WOFW configuration

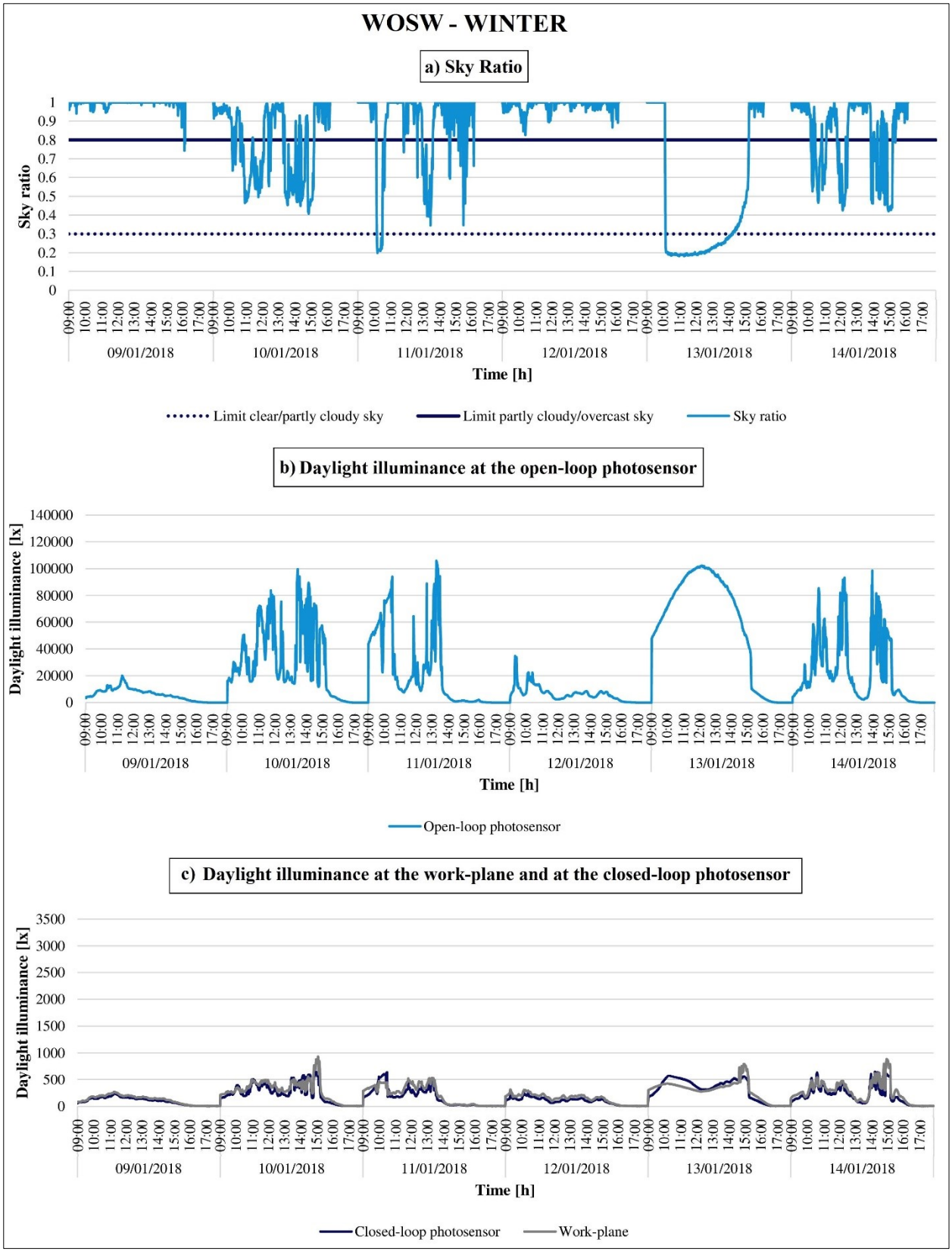

Figure V. 5: Winter daylight measurements referred to WOSW configuration

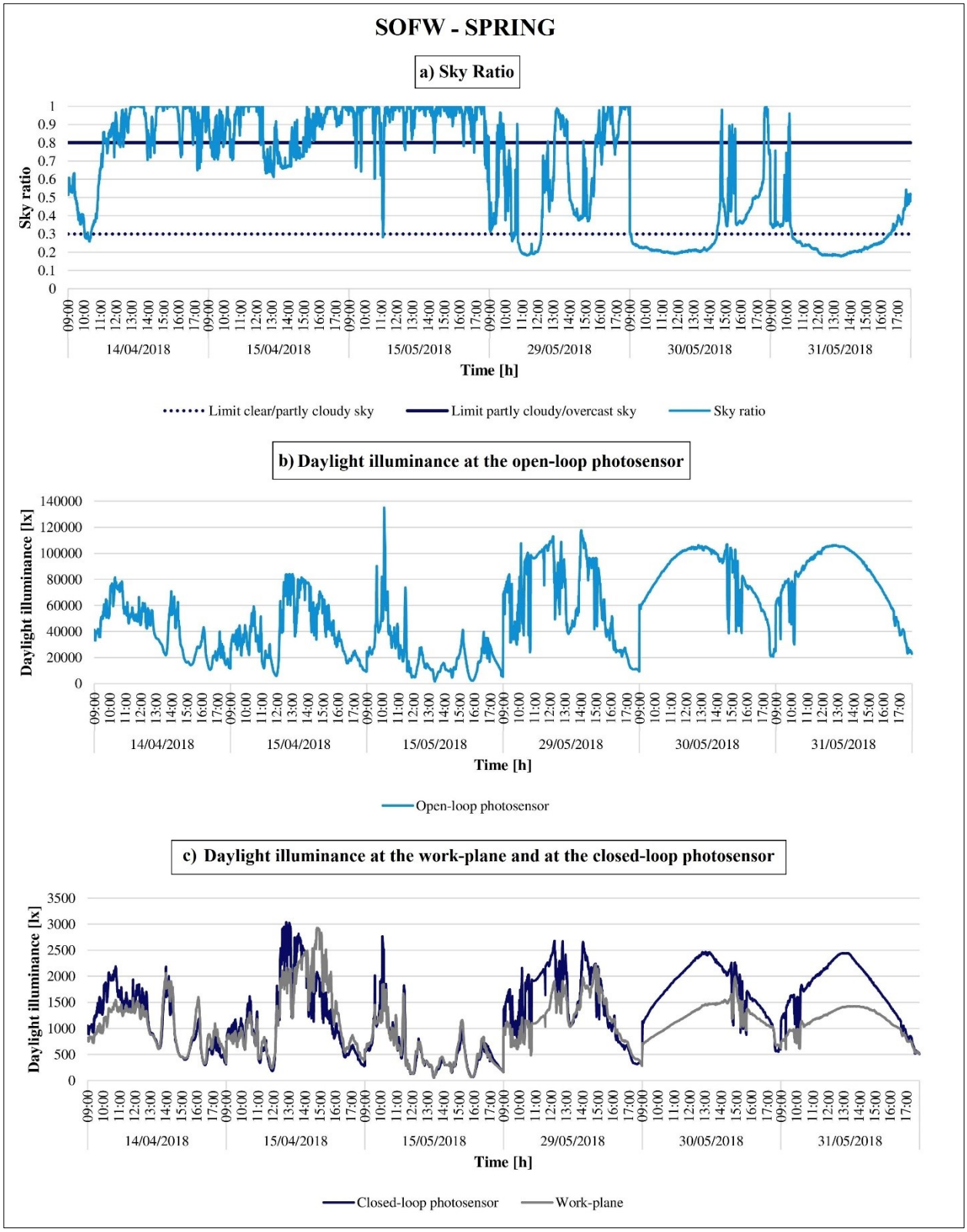

Figure V. 6: Spring daylight measurements referred to SOFW configuration

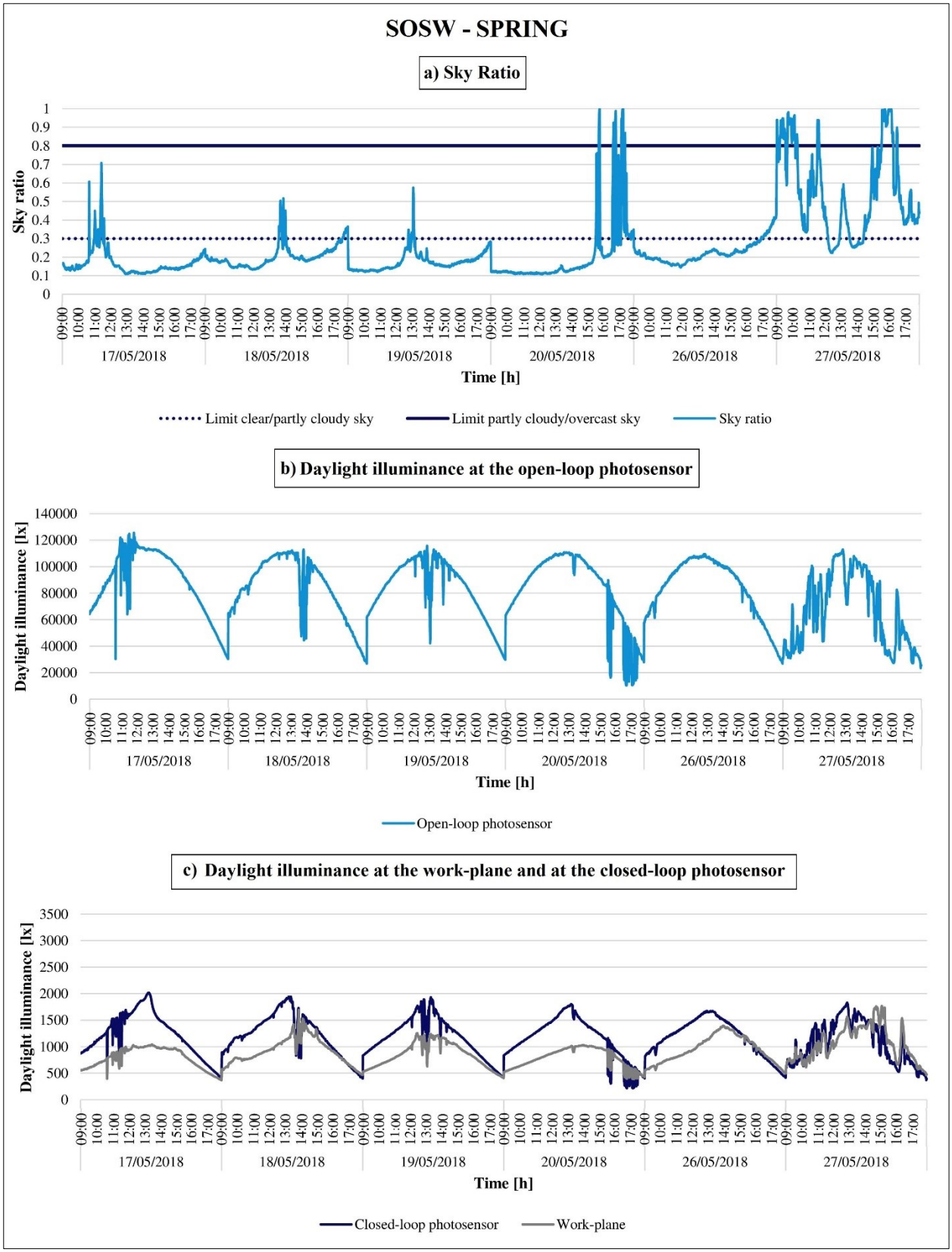

Figure V. 7: Spring daylight measurements referred to SOFW configuration

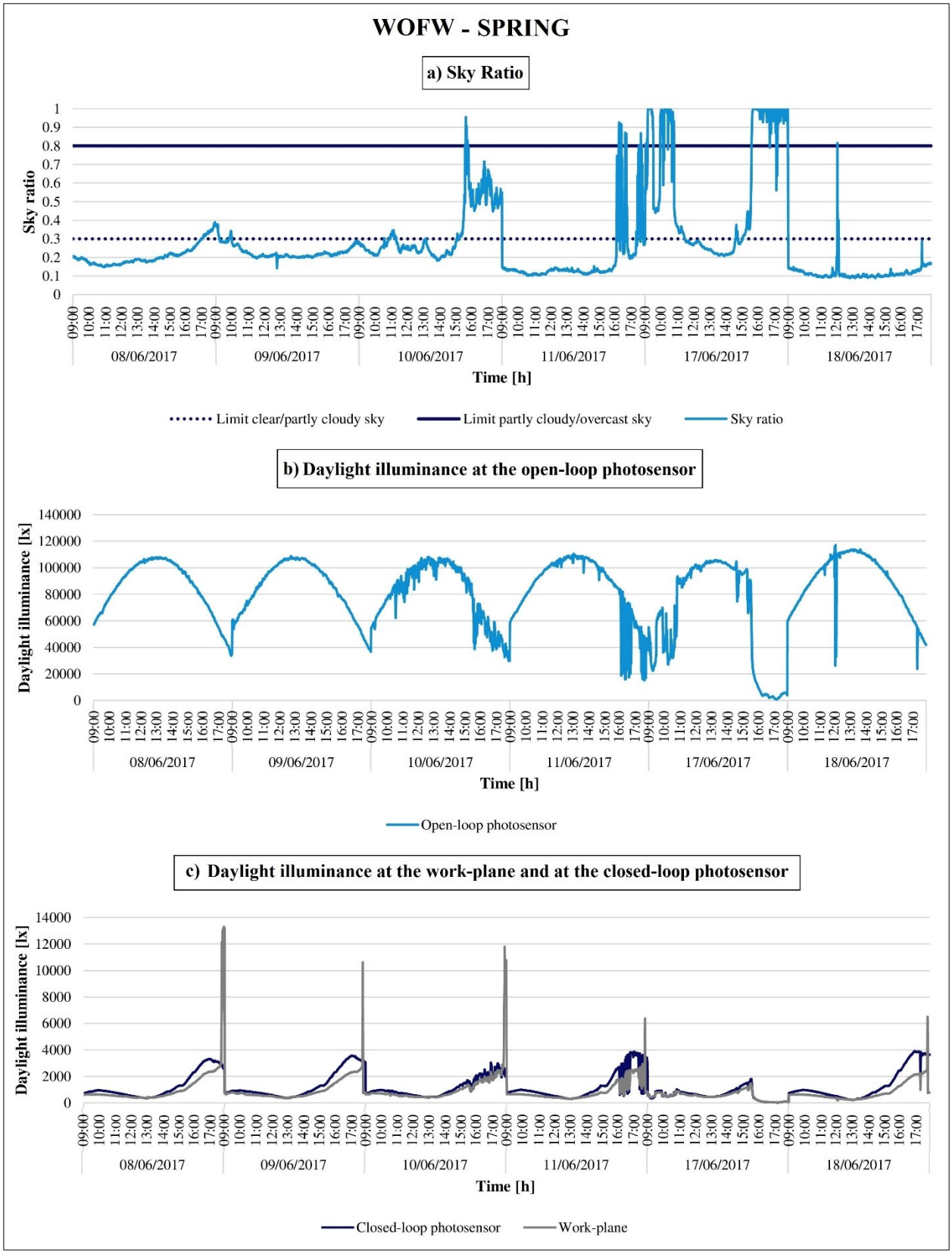

Figure V. 8: Spring daylight measurements referred to WOFW configuration

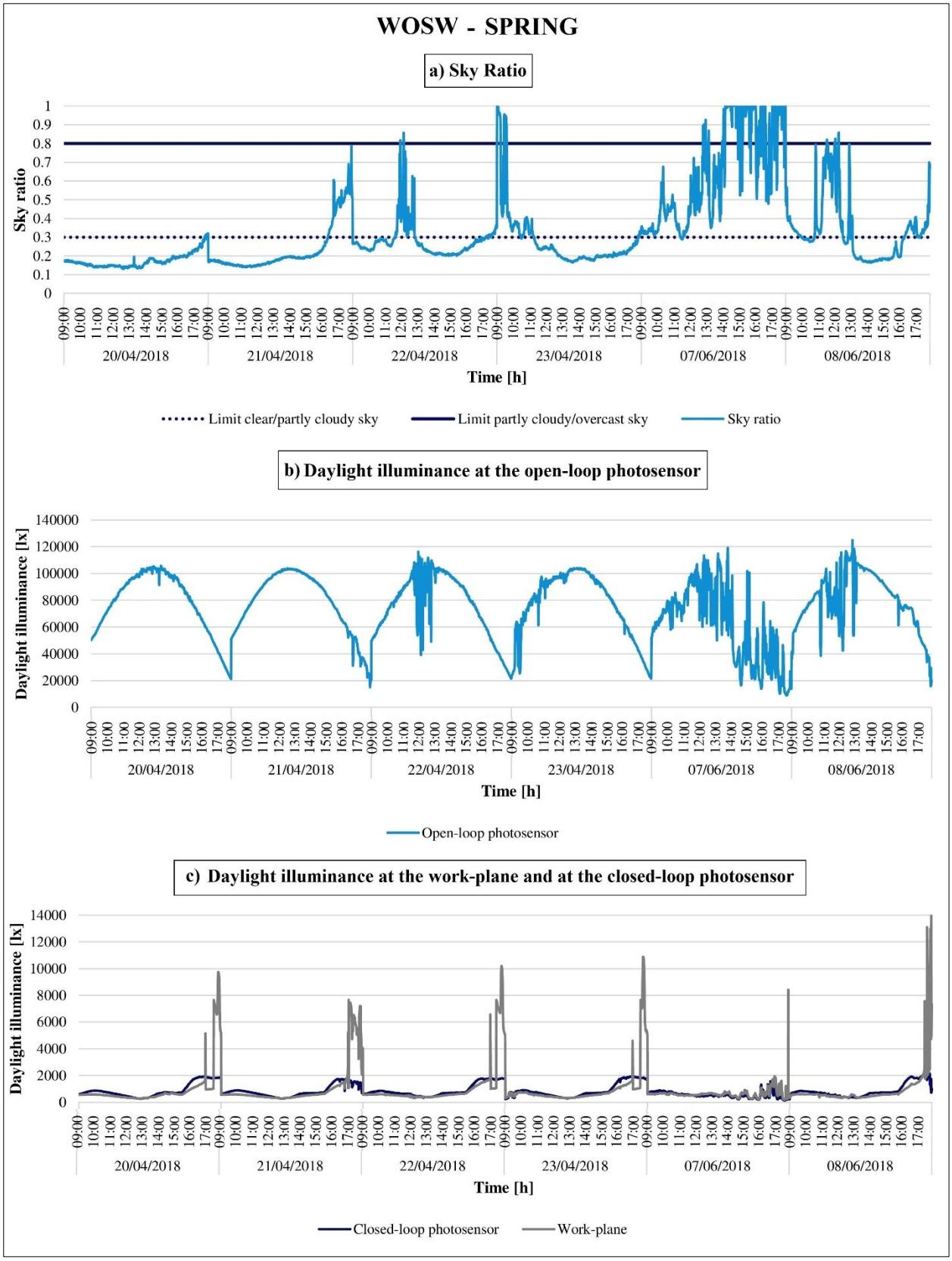

Figure V. 9: Spring daylight measurements referred to WOSW configuration

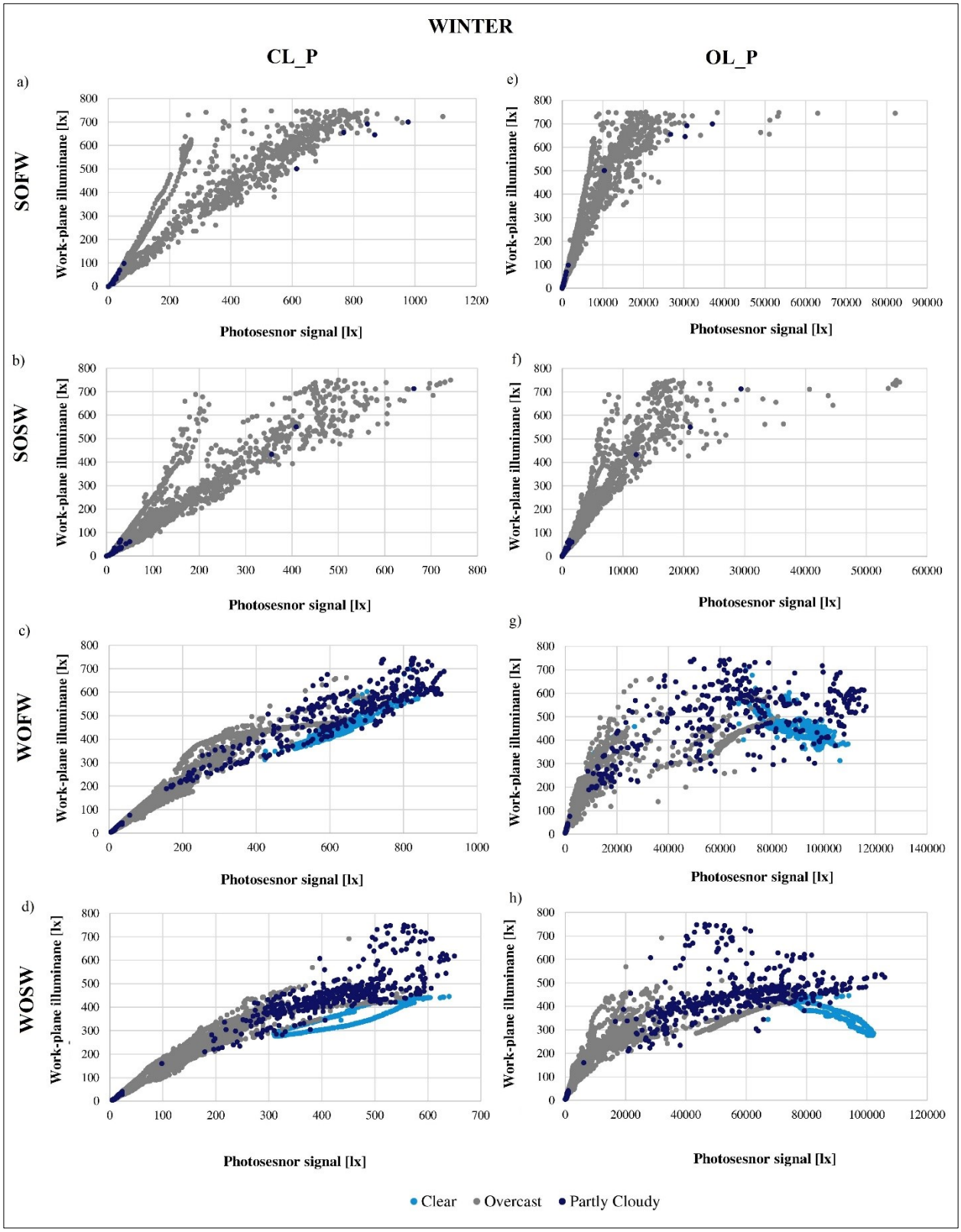

Figure V. 10: Winter relationship between work-plane illuminance and photosensor signal

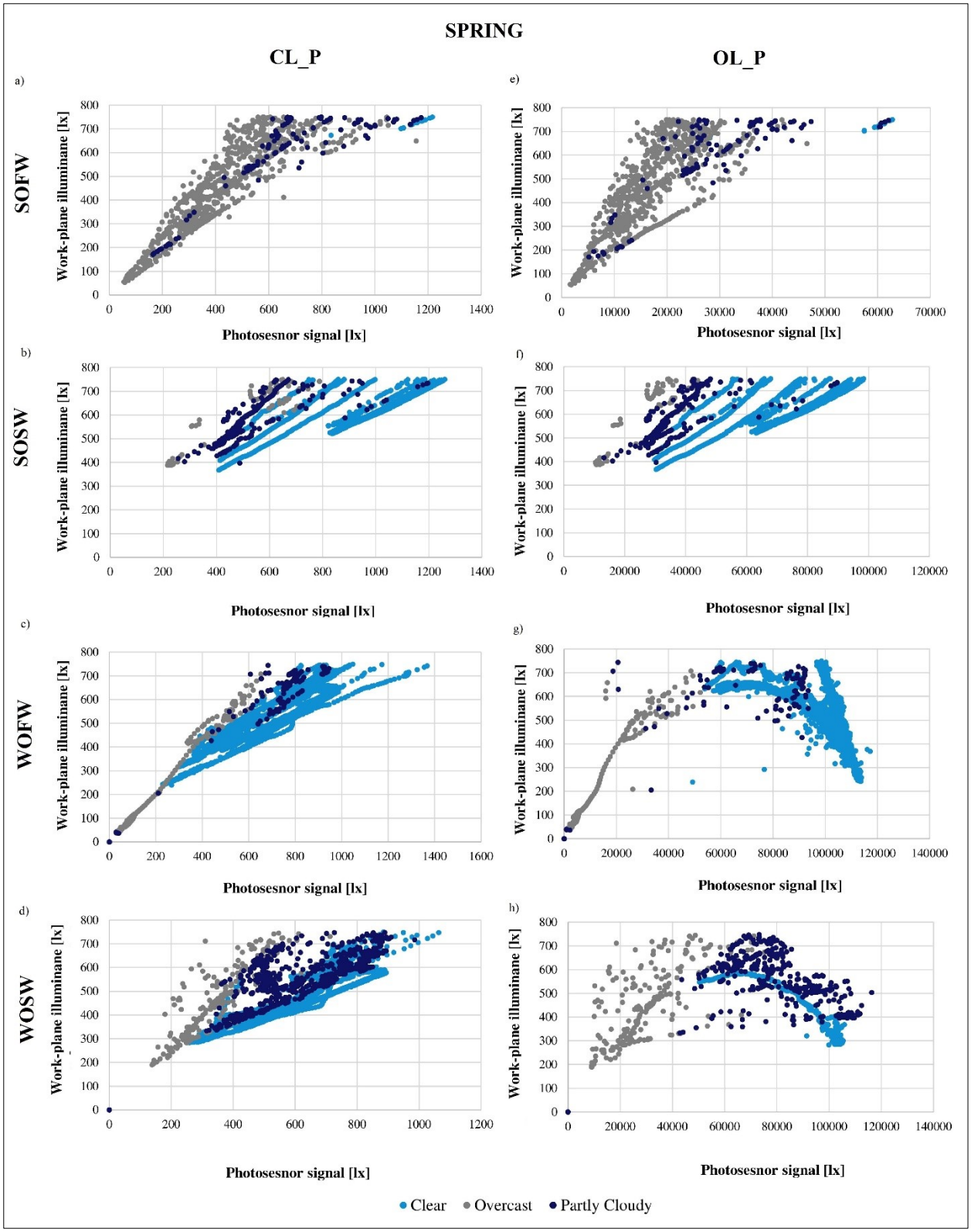

Figure V. 11: Spring relationship between work-plane illuminance and photosensor signal

V.2. DLCSs performances results

DET was used to simulate different DLCSs and evaluate their performances. Figures from V.12 to V.19 represent trends of $\delta(t)$ on the principal vertical axis and of the $\bar{E}_{tot}$(t) on the secondary vertical axis. Each figure reports results of all considered control strategies (open-loop and closed-loop switching, open-loop and closed-loop stepped and open-loop and closed-loop dimming) and is referred to a specific season and façade configuration. Based on the simulations, performance parameters were then calculated. They are represented in Figures from V.20 to V.23. Finally, Figure V.24 represents energy savings.

Let us start the analysis from switching systems, the functioning of which is represented in graphs indicated with the *a* letter (for open-loop systems) and *b* letter (for closed-loop ones) in Figures from V.12 to V.19. Referring to SOFW configuration, the daylight measurements analysis, highlighted that, excluding few days, weather conditions were substantially variable determining very fluctuating illuminance values at the photosensors (see Figures V.2 and V.6). The switching systems (both open-loop and closed-loop ones) turn luminaires on for most of the day during winter (see Figures V.12-a and V.12-b) and during the first three days in spring. On the contrary, during the last three days in spring, lights are always off, except for the last part of the evening (see Figures V.13-a and V.13-b). The instable weather conditions determine that the electric light is continuously turned on and off to match the daylight variations. During spring, the number of switching on and off actions is mostly the same for both open-loop and closed-loop photosensor (31 and 29 respectively- see Table V.I), whereas during winter, the closed-loop one performs worse from this point of view, determining most electric light fluctuations than the open-loop one (42 and 28 respectively -see Table V.1). It must be noticed that, thanks to the use of the time delay, switching off actions are never too brusque, since they occur after 30 minutes the lights are turned on. On the contrary, switching on actions can be sudden and can occur immediately after a switching off one. Considering SOSW, in winter sky was generally overcast and daylight availability scarce (see Figure V.3). As a consequence, the open-loop maintains luminaires always on (see Figure V.14-a). The closed-loop system functioning is similar except for few switching on and off actions occurring in the 2nd and 4th day (see Figure V.14-b). In spring, for both OL_P and CL_P, luminaires are generally on during the first and the last part of the day and off during the central one (see Figures V.15-a and V.15-b). The on and off actions are less frequent then the previously spring analysed cases. Looking at graphs related to west orientation (see Figures V.16-a, V.17-a, V.18-a and V.19-a), it is immediately clear that, irrespective of the season and façade configuration, the OL_P is not adequate to manage the luminaires control. This is due to the fact that, given the room orientation, outdoor illuminances and indoor ones have completely different trends.

Table V. 6: Number of on-off and off-on actions for each façade configurations and control system typology

Façade conf.	DLCS typology	Winter	Spring
SOFW	OL_P Switching	28	31
	CL_P Switching	42	29
	OL_P Stepped	148	109
	CL_P Stepped	32	17
SOSW	OL_P Switching	4	24
	CL_P Switching	10	26
	OL_P Stepped	39	104
	CL_P Stepped	13	2
WOFW	OL_P Switching	28	14
	CL_P Switching	0	18
	OL_P Stepped	162	92
	CL_P Stepped	29	14
WOSW	OL_P Switching	20	28
	CL_P Switching	0	16
	OL_P Stepped	144	117
	CL_P Stepped	12	25

This determines that often $\bar{E}_{tot}(t)$ is lower than $\bar{E}_{task}$ determining light deficit. This deficit sometimes is significant (about 400 lx – see for example 23/12 in Figure V16-a). On the contrary, the CL_P does not generate deficit (see Figures V.16-b, V.17-b, V.18-b and V.19-b). However, in winter, for both configurations (see Figures V.16-b and V.18-b) luminaires are on for the entire day. The performance analysis evaluation gives a synthetic evaluation of the switching systems

performances, confirming the observation made until now (see Figures from V.20 to V.23). For all the considered cases, switching systems operates in ILE conditions for most of the day. This is due to the fact that, even if daylight illuminances are slightly lower than regulations prescriptions, luminaires are fully on. Moreover, considering that the system is not dimmable, even when it is dark, and luminaires must be switched fully on, due to the oversizing of the lighting system for maintenance reasons, a significant ILE occurs. $ILE_{\%}$ ranges from 32.6% to 49.3% considering south orientations (see Figures V.20-c, V.20-d, V.21-c and V.21-d), whereas for west orientations it is always higher than 35.0%, reaching 79.8% for WOSW, in spring considering the CL_P (see Figures V.22-c, V.22-d, V.23-c and V.23-d). The fact that switching systems maintain high $\bar{E}_{tot}(t)$ levels, have the positive effect that, generally, deficit conditions do not occur or are completely negligible ($LD_{\%}$ around 1.0%). As it was previously revealed, the OL_P represents an exception in this sense when the window is west-oriented. For example, considering winter, it is possible to observe DIA^{-} values equal to 19.2% and 12.8% corresponding to $LD_{\%}$ equal to 7.5% and 6.2%, referred to WOFW and WOSW respectively (see Figures V.22-a, V.22-c, V.22-a and V.22-c). Generally, $LW_{\%}$ assumes low values in winter for all considered cases. Higher values were observed for spring: for example, it is equal to 25.4% considering OL_P and WOFW configuration (see Figure V.22-d). This was easily predictable considering that the correlation between the photosensor signal and the work-plane illuminance turned out to be not good see Figure (V.11-g). Looking at Figure V.24 the consequences in terms of energy saving can be understood. Considering SOFW configuration in spring, energy savings are equal to 19.3% and 23.6% considering OL_P and CL_P respectively (see Figure V.24-a). As for the SOSW, they are equal to 14.9% and 11.8%, depending on the photosensor (see Figure V.24-c). In spring, energy savings are much higher than in winter and, considering SOFW, they achieve values surely comparable with those referred to dimming systems. Specifically, for SOFW they are equal to 51.8% and 58.3% considering OL_P and CL_P respectively (see Figure V.24-b). As for SOSW, savings are about 40.0% for both photosensors (see Figure V.24-d). As for the west orientations, considering winter (see Figures V.24-e and V.24-g), energy savings are negative. This happens because luminaires are always on. In this situation, the energy due to auxiliary components (photosensors and controllers) determine consumptions higher than a standard lighting system, without automated control. In spring, the closed-loop photosensor determines savings equal to about 22.0% and 10.4%, considering WOFW and WOSW respectively (see Figures V.24-f and V.24-h). Energy savings related to OL_P are obviously not significant, since they are the results of a deficit functioning.

Let us consider the case of stepped systems. Taking a look to graphs indicated with c letter in Figures from V.12 to V.19, it is immediately clear that, for this application, considering the OL_P, stepped systems perform worse than simple switching systems. As it can be seen in Table V.2, irrespective of the season and façade configurations, electric light oscillations are more frequent and sudden (the maximum value is observed for WOFW in winter, corresponding to 162 on-off and off-on actions). This is due to the fact that the OL_P, given its location, is really sensitive to the frequent outdoor daylight variations, and the dead-band alone is not able to reduce the connected continuous on-off and off-on actions. On the contrary, considering the CL_P (letter d in Figures from V.12 to V.19) the electric light oscillations are not so frequent as for the OL_P case (comprised between 2 and 32). However, the CL_P for all observed cases (see Figures from V.12-d to V.19-d), determines that the system operates often in deficit conditions. This is due to the fact that the system is calibrated without accounting for daylight presence and it is based on $S_{el,\delta max}$ exclusively. As it was previously observed regarding switching systems, the OL_P is not adequate if the office is west-oriented, often determining deficit conditions (see Figures from V.16-c to V.19-c). The only one case for which good performances are observed is the open-loop system installed in south oriented offices (see Figures from V.12-c to V.15-c). All these observations are confirmed by the performance evaluation reported in Figures from V.20 to V.23. Specifically, looking at Figures V.20-c, V.20-d, V.21-c and V.21-d it is clear that, by using the open-loop photosensor, stepped systems guarantee better performances compared with switching ones. Indeed, they are

characterized by lower $ILE_{\%}$ values, thanks to the fact that, not only there are two switching steps, but also the maximum light output is 80% and not 100%. $LW_{\%}$ values are comparable to those referred to switching systems and $LD_{\%}$ is negligible also in this case. All the other cases are characterized by high $LD_{\%}$ values. The peak values are observed for OL_P and CL_P in spring and WOSW configuration (see Figure V.23-d). It is interesting to observe that if the evaluation of these systems had been done according to achieved energy savings exclusively, they would appear the most performing systems. Since, excluding values referred to WOFW and WOSF in winter, they are always characterized by the highest energy savings (see Figure V.24). However, the performance evaluation demonstrated that these savings are partly due to the effect of the deficit operating conditions. On the contrary, the OL_P case with south orientations is really a good option. The system guarantees energy savings comparable with those obtained by dimming systems. Specifically, winter savings are equal to 47.8% and to 32.9% considering SOFW and SOSW respectively (see Figures V.24-a and V.24-c). Spring savings are even higher, being equal to about 78.0% for both façade configurations (see Figures V.24-b and V.24-d).

Finally, let us observe results related to dimming systems (see Figures from V.12 to V.19 letters e and f). The first thing that can be observed is that, irrespective of the orientation, photosensor and season, these systems have a great capability to follow daylight oscillations both when they are significant (see for example $\delta(t)$ trends in Figure V.16 letters e and f) and when they are less strong (see for example Figure V.17 letter e). This determines that the $\bar{E}_{tot}(t)$ values are generally very close to the $\bar{E}_{task}$. Furthermore, even when deficit occurs, it is negligible (see for example Figure V.16 letter e). As a consequence, indoor light conditions are pretty stable and illuminance levels pretty constant. On the contrary, switching systems determine a completely different luminous environment. Considering that electric light levels are fixed, even when luminaires are on the indoor daylight trend is easily recognizable (see for example Figure V.15 letters a and b). This could be an aspect appreciated by users. Another important issue to focus on, is the fact that sometimes, in spring, luminaires are on at the minimum light output and this guarantee to fulfil LR (see for example Figure V.15 letters e and f). Moreover, it is clear that often the impossibility to turn luminaires completely off, determines significant intrinsic excesses (see for example the last part of the monitored days in Figure V.19 letter f). According to results of Figures V.20 and V.21, for south orientations, irrespective of the season and adopted photosensor, the system mostly works in ideal or intrinsic excess conditions, with $ILE_{\%}$ values ranging from 12.8% to 38.2%. $LW_{\%}$ and $LD_{\%}$ values are always negligible. Considering the west orientation (see Figures V.22 and V.23), it can be observed that in winter $ILE_{\%}$ is lower than in spring, since the system works in minimum light output conditions less frequently, due to weather conditions. As for the OL_P, irrespective of the season, $LW_{\%}$ values are higher than for the CL_P. This is due to the fact that the correlation between the photosensor signal to the work-pane illuminance is not very good. However, it must be underlined that for this control strategy, differently from the others, deficit is negligible. Generally, this is the control typology for which the differences between the performance obtained by means of OL_P and CL_P are the lowest, except the case of west orientations, in spring (see Figures V.22-d and V.23-d). Given the good daylight integration performances, energy savings results are significant for all the observed cases. They are always high, generally comprised between about 30.0%-40.0% in winter and between 40.0%-60.0% in spring (see Figure V.24). Energy savings are similar to those achievable by means of switching and stepped systems, when indoor daylight levels are generally higher than task illuminance. In this situations lights could be completely turned off, but dimming systems, differently from the others, cannot do that (see Figure V.24 letter b).

It must be underlined that DLCSs performances were simulated considering different calibration conditions in winter and spring, to account for the difference in the ratio of the work-plane illuminance to the photosensor signal due to the season. As it can be inferred from Table V.2 this can have positive effect. Indeed, referring to SOFW façade configuration, if for example the winter functioning has been based on calibration ratio observed in spring, energy savings would

decrease both for open-loop switching and dimming systems. This depends on the $LW_{\%}$ increase. The $LD_{\%}$ would decrease, but this reduction was negligible if compared whit the value related to winter calibration.

Table V. 7 : Open-loop switching and dimming systems winter performances evaluated calibrating the system in winter (winter cal.) and in spring (spring cal.) referred to SOFW configuration

	OL_P switching		**OL_P dimming**	
	Winter cal.	**Spring cal.**	**Winter cal.**	**Spring cal.**
DIA	95.62	90.03	75.25	65.19
DIA^{+}	3.92	9.78	24.20	34.81
DIA^{-}	0.46	0.19	0.56	0.00
$ILE_{\%}$	47.25	47.83	19.92	19.93
$LW_{\%}$	5.09	12.69	1.75	4.66
$LD_{\%}$	0.03	0.01	0.02	0.00
Energy savings	19.27	12.98	41.79	39.53

The effect is similar considering closed-loop switching systems, whereas the closed-loop dimming system is not affected by this factor. This is explicable considering that, as it is reported in Table IV, the calibration ratios are almost equal in the two observed seasons.

Table V. 8: Closed-loop switching and dimming systems winter performances evaluated calibrating the system in winter (winter cal.) and in spring (spring cal.) referred to SOFW configuration

	CL_P switching		**CL_P dimming**	
	Winter cal.	**Spring cal.**	**Winter cal.**	**Spring cal.**
DIA	96.08	95.03	79.88	79.97
DIA^{+}	2.87	4.81	19.63	19.51
DIA^{-}	1.05	0.15	0.49	0.52
$ILE_{\%}$	43.11	47.07	19.88	19.72
$LW_{\%}$	3.72	6.25	1.71	1.68
$LD_{\%}$	0.06	0.01	0.01	0.01
Energy savings	23.6	18.58	41.79	41.99

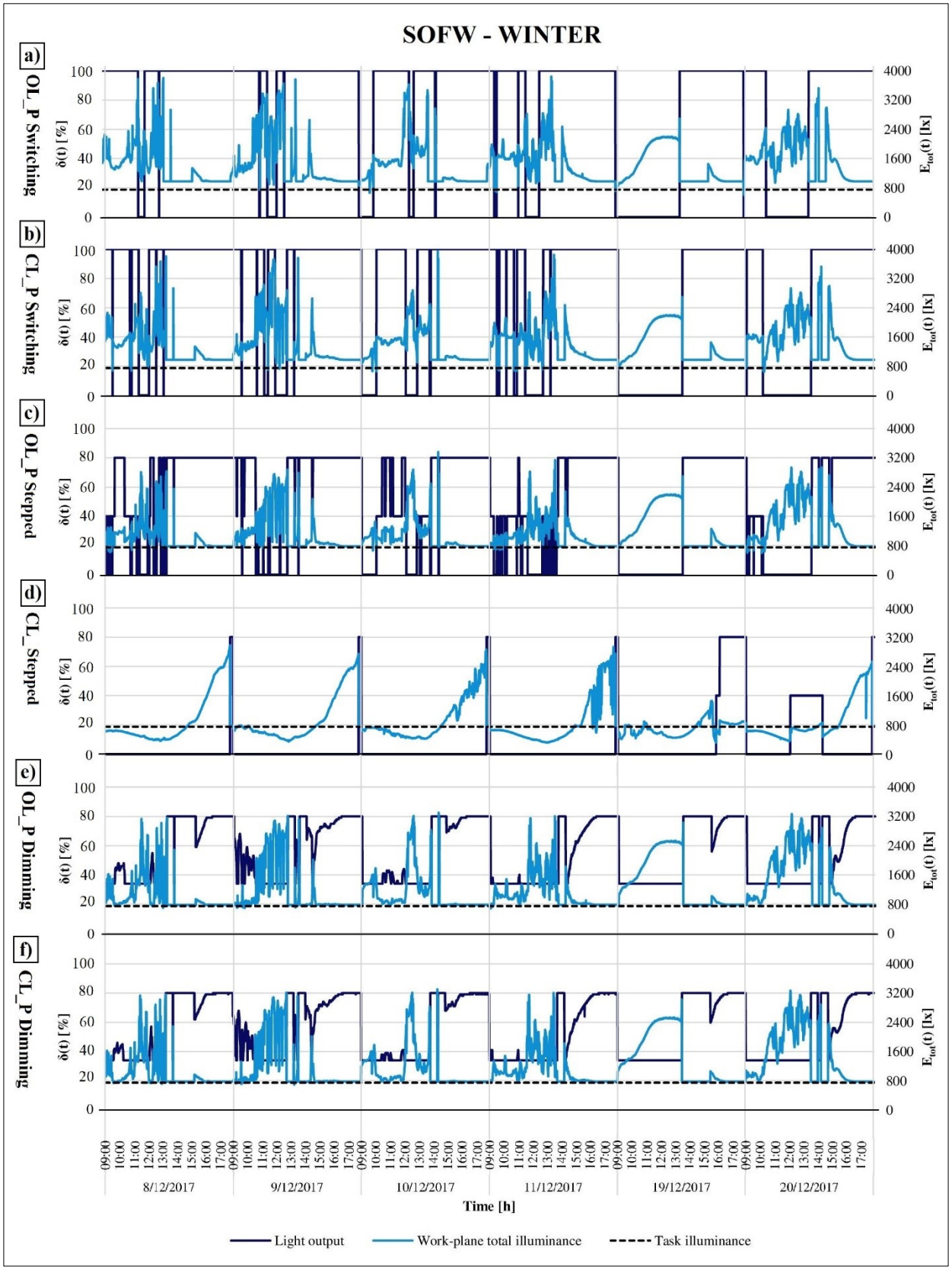

Figure V. 12: Winter DLCSs functioning referred to SOFW configuration

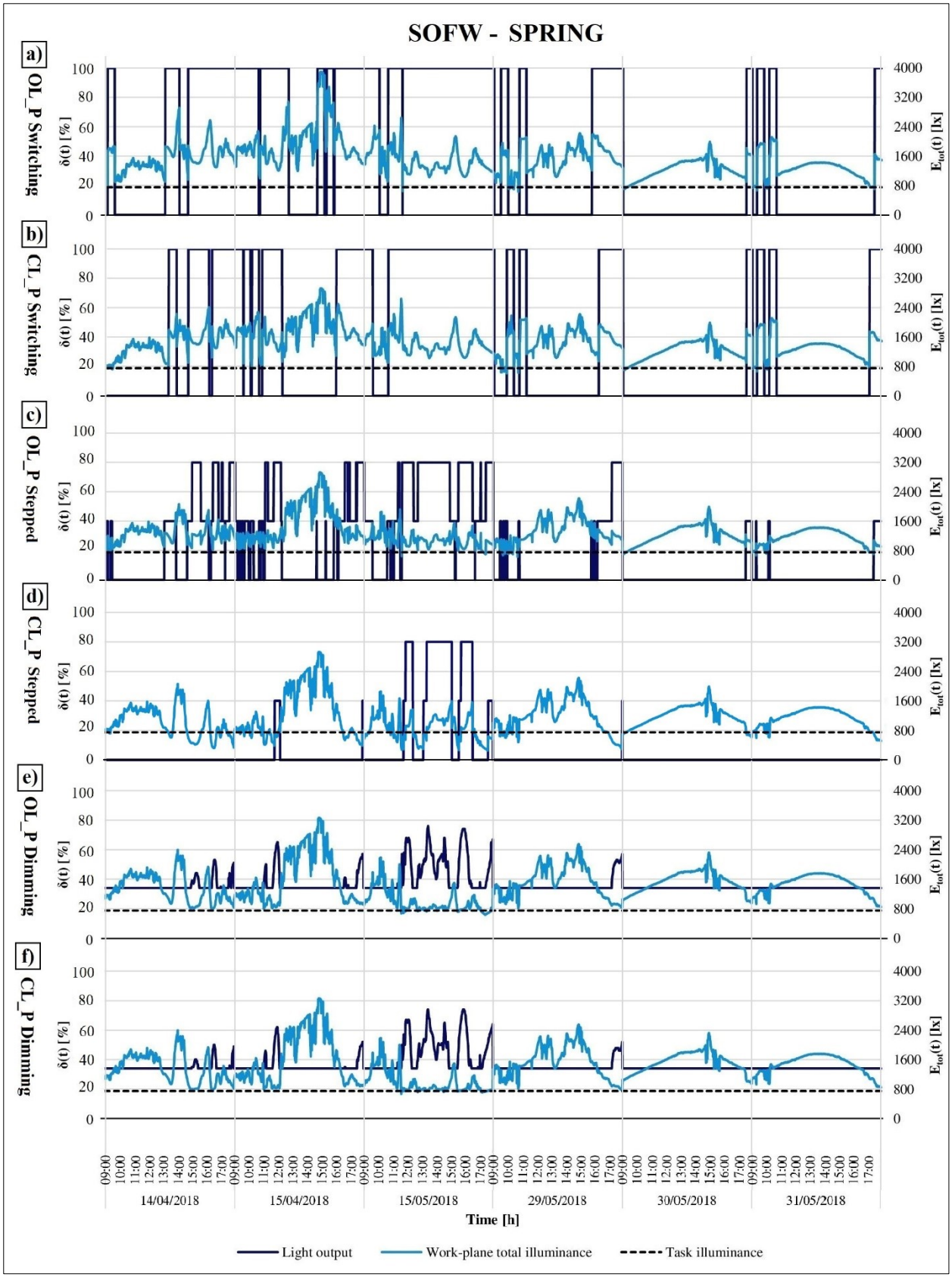

Figure V. 13: Spring DLCSs functioning referred to SOFW configuration

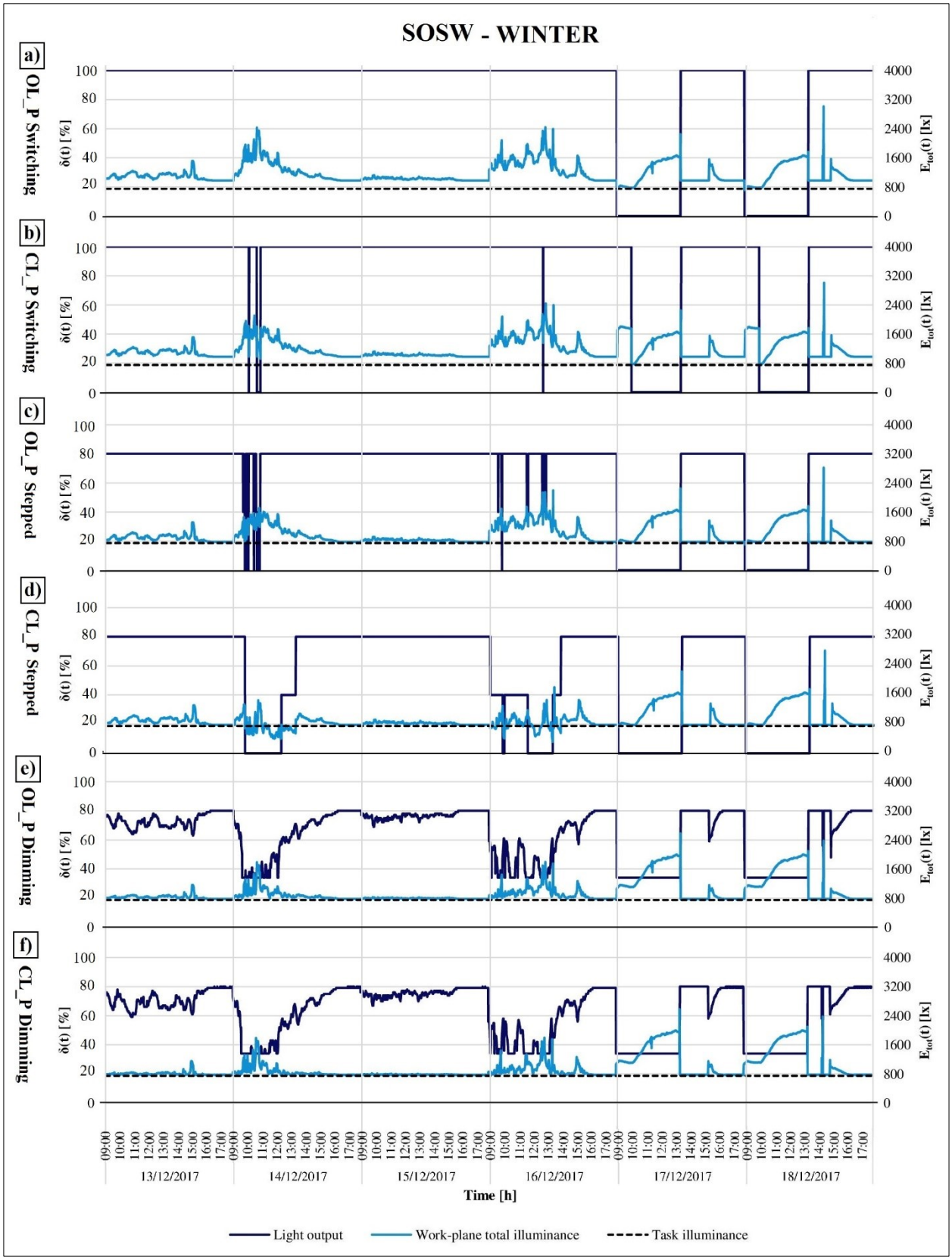

Figure V. 14: Winter DLCSs functioning referred to SOSW configuration

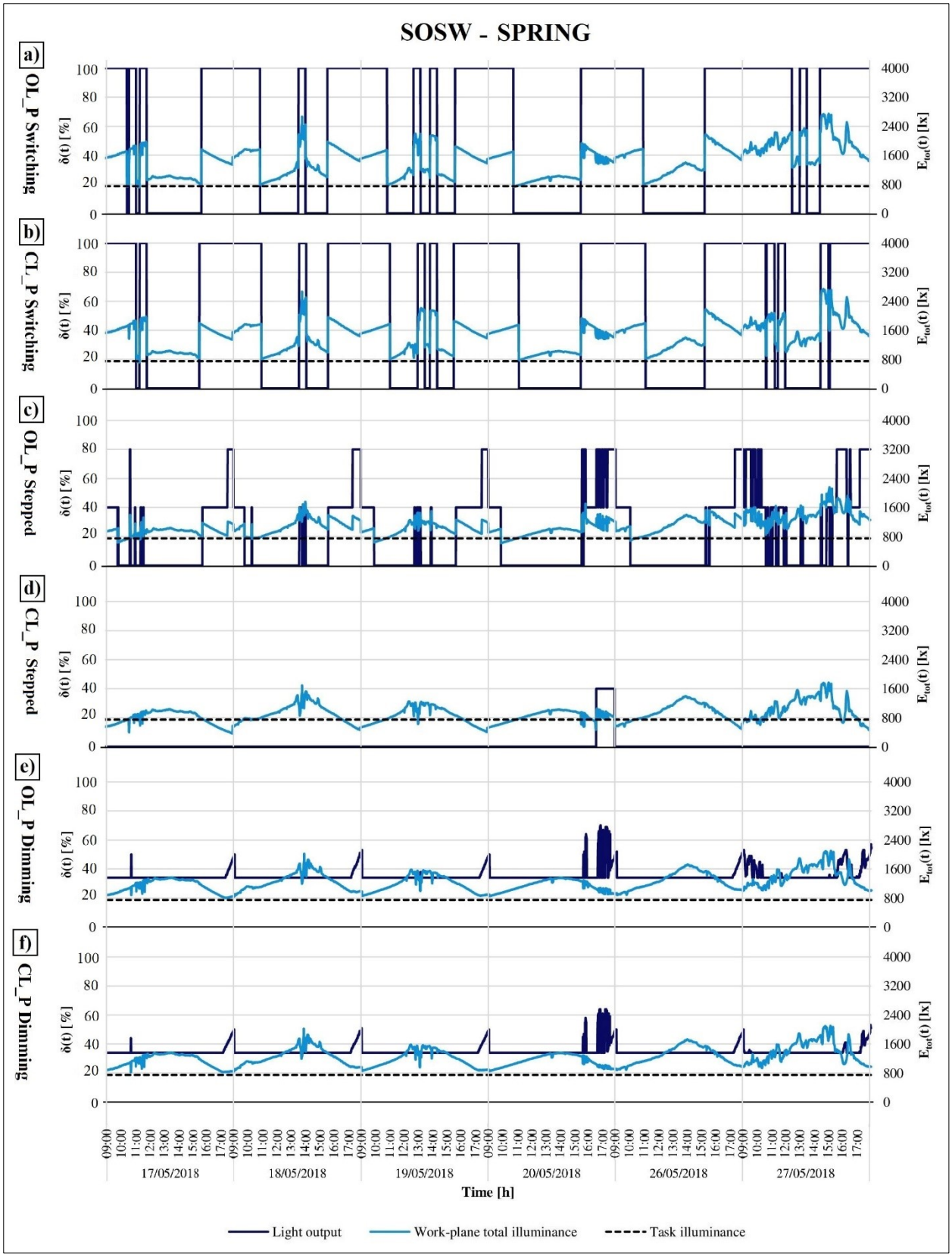

Figure V. 15: Spring DLCSs functioning referred to SOSW configuration

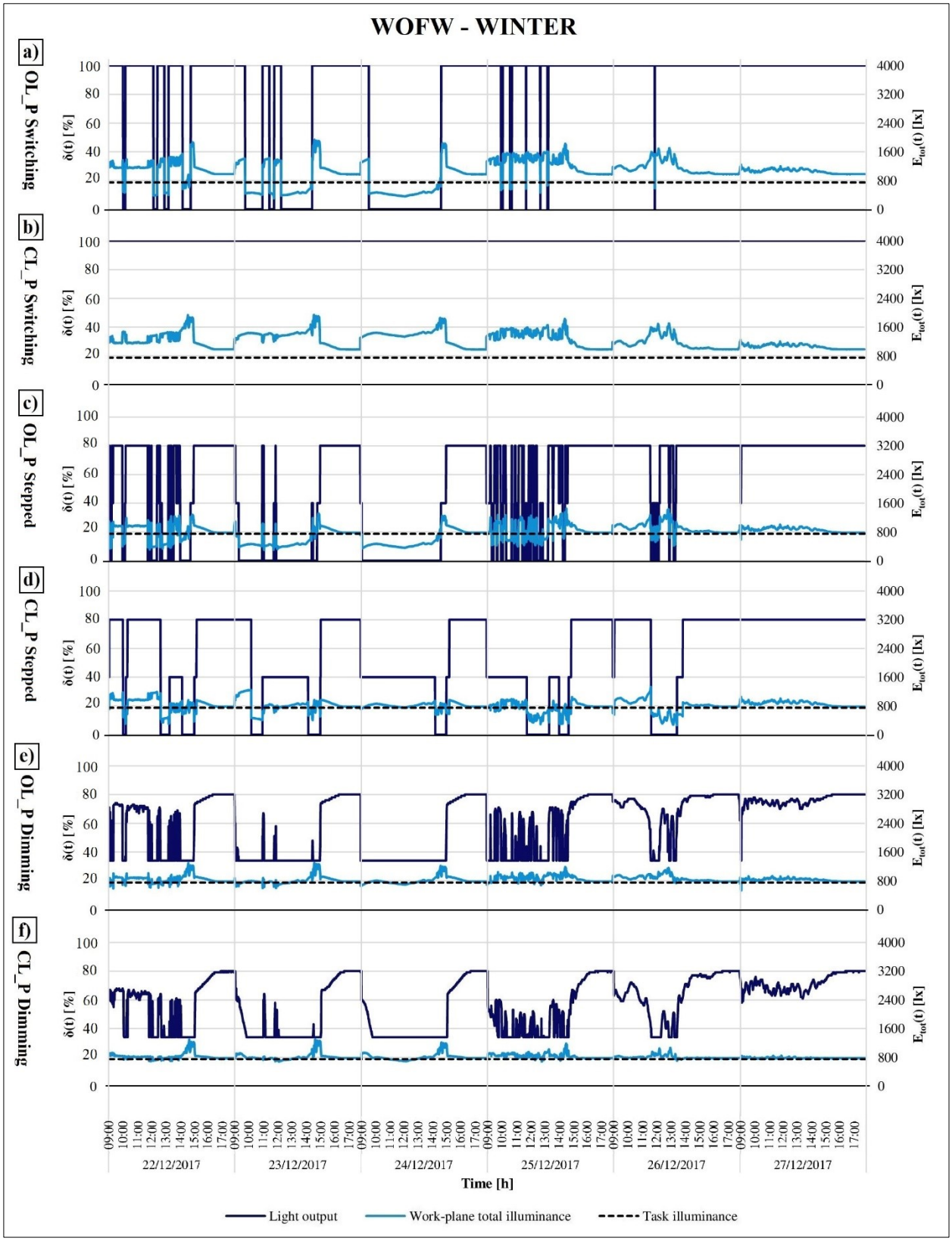

Figure V. 16: Winter DLCSs functioning referred to WOFW configuration

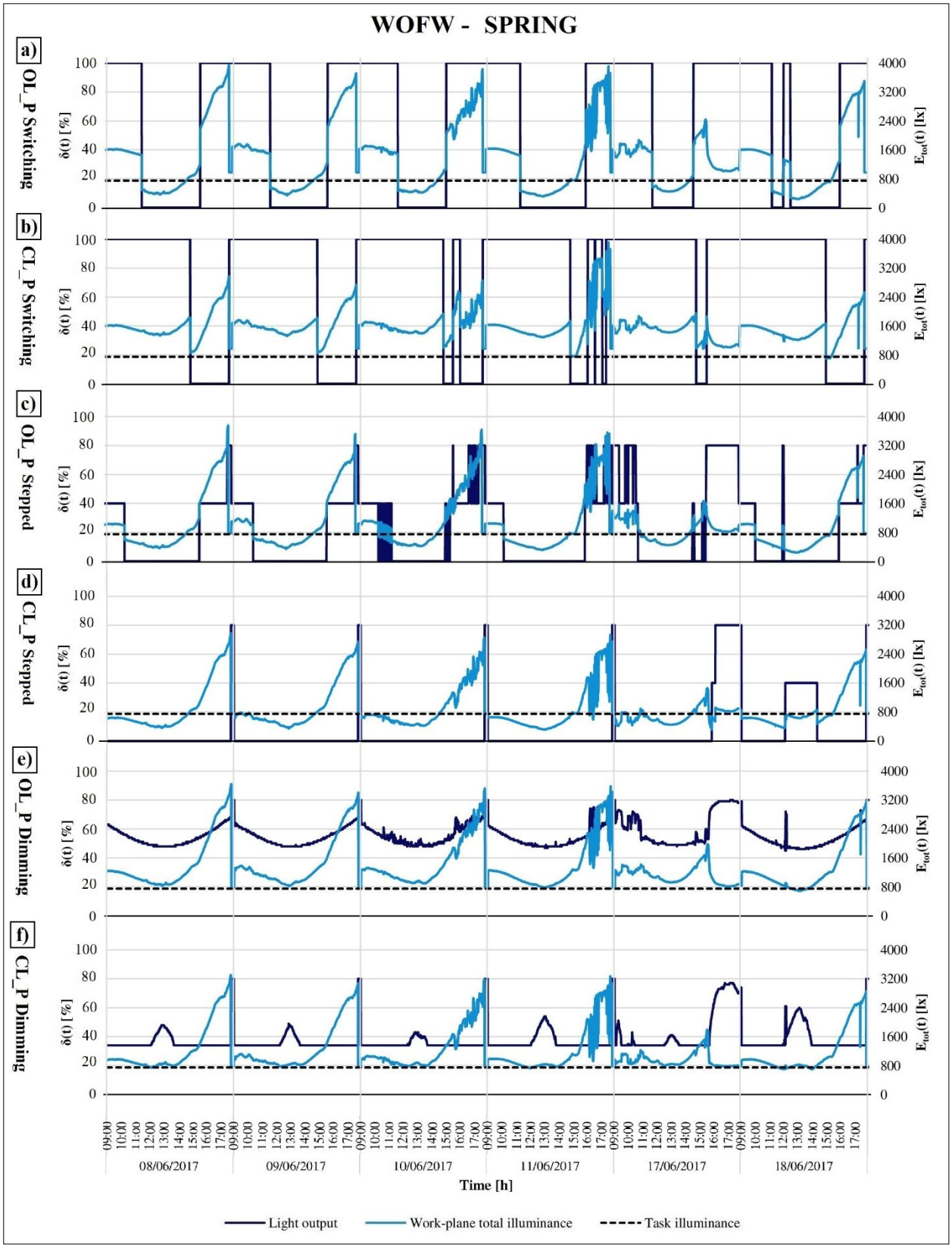

Figure V. 17: Spring DLCSs functioning referred to WOFW configuration

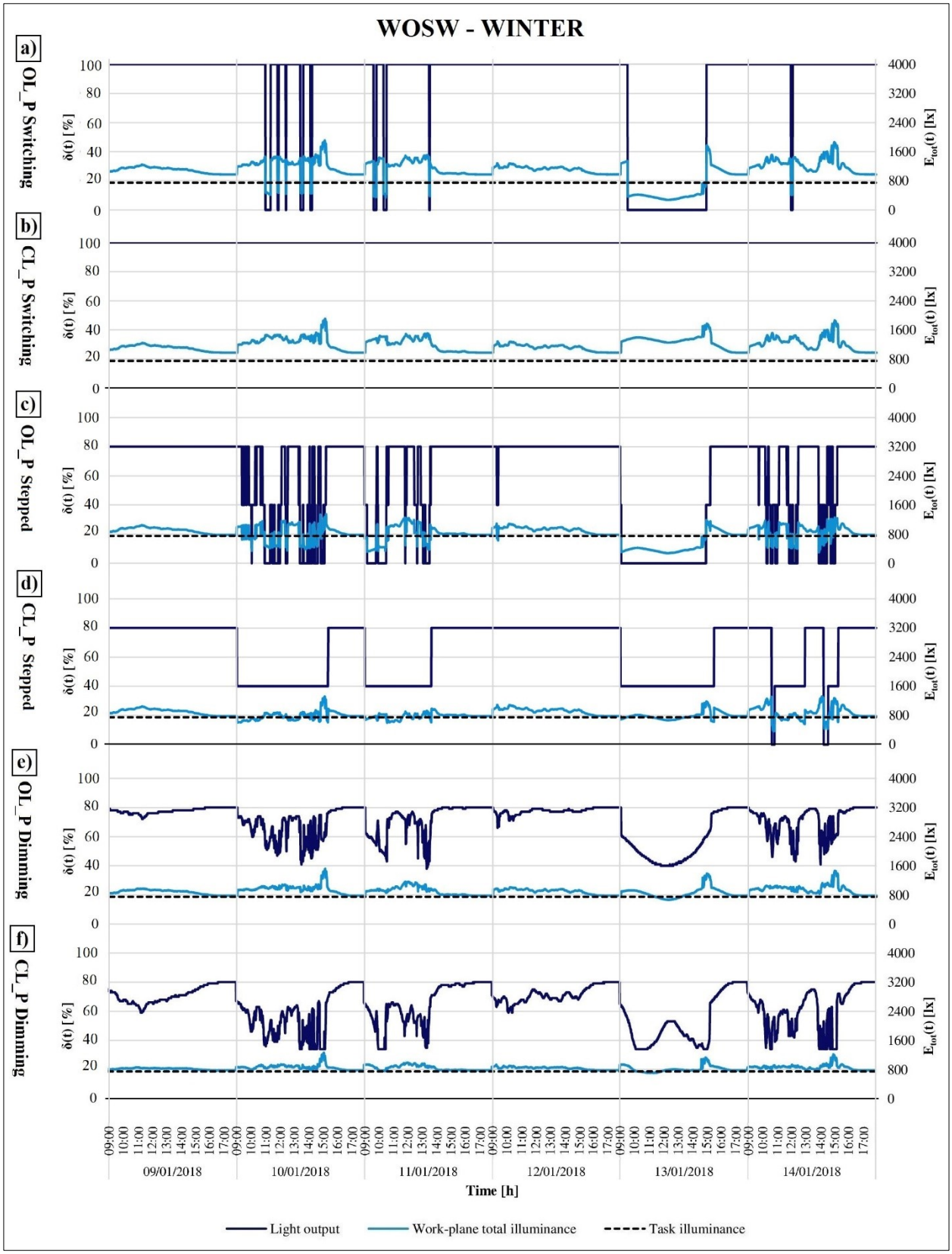

Figure V. 18: Winter DLCSs functioning referred to WOSW configuration

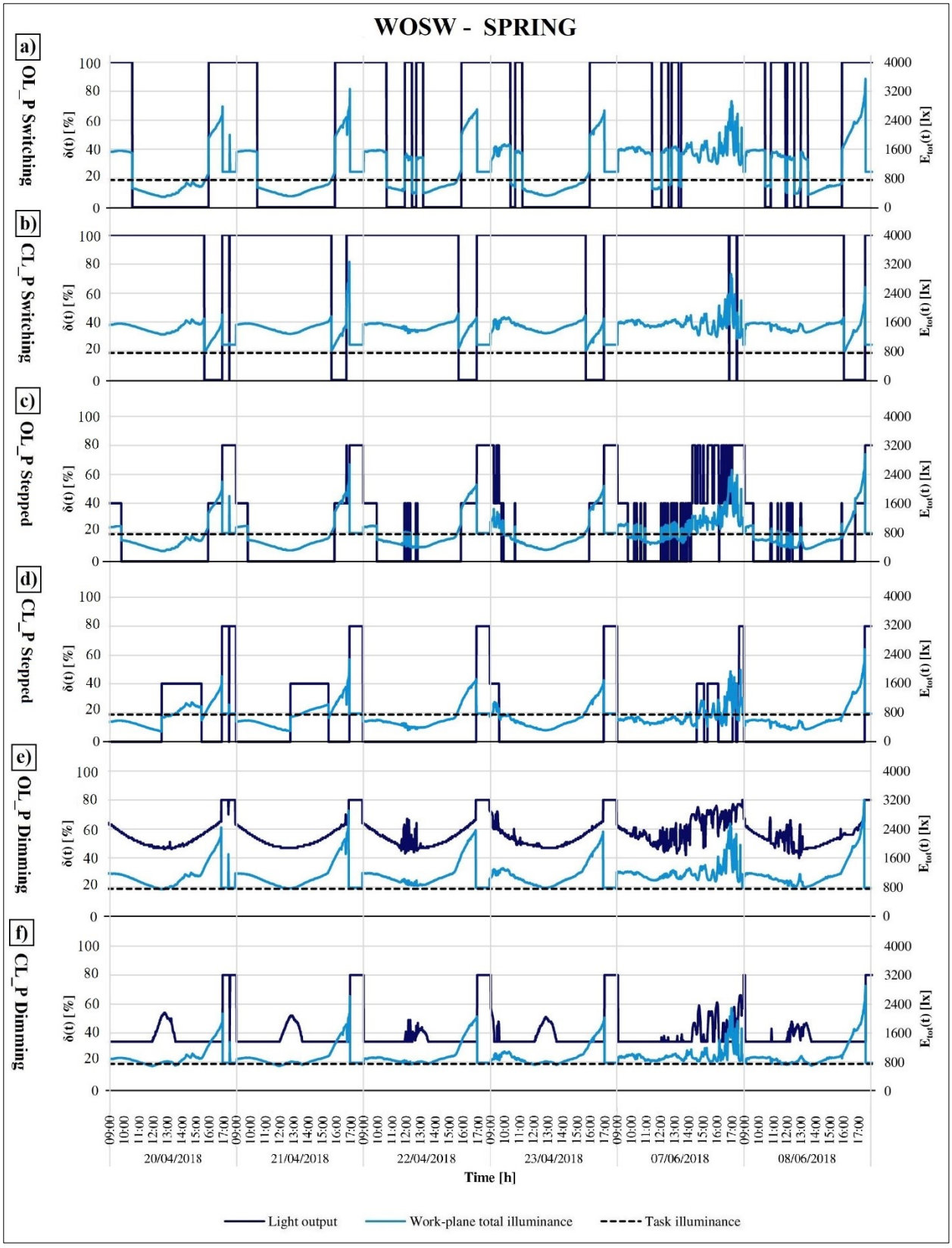

Figure V. 19: Spring DLCSs functioning referred to WOSW configuration

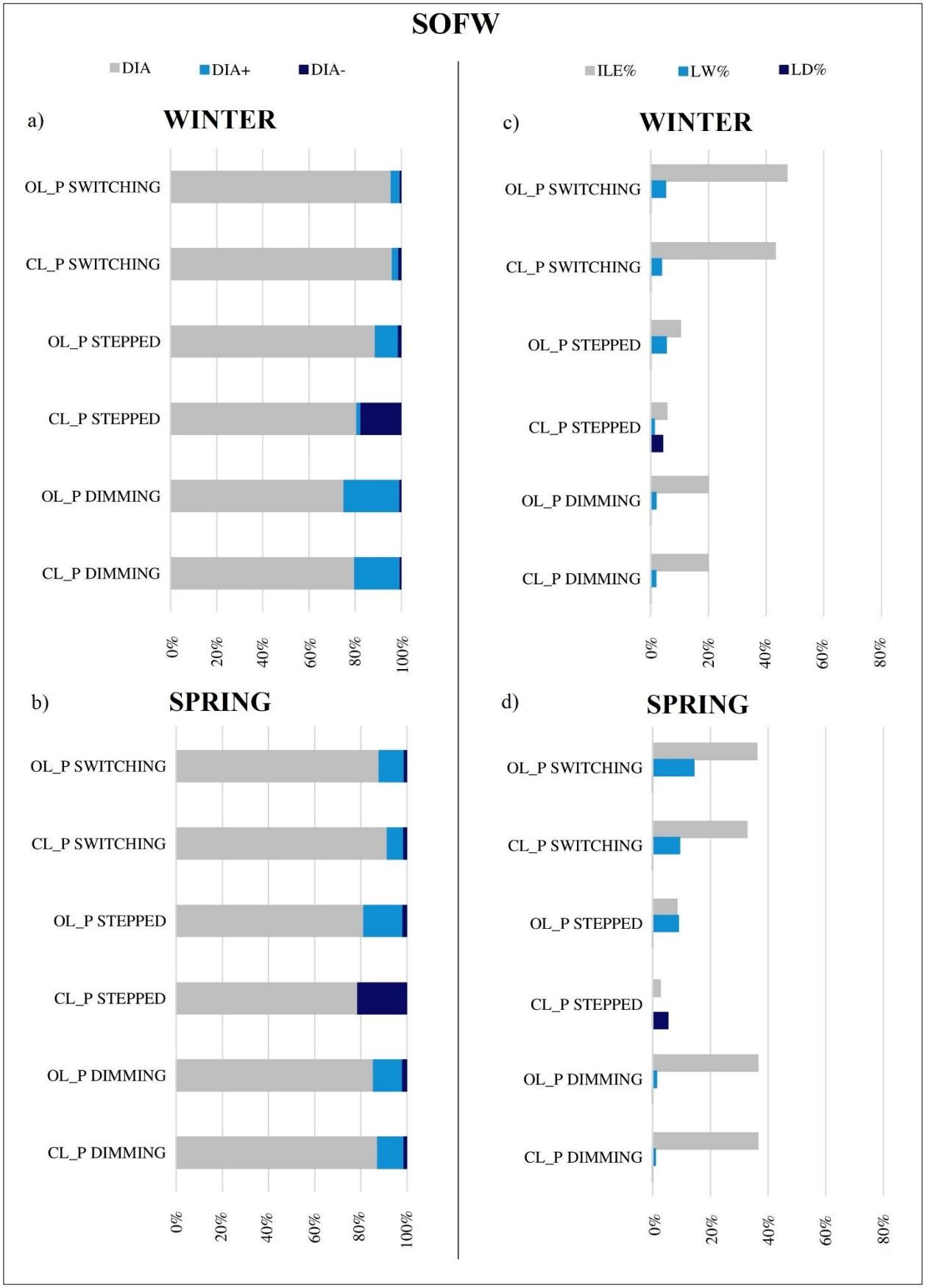

Figure V. 20: DLCSs performance evaluation referred to SOFW configuration

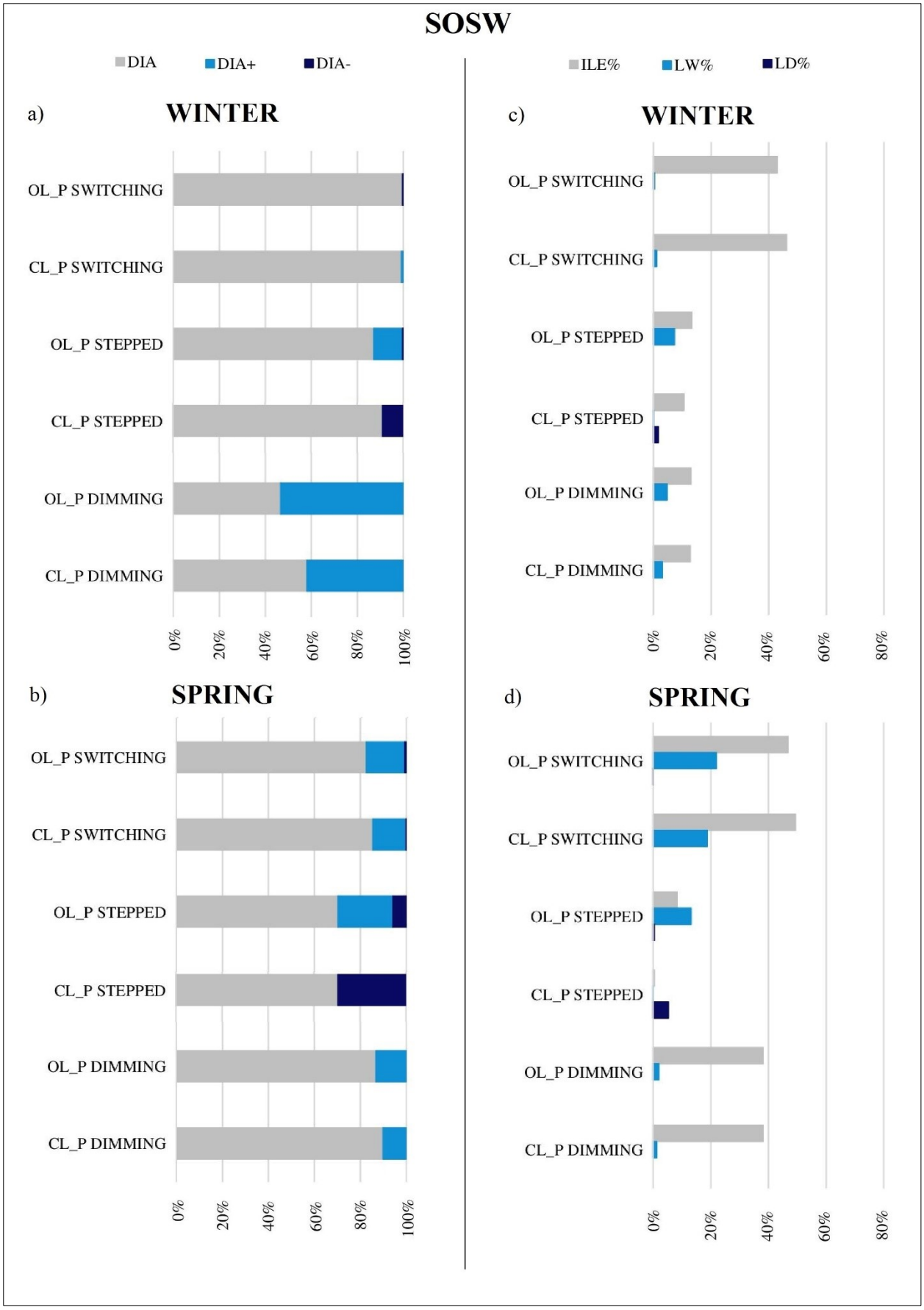

Figure V. 21: DLCSs performances evaluation referred to SOSW configuration

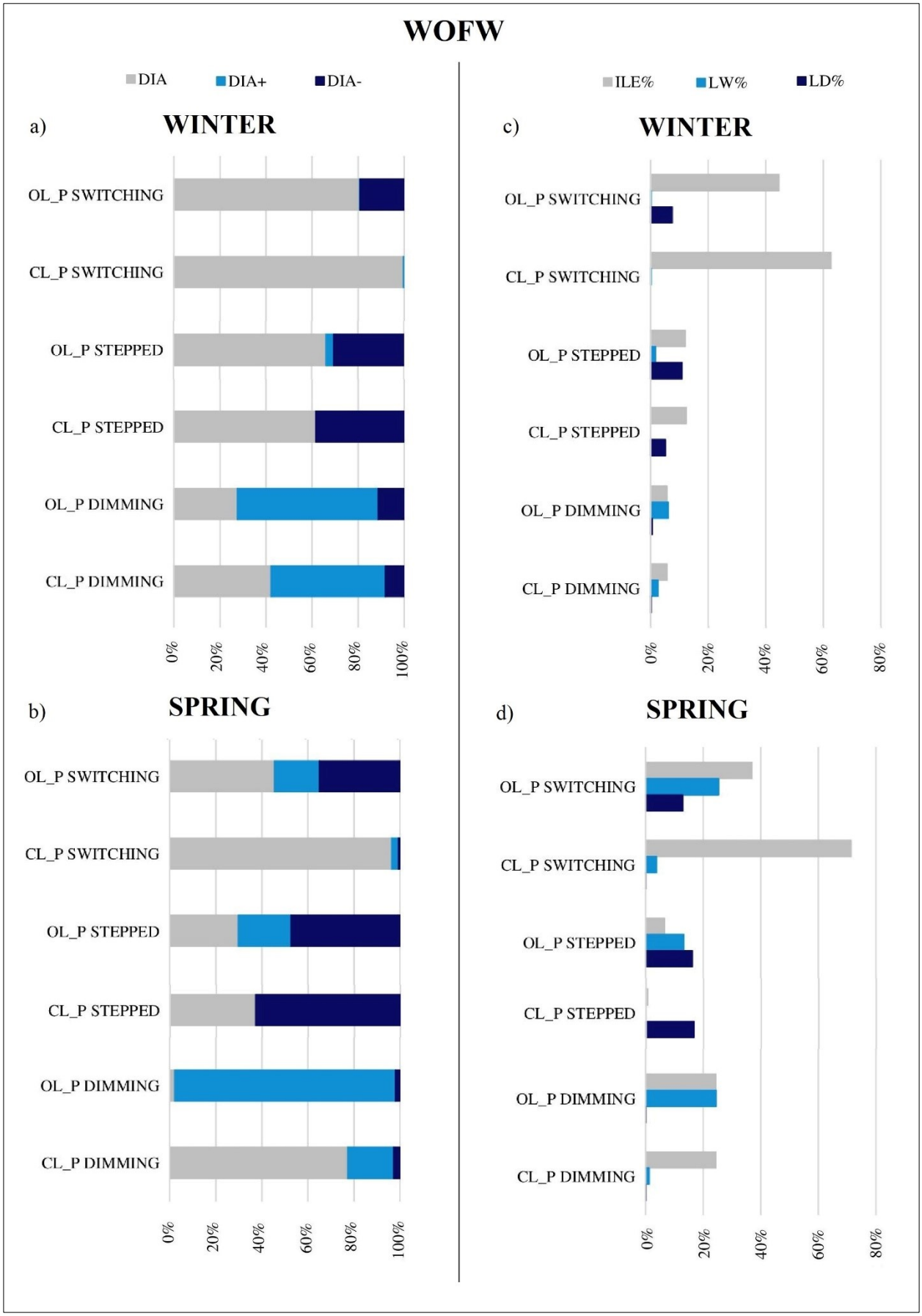

Figure V. 22: DLCSs performances evaluation referred to WOFW configuration

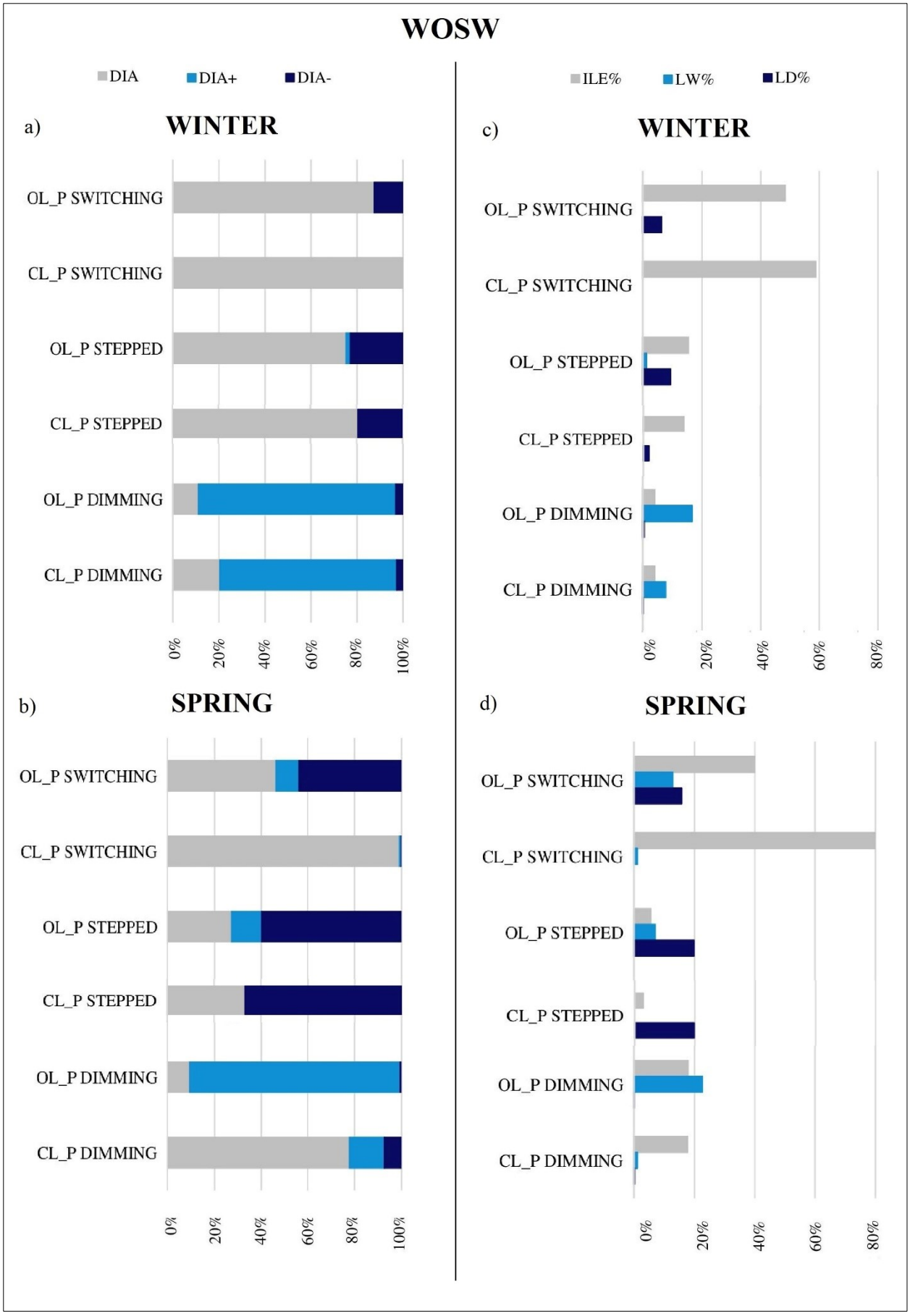

Figure V. 23: DLCSs performances evaluation referred to WOSW configuration

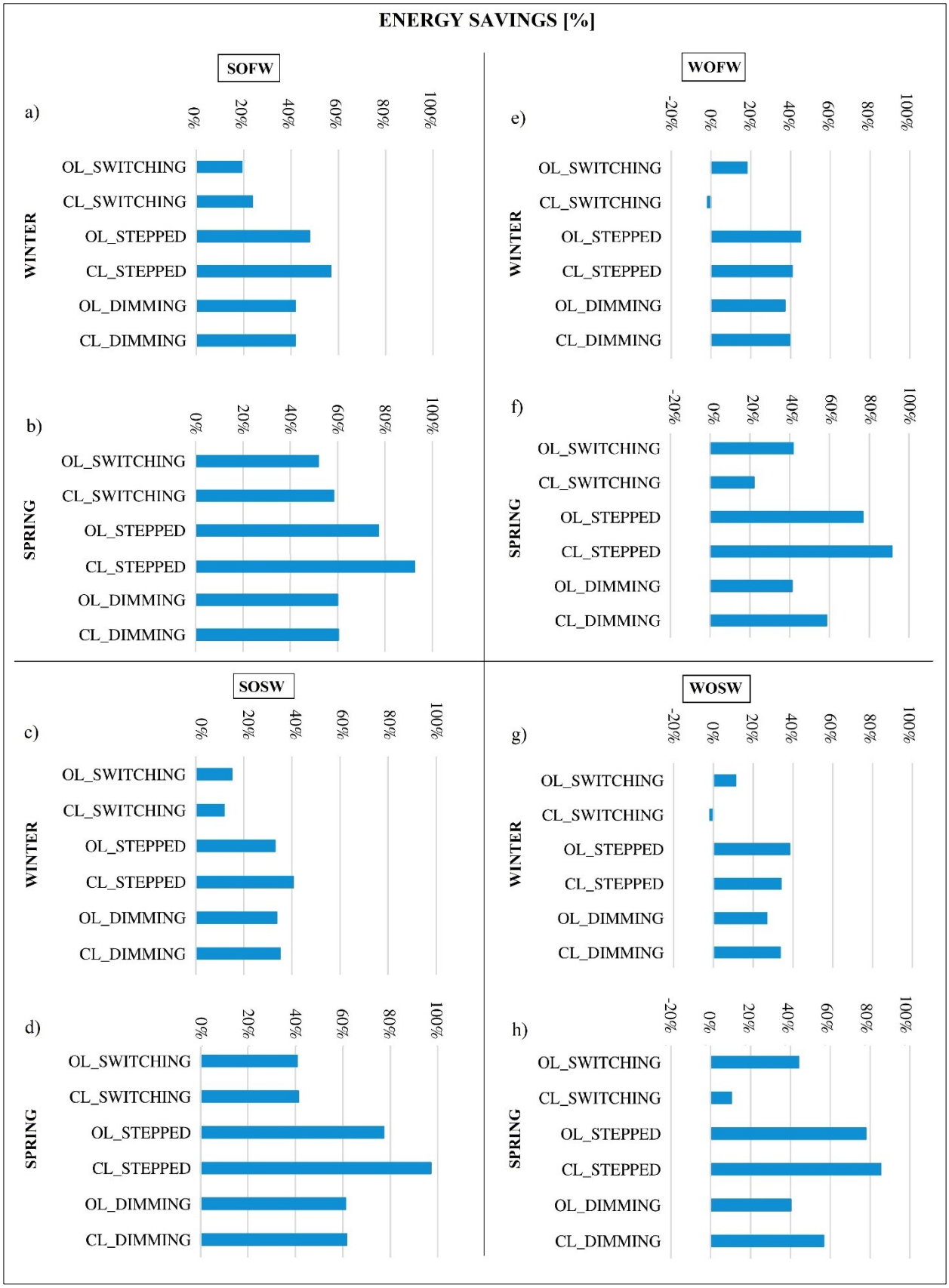

Figure V. 24: Energy savings evaluation referred to all configurations

VI. Discussion

In summary, the obtained results demonstrated that the effectiveness of the control systems is affected by numerous factors and each application represents a specific case, that must be in-depth studied, in order to obtain the most suitable technical solution. However, some general observations can be done, as it is clear by looking at the recapitulatory graphs in Figure VI.1.

Switching systems represent the simplest control strategy. They are characterized by significant $ILE_{\%}$ values (ranging from 32.6% to 79.8% as for the analysed cases), often determining that achievable energy savings are not so relevant, if compared with those guaranteed by other control systems. However, it was showed that switching systems can represent a useful option, when daylight illuminances at the work-plane generally assumes values higher than the task illuminance. This is in accordance with [39]. Moreover, it must be noticed that, when a closed-loop photosensor is used, these systems generally do not determine deficit conditions.

As for stepped systems, different observations must be done, depending on the photosensor typology. Specifically, when they are managed by open-loop photosensors and the correlation between the outdoor daylight conditions and indoor ones is good (south orientations in the specific application), they guarantee better performances than switching systems. Specifically, they are characterized by lower $ILE_{\%}$ values (in the analysed cases ranging from 8.3% to 13.2%), $LW_{\%}$ ones are comparable with those referred to switching systems and $LD_{\%}$ is always lower than 1.0%. Correlated energy savings are higher compared with switching systems and similar or higher than those guaranteed by dimming ones. However, they are characterized by a not negligible problem: the continuous switching on-off and off-on actions, due to the fact that the system is not able to manage the frequent daylight oscillations detected by the outside-located photosensor. On the contrary, as for the switching systems, results demonstrated that the setting of the switching-linked time-delay strictly improve their performance from this point of view (see Table V.6), as it was reported in a previous research [26]. For example, considering the SOFW case and the OL_P in winter, switching actions are 28 for the simple switching and 148 for the stepped one, that is calibrated without considering a time delay. As for the stepped systems managed by closed-loop photosensors, they are characterized by the highest values of $LD_{\%}$ (comprised between 1.9% and 19.7% for the analysed cases). This is due to the fact that they are calibrated considering the ratio of the work-plane illuminance to the photosensor signal exclusively in presence of electric light and not accounting for daylight. A similar problem was revealed by previous researches [40, 41] about integral reset systems, which are exclusively calibrated on electric light as well.

Finally, the dimming systems turned out to be the most adaptable to different daylight conditions, being generally characterized by lower $ILE_{\%}$ values (ranging from 4.1% to 38.2% in the specific case) and with $LD_{\%}$ always close to 0.0%. Results demonstrated that they represent the better solution when daylight illuminances are generally lower than the task one, as it was demonstrated in [38].

Finally, irrespective of the control strategy, it was highlighted that calibration conditions are crucial to obtain a proper functioning of control systems and that there is a straight correlation between the $\overline{E}_{dl}/S_{dl}$ ratio variations and weather and season ones (see Tables from V.2 to V.5, V.7 and V.8), as it was previously stated in [28-30].

Moreover, performed analyses underlined that, as it was reported in [65], to calibrate control systems accounting for seasonal variations improve their performances.

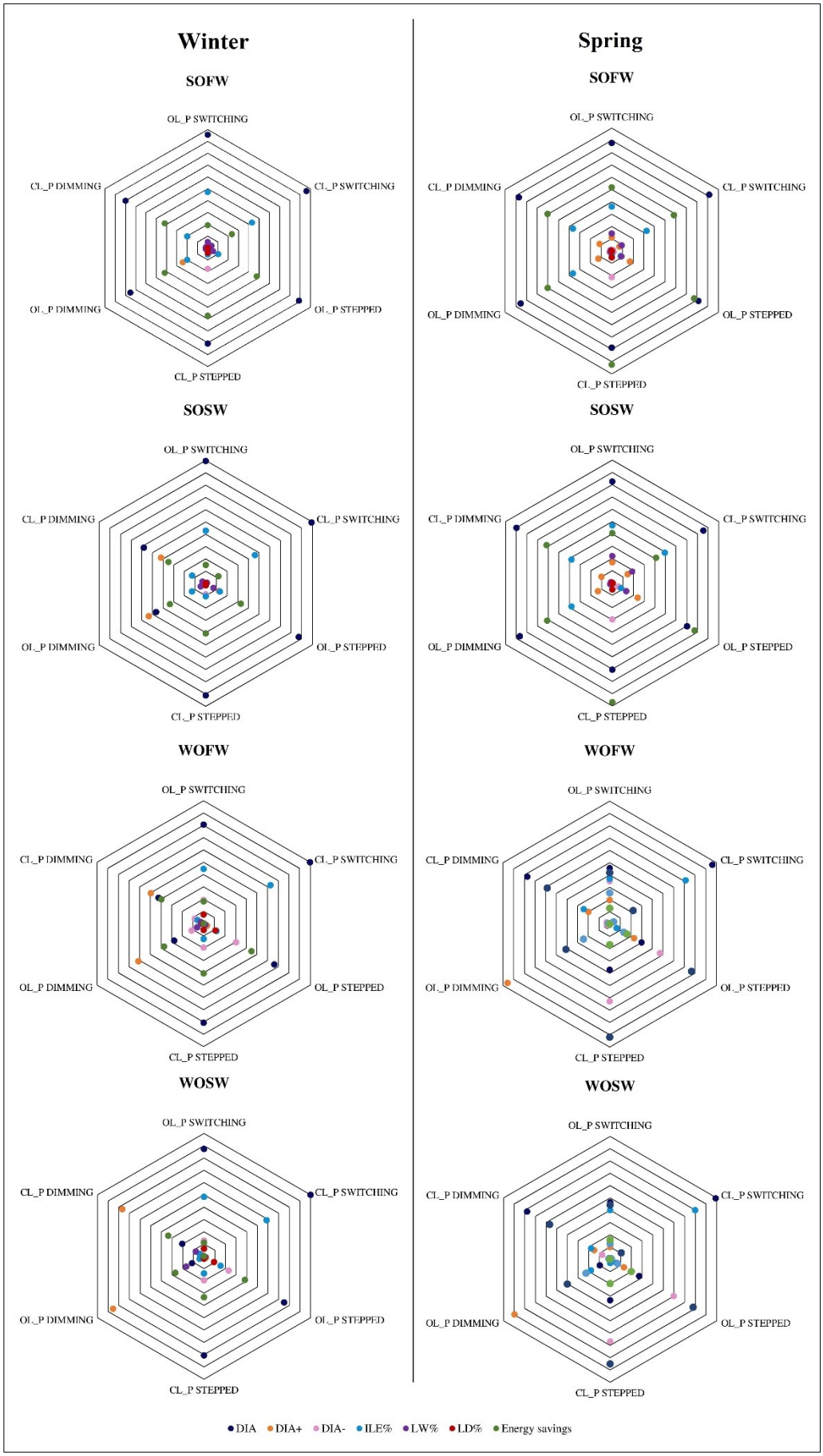

Figure VI. 1:Recapitulatory graphs related to DLCSs performance parameters

VII. Merits, limitations and future steps of the research

The presented study introduces the following novelties:

- The proposed assessment methodology allows evaluating DLCSs performances from a new point of view. It is useful to describe the capability of the control systems in maintaining proper light conditions at the work-plane and in integrating daylight, instead of focusing exclusively on the achievable savings.
- A calculation tool (DET) is specifically developed to allow proposed parameters to be easily calculated.
- The calculation tool presents, beyond the performance evaluation module (to calculate the proposed performance parameters) a simulation module as well. It is able to simulate the dynamic functioning of different typologies of control systems starting from measured or simulated daylight data.
- The DET simulation module overcomes the limits of just available software. Specifically, it calculates the control systems functioning starting from the photosensor detections and accounting for all the calibration parameters ($\overline{E}_{dl,tc}/S_{dl,tc}$ calibration ratio, maximum and minimum light output, dead-bands, time-delays, etc). Moreover, it calculates energy consumptions considering the relationship between light output and the absorbed power, the impact of power absorbed by luminaires in stand-by conditions and of auxiliary devices such as photosensors and controllers.
- Results obtained by the analysis of the case study are in good agreement with previous researches and allows obtaining useful information about the functioning of different typologies of DLCSs.

However, as for the case study analysis, it must be underlined that it is based on two simplifications.

It is assumed that the photosensor signal coincides with the illuminance at the photosensor. This means that photosensors spatial and spectral responses are neglected. However, as it was reported in section I.3 these characteristics strictly affect systems performances.

Moreover, daylight measurements were performed without shielding the direct radiation. The evaluation of the potential effect of a shading system is performed ex post. It was simply considered that, when daylight illuminances at the work-plane were higher than 3000 lx a glare risk occurred. So, the luminaires had to be turned on at maximum light output to account for the daylight availability reduction due to the use of a shading device.

These two aspects deserve a specific treatise. However, it must be underlined that DET is structured to receive work-plane illuminances and photosensor detections as input data. Consequently, the evaluation of the daylight availability variations due to shading devices and the correct definition of the photosensor signals are problems that must be faced before using DET and that do not invalidate its way to operate. The better the inserted input data are, the more reliable the DET output results will be.

Despite these aspects, the obtained outcomes represent a good start point for further research projects.

First of all, the results obtained with DET should be compared with the functioning of real control systems. Moreover, a comparison with results provided by other software could be useful to quantify the specific uncertainties of each calculation model. This comparison would be useful also to underline which aspects of the implemented algorithms have a major effect in determining the properness of the DLCSs functioning simulation. Furthermore, it would be interesting to compare results obtained by means of DET with those obtained by applying the calculation procedure proposed by the EN 15193-1:2017 [86].

As for the specific case study, similar experiments could be repeated referring to other daylight conditions (spaces characterized by different architectural features, façade configurations and orientation), to verify if the obtained results are generalizable.

Parameters affecting systems performances should be furtherly studied and optimizing criteria to identify the most appropriate technical choices should be found.

Moreover, it is important to experiment strategies to optimize systems performances by

adapting their functioning to seasonal changes of the indoor daylight availability.

Last but not the list, once the optimization design criteria are found, the functioning of the so calibrated DLCSs should be experimented in real spaces and users' opinions about their way to operate should be analysed.

Conclusions

The goal of the thesis was to propose a methodology useful to evaluate daylight-linked control systems (DLCSs) performances. For this purpose, the work was divided in different steps:

- State-of-the-art analysis aiming at understanding what are the parameters mostly influencing DLCSs performances;
- Proposal of new performance parameters able to evaluate the capability of DLCSs in integrating daylight (Daylight Integration Adequacy -DIA-; Percentage Intrinsic Light Excess -$ILE_{\%}$-; Percentage Light Waste -$LW_{\%}$- Percentage Light Deficit -$LD_{\%}$-).
- Development of a simulation tool (DET) useful to simulate DLCSs functioning, overcoming the limits of the available software, and to calculate the above-mentioned parameters;
- Setting up of a test-room, where daylight measurements were performed;
- Use of the measured data to simulate the functioning of different control systems by using DET and to evaluate how they would operate, once installed in the test-room.

The state-of-the-art analysis underlined the difficulties connected to DLCSs design and highlighted how each stage of the project, even those not strictly connected to the lighting system design, implies technical choices affecting the functioning of the control systems. For example, façade configuration is crucial: orientation, window to wall ratio, use of shading devices have a primary role in determining the ratio of the work-plane illuminance to the photosensor signal and consequently DLCSs performances. Obviously, the characteristics of the control itself are fundamental such as the adopted control strategy (choice between open-loop or closed-loop systems or between switching or dimming systems) or the characteristics of the photosensors (spectral response, spatial response, location). However, each choice connected to the lighting system setting can have an impact on the way DLCSs operate: the choice of the luminaires, their location and arrangement in control zones, the choice of auxiliary components. Finally, the commissioning is the phase during which all the aspects defined with the design process become real and operative. Indeed, by means of the calibration, the way the system operates is univocally established.

Independently from the description of the factors affecting DLCSs performances, the most important result of the state-of-the-art analysis is that it underlined how the weight of each affecting factor cannot be univocally defined: a design strategy perfect for a case study could be completely unsuitable for another one. As a consequence, a study suggests using switching systems, another one opts for dimming controls; one underlined the benefits of photosensors characterized by narrow field of view and another those of photosensors with wide spatial response; one found that switching-time delay is the most effective strategy to reduce electric light oscillations and another one suggests using daylight-linked time delay. The truth is that each case study is unique and needs to be treated on its own merit. In this sense, the most important problem is the general lack of a specific DLCSs design culture.

From this awareness the goal of the thesis is born: providing a mean to evaluate DLCSs performances on a case-by-case basis. So, performance parameters were introduced and the tool to calculate them was developed.

The concept, which the new performance parameters are based on, is that, since the goal of DLCSs is to integrate daylight, they must be evaluated according to their capability in doing that. In this regard, it was underlined that it is possible to recognize four different operating conditions for DLCSs: ideal functioning, light deficit, intrinsic light excess and light waste. In the first case the integration of electric light and daylight is perfect, and the sum of daylight work-plane illuminances and electric light illuminances determined by the control is equal to the required task illuminance. Ideal functioning is really rare, due to the technical characteristics of DLCSs, so light deficit or excesses can occur. When light deficit occurs, electric light is not sufficient to integrate daylight and prescriptions are not fulfilled. On the other hand, occasionally, total illuminances at the work-plane (daylight plus electric light) can be higher than prescriptions. Sometimes the excess is due to the control strategy characteristics and cannot be avoided unless the strategy itself is changed. This excess was defined Intrinsic Light Excess. Other times, the excess is

due to an improper system functioning and, in this case, it is defined waste. The proposed performance parameters describe the percentage occurrence during time of the different operating conditions (DIA, DIA^+, DIA^-) and quantify the light deficit, the intrinsic light excess and the waste as percentage of the light requirements prescribed by regulations ($LD_{\%}$, $ILE_{\%}$and $LW_{\%}$).

The use of these parameters allows overcoming the limits of the evaluation exclusively based on achievable energy savings, that, as it was often repeated along the thesis, is not adequate to evaluate if the DLCS properly operates. Moreover, the parameters have a double value: they can used both during design stage to compare different design solutions, identifying the most suitable one, and to evaluate DLCSs performances during their operating life. In this case, they help to identify the causes of improper functioning and to find solutions to remove them.

As it was underlined in Section 3 one of the problems in designing DLCSs is the lack of an adequate tool to simulate their functioning. For this reason, DET was developed. It is an Excel macro and it contains a simulation module and an evaluation one. The simulation module allows simulating DLCSs functioning, starting from daylight availability data obtained by means of both dynamic daylight simulations and field measurements. The simulation module introduces some novelties compared to the available calculation tools: the variations over time of the ratio of daylight work-plane illuminance to the photosensor signal are considered, the calibration phase is in-depth modelled, effect of parameters as dead-bands, time-delays, maximum and minimum light outputs can be evaluated. Finally, the evaluation module allows DIA, DIA^+, DIA^-, $ILE_{\%}$, $LD_{\%}$ and $LW_{\%}$ to be calculated.

Daylight measurements in the test-room were used to simulate by means of DET different DLCSs. The test-room has a double orientation, so, by modifying the window to wall ratio by means of simple cardboards attached to the windows frame, it was possible to obtain data referred to 4 different façade configurations: south orientation with French window, south orientation with simple window, west orientation with French window, west orientation with simple window. Moreover, measurements were repeated during winter and during spring for each configuration. The following controls were considered: open-loop and closed-loop switching, open-loop and closed-loop stepped, open-loop and closed-loop dimming.

The conspicuous amount of obtained results allowed evaluating the effect of different parameters on the analysed DLCSs. Different conclusions were obtained and, even if they are specific for the observed case studies, they can be food for thought for further studies or for design applications.

The comparison between open-loop and closed-loop systems underlined that the two strategies can be both profitable for those applications for which indoor work-plane illuminance trends well match the outdoor ones (south orientation in the specific case). On the contrary, when this correspondence is not observed (west orientations in the specific case), the use of open-loop systems is generally not preferable. However, if this is true for switching and stepped systems, the use of dimming ones allows obtaining good performances for all the observed cases, even with open-loop photosensors. This is an important result: it implies that a single outdoor photosensor could be used to control luminaires in different spaces.

The comparison between switching, stepped and dimming systems underlined that even though dimming is the strategy that generally performs better, the choice of a strategy or another is strictly related to the daylight availability and to the most recurring indoor daylight levels. For example, it was demonstrated that, for south orientations, during spring, since indoor daylight levels are generally higher than prescriptions, switching or stepped systems able to completely turn off lights, guarantee performance comparable with the dimming one, that, conversely, are always on at a minimum light output, even if electric light is not required. On the contrary, when daylight levels are usually low and the electric light requirement are generally higher than the minimum light output, dimming systems performances are optimized. Based on these observations, design optimization criteria should be investigated considering the following issues: the yearly indoor daylight availability; the weather conditions frequency; the comparisons between light requirement and electric light trends provided by the different control strategies.

Moreover, it was underlined that switching, stepped and dimming systems determine a very different luminous environment. Switching and stepped systems create a strongly perceivable contrast between electric light and daylight trends, both easily identifiable. On the contrary, dimming systems maintain constant indoor levels, making more difficult to perceive the indoor daylight trends. This aspect should be investigated with field surveys, aiming at analysing users' preferences regarding this aspect. Previous studies underlined that users' preferred light levels are different according to the moment of the day. Based on that, the proposed parameters could be easily revised, considering that the goal of the DLCS is not to maintain constant light levels, but to adapt them to a user-defined daily profile. Furthermore, if switching systems turned out to be the most suitable solution, technical strategies to reduce too frequent electric light oscillations must be deepened. The case study analysis demonstrated the effectiveness of switching-linked time delay. However, it was underlined that to completely solve the problem, time delay should be considered also when luminaires must be turned on. This means to accept the risk of light deficit. Previous studies reported that sometimes users prefer light levels lower than requirements. So, it is possible that people would prefer occasional light deficit conditions, compared with too frequent switching on actions. This aspect should be investigated by means of field surveys as well.

Results emphasised how the commissioning phase is crucial in defining the performance of DLCS. They underlined that the system resetting over time is desirable to adapt the control functioning to daylight availability seasonal variations. Moreover, to observe how the light output trends of the DLCSs vary depending on different weather conditions, demonstrated that DLCSs functioning changes during the same season depending on the specific weather conditions. This seems to suggest that the lighting control performances could be improved if the control algorithm was based not only on daylight levels detected by photosensors, but also on data collected by a weather station. This is a strategy already used for shading devices management.

Other two aspects that are neglected in this context, since they deserve a specific treatise, are the following: the in-depth evaluation of the photosensor spectral and spatial response (for the case study standard illuminance meters were used instead of real photosensors) and a more specific evaluation of shading devices use.

In any case, independently from the specific presented outcomes, the most significant result of the thesis is the proposal of a new methodology that can be easily used both in design practice and in research field. Moreover, the methodology is prone to be specifically adapted depending on the criteria which DLCSs are based on. Currently, the DLCSs goal is to maintain constant work-plane illuminances. Previous researches demonstrated that this criterion is not alone sufficient to guarantee proper comfort conditions. For example, the control could be calibrated to maintain certain illuminance values at the user's eyes height and not at the work-plane. In this sense, also non-visual light effects could be considered. Moreover, it could be evaluated the possibility to integrate daylight considering that the total light requirement is not stable during the day, but it varies depending on the time. In all these cases, the use of the proposed parameters can be easily extended to the specific control profiles, in order to account for other aspects of comfort.

Appendix

The following paragraphs describe control algorithms implemented in DET. The functioning of each control system will be explained, the related equations will be reported and the way DET models controls will be presented

A.1. Open-loop switching

Open-loop switching systems turn on and off light depending on daylight sensed by the photosensor.

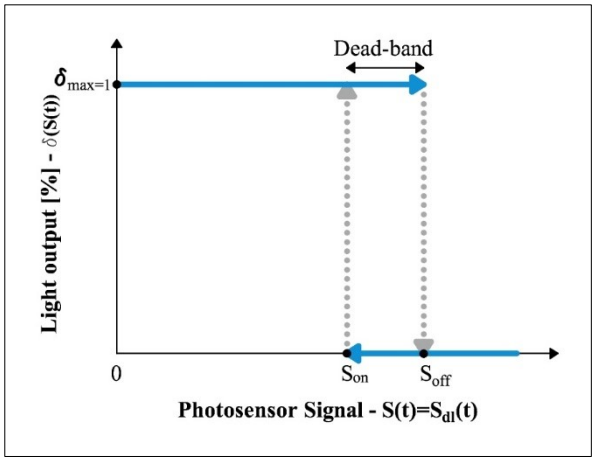

Figure A 1: Open-loop switching control algorithm

The algorithm is based on two set points: S_{on} and S_{off}. Specifically, S_{on} is the photosensor signal corresponding to a work-plane illuminance equal about to the task illuminance required by regulations [73]. When the signal goes below S_{on}, luminaires are immediately turned on. On the other hand, S_{off} is the signal corresponding to switching off actions. It is:

$$S_{off} = S_{on} + dead - band \quad \text{(A1)}$$

The dead-band is set to prevent rapid on-off and off-on actions that could annoy users. Generally, the dead-band extent is equal to about 10%-25% of S_{on} [55]. S_{on} and the dead-band are set during commissioning. Excessive switching can be prevented thanks to a time delay as well. There are different time delay typologies, but in DET the switching-linked one is implemented, since a previous research [26] demonstrated that it is the technique guarantying the best performances. The switching-linked time delay operates so that, after a switch on action, luminaires cannot be switched off until the time delay has passed, whereas they are switched on as soon as the photosensor signal goes below S_{on}. Generally, time delays range from 2 to 30 minutes [55].

The light output $\delta(S(t))$ can be calculated as a function of the photosensor signal, $S(t)$, that in turn depends on the time. In open-loop systems $S(t)$ coincides with the daylight component, $S_{dl}(t)$. From now on, for ease of reading, $\delta(S(t))$ is indicated as $\delta(t)$. Specifically, $\delta(t)$ is:

$$\delta(t) = \begin{cases} \delta_{max} = 1 & if \quad S(t) \le S_{on} \\ 0 & if \quad S(t) \ge S_{off} \\ \delta_{t-1} & if \quad S_{on} < S(t) < S_{off} \end{cases} \quad [\%] \quad \text{(A2)}$$

The parameters to be inserted in DET to simulate open-loop switching controls are: S_{on}, the dead-band (indicated as percentage of S_{on}) and the time delay in minutes (0 if it is not needed). It must be underlined that to simulate systems with switching-linked time delay it is necessary that input data time step is 1 minute. Starting from data provided by users, DET calculates $\delta(t)$ as it is reported in Figure A2. The first step of the workflow is the evaluation of S_{off}. Then two different algorithms are considered depending on time delay setting. For both algorithms, the light output is calculated as a function of the time for each photosensor signal value inserted by the user. The calculation is iterated according to a daily cycle, considering that, at the beginning of each simulation day, luminaires are off. Based on the first daily photosensor detection, the system simply turns on or off luminaires if the signal is lower or higher than S_{on} respectively. Then, from the second detection on, the effect of the dead-band is considered.

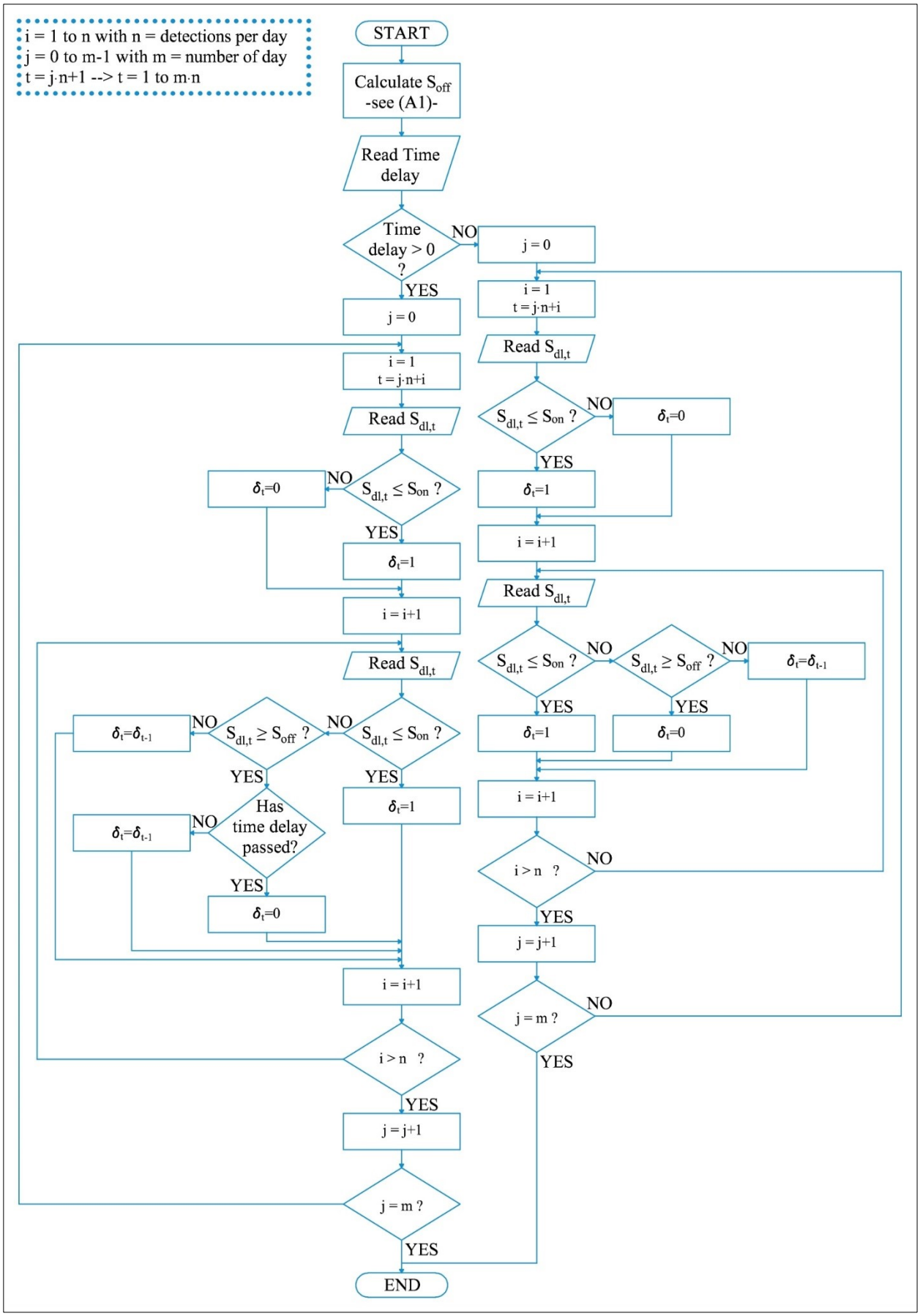

Figure A 2: Open-loop switching systems simulation workflow in DET

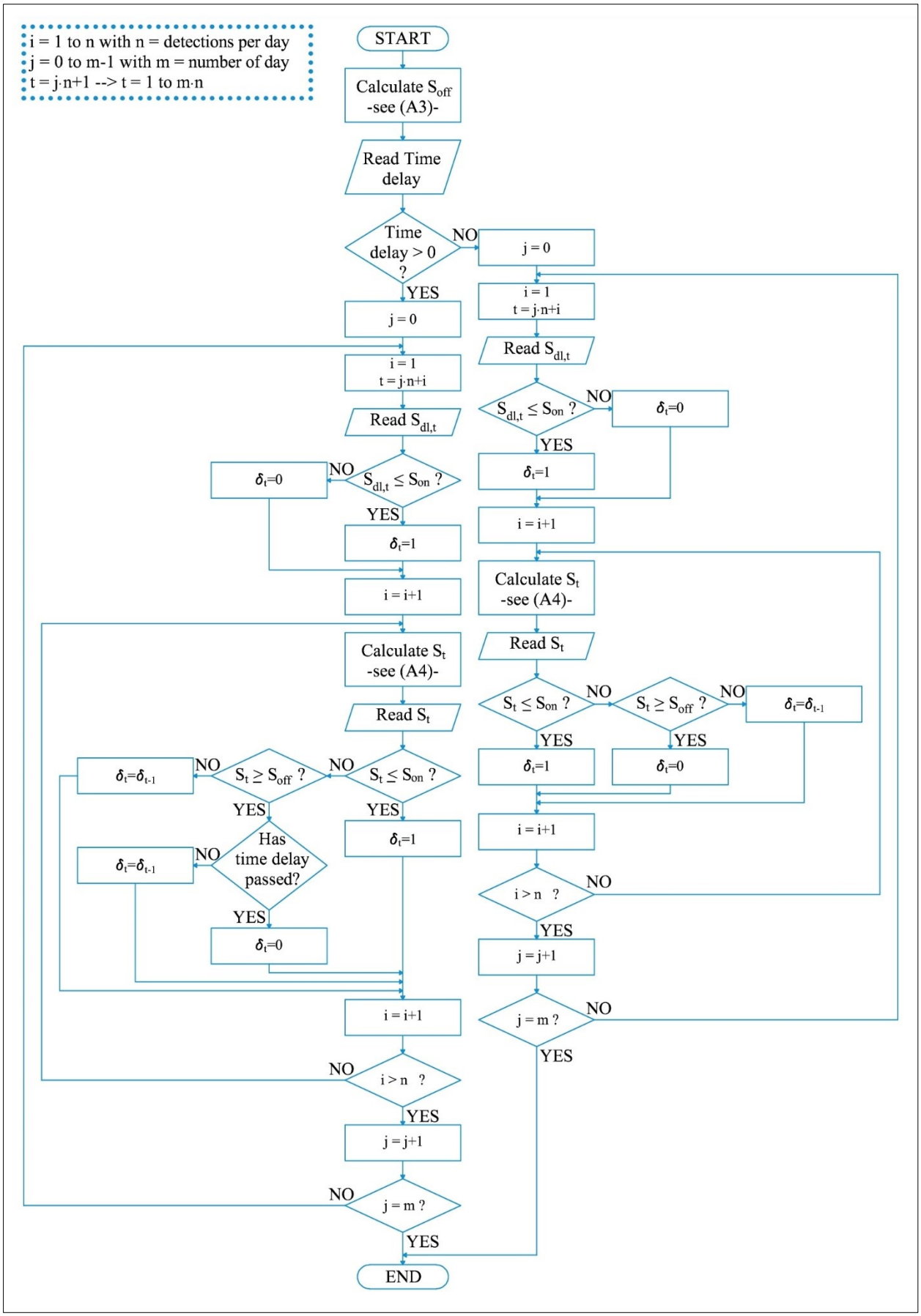

Figure A 3: Closed-loop switching systems simulation workflow in DET

A.2. Closed-loop switching

Closed-loop switching systems are very similar to open-loop ones.

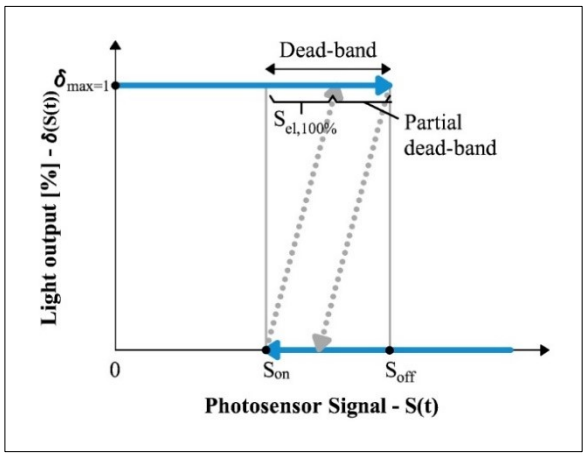

Figure A 4: Closed-loop switching control algorithm

The algorithm is based on the two S_{on} and S_{off} set points as well, and a dead-band is set to prevent too frequent electric light oscillations. The only difference is the way the dead-band extent must be evaluated. When luminaires are switched on and off, since the photosensor detects both daylight and electric light, its signal is subjected to suddenly increases or drops. The corresponding signal shift is equal to the electric light component of the photosensor signal registered when luminaires are on at 100% ($S_{el,100\%}$). For this reason, the dead-band must be higher than $S_{el,100\%}$, in order to avoid that, after a switching on action, a switching off one immediately occurs and vice-versa. S_{on} and the dead-band are identified during commissioning. S_{on} can be set during night (in this case it is equal to $S_{el,100\%}$), but it can be set in presence of daylight as well. This is useful to account for the fact that, when daylight is present, the ratio of the work-plane illuminance to the photosensor signal is different from that determined by electric light. The difference between the dead-band and $S_{el,100\%}$ can be called partial dead-band and can be evaluated as a percentage of S_{on}. According to [55] for closed-loop systems, total dead-bands 1.2-2 times higher than S_{on} are reasonable. Once partial dead-band is defined, S_{off} is:

$$S_{off} = S_{on} + S_{el,100\%} + partial\ dead\ band \quad \text{(A3)}$$

$\delta(t)$ can be evaluated according to the (A2) as well.

To simulate these systems DET needs the following parameters: S_{on}, the partial dead-band, $S_{el,100\%}$ and the time delay. The closed-loop switching systems simulation workflow is reported in Figure A3. It is similar to that reported in Figure A2, related to open-loop systems. The only difference is that, in open-loop systems, $S(t)$ coincides with $S_{dl}(t)$ for the entire day, whereas, for closed-loop systems, this happens only for the first detection of the day, when luminaires are considered being turned off. Then, if luminaires are switched on, $S(t)$ is the sum of the daylight signal, $S_{dl}(t)$, and the electric light one, $S_{el}(t)$. So, starting from the second detection of the day, $\delta(t)$ cannot be evaluated according to $S_{dl}(t)$, but according to $S(t)$. $S_{el}(t)$ depends on the light output set according to the previous photosensor detection, i.e. δ_{t-1}. So, for each daylight photosensor detection inserted by users, $S_{dl,t}$, DET calculates S_t as:

$$S_t = S_{dl,t} + S_{el,t} = S_{dl,t} + \delta_{t-1} \cdot S_{el,100\%} \quad \text{(A4)}$$

and finally, evaluates δ_t based on S_t.

A.3. Open-loop stepped

Open-loop stepped systems regulate light output according to sequential steps, as it can be inferred from Figure A5. Specifically, the figure represents the case of a tri-level stepped system, but two-levels stepped controls are common as well.

To calibrate such a system the following parameters are needed: S_{up}, δ_{max} and the number of steps. S_{up} is the photosensor signal corresponding to a daylight illuminance level at the work-plane equal to about the task illuminance required by regulations [73]. Starting from S_{up}, further set-points are then defined, (e.g. $1/3\,S_{up}$ and $2/3\,S_{up}$ in three-levels systems; $1/2\,S_{up}$ in two-levels ones).

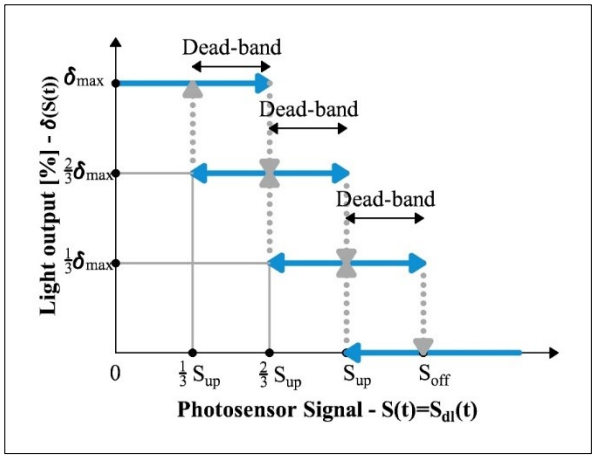

Figure A 5: Open-loop stepped control algorithm

In the same way, further light output levels are set (e.g. $1/3\,\delta_{max}$ and $2/3\,\delta_{max}$ in three-levels systems; $1/2\,\delta_{max}$ in two-levels ones). Every time $S(t)$ goes below one of the setpoints, light output is consequently regulated. Differently from simple switching systems, δ_{max} is not necessarily equal to 100%. Indeed, daylight-based control strategy can be associated to lumen maintenance once. So, δ_{max} can be differently set during light system life cycle, to account for luminaires luminous flux decay during time. Consequently, at the beginning of the system life, δ_{max} can be lower than 100%. Also for stepped systems, dead-bands are set to reduce continuous increases and drops of electric light levels, as well as for switching systems. The dead-band extent is equal to:

$$Dead-band = \frac{S_{up}}{k} \qquad \text{(A5)}$$

with k equal to the number of steps. Dead-bands introduction determines that luminaires are turned on at δ_{max} when the photosensor signal is lower than $1/k\,S_{up}$ ($1/3\,S_{up}$ in Figure A5) and that they are switched off when the photosensor signal is higher than S_{off}, with:

$$S_{off} = S_{up} + dead-band \qquad \text{(A6)}$$

From Figure A5, it can be observed that, when photosensor signal ranges from $1/3\,S_{up}$ to S_{off}, $\delta(t)$ can assume two different values depending on the light output history. For example, if the signal is comprised between $1/3\,S_{up}$ and $2/3\,S_{up}$, $\delta(t)$ is equal to $2/3\,\delta_{max}$ if the light output previously set by the system was equal or lower than $2/3\,\delta_{max}$, else $\delta(t)$ is equal to δ_{max}. Generalizing, irrespective of the k number of the steps, when the signal is comprised between $1/k\,S_{up}$ and S_{off}, $\delta(t)$ can assume two different values, one higher than the other. Let us call these two quantities δ_{high} and δ_{low}. For each photosensor detection t, to evaluate δ_{low}, the percentage difference between S_t and S_{up}, ($\Delta^{\%}_{S,t}$), must be evaluated as:

$$\Delta^{\%}_{S,t} = 1 - \frac{S_t}{S_{up}} \qquad \text{(A7)}$$

The light output necessary to integrate daylight ($\delta_{necessary,t}$) would be:

$$\delta_{necessary,t} = \Delta^{\%}_{S,t} \cdot \delta_{max} \quad [\%] \qquad \text{(A8)}$$

Since the system is a stepped one, only a defined number of δ_i is admitted, with i ranges from 0 and k. Specifically, the minimum value of δ_i is 0, the maximum one is δ_{max} and each value of δ_i between 0 and δ_{max} is equal to the sum of δ_{i-1} and δ_{max}/k. δ_{low} can be evaluated as:

$$\delta_{low} = \min \delta_i : \ \delta_i > \delta_{necessary,t} \quad [\%] \qquad \text{(A9)}$$

Then, δ_{high} is:

$$\delta_{high} = \delta_{low} + \frac{\delta_{max}}{k} \quad [\%] \qquad \text{(A10)}$$

Based on these premises, the control equations for open-loop stepped systems, irrespective of the k number of the steps, are the following:

$$\delta(t) = \begin{cases} \delta_{max} \ if \ \ S(t) \le \dfrac{S_{up}}{k} \\ 0 \quad\ if \ \ S(t) \ge S_{off} \\ \delta_{low} \ if \ \dfrac{S_{up}}{k} < S(t) < S_{off} \ and \ \delta_{t-1} \le \delta_{low} \\ \delta_{high} \ if \ \dfrac{S_{up}}{k} < S(t) < S_{off} \ and \ \delta_{t-1} > \delta_{low} \end{cases} \quad [\%] \qquad \text{(A11)}$$

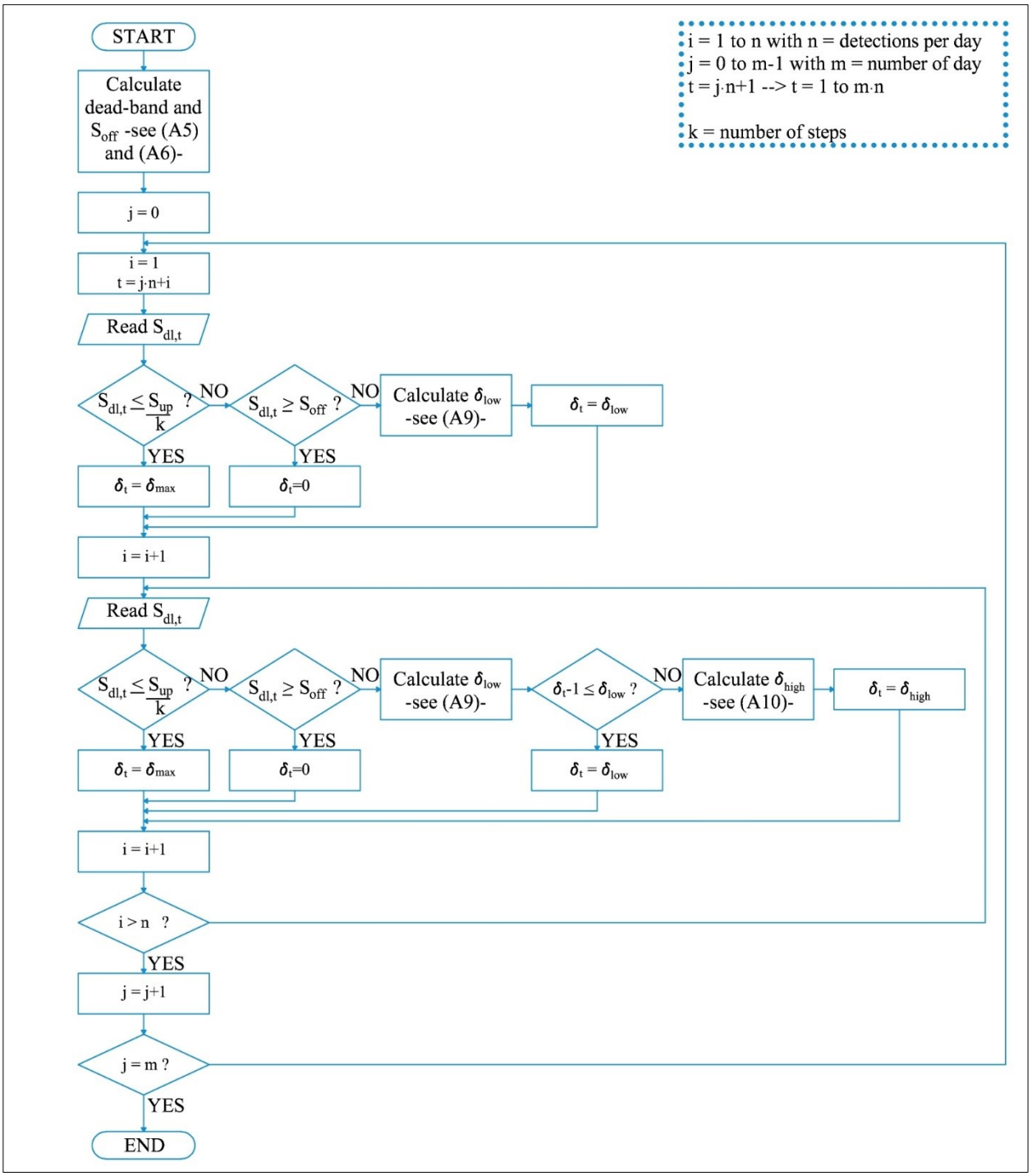

Figure A 6: Open-loop stepped systems simulation workflow in DET

DET workflow for open-loop stepped systems simulation is reported in Figure A6. The first workflow step is the calculation of the S_{off} value and the dead-band based on the input data given by the users (i.e. S_{up}, δ_{max} and the number of steps). As it was previously explained regarding switching systems, the simulation is performed according to a daily cycle. Consequently, it is considered that at the beginning of the day luminaires are off and that dead-bands effect is considered starting from the second photosensor detection on.

A.4. Closed-loop stepped

Closed-loop stepped systems regulate light output according to sequential steps, similarly to open-loop once. However, the control algorithm is substantially different, since the photosensor detects both daylight and electric light (see Figure A7). To calibrate these systems, it is necessary to

set four different parameters: S_{up}, δ_{max}, the partial dead-band and the number of steps (Figure A7 reports the case of a tri-level stepped system).

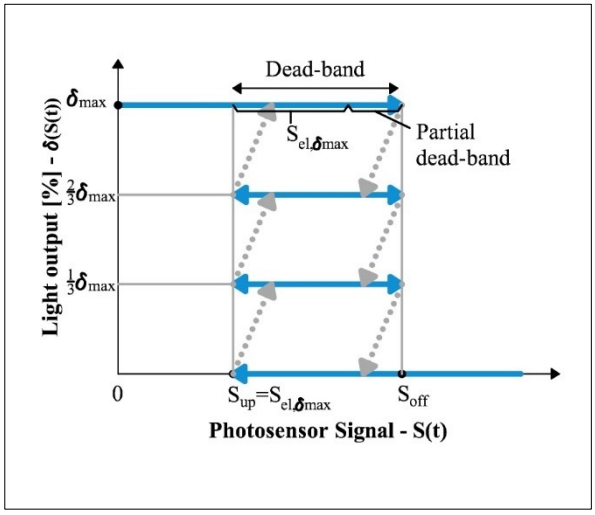

Figure A 7: Closed-loop stepped control algorithm

If S_{up} is equal to $S_{el,\delta max}$, the functioning of the system can be managed by means of two only set-points (S_{up} and S_{off}). This happens because each light output increment determines a corresponding photosensor signal increase. Consequently, after each regulation action, the signal assumes a value belonging to the dead-band. As well as for closed-loop switching systems, the dead-band is equal to the sum of $S_{el,\delta max}$ and of a partial dead-band. So, S_{off} is:

$$S_{off} = 2 \cdot S_{el,100\%} + partial\ dead - band \qquad \text{(A12)}$$

Every time the photosensor signal goes below S_{up}, there is a light output increment. In this case, for each photosensor detection t, similarly to open-loop systems, this increment can be evaluated according the (A9). Consequently, δ_t can be evaluated as:

$$\delta_t = \delta_{t-1} + \min \delta_i : \delta_i > \left(1 - \frac{S_t}{S_{up}}\right) \cdot \delta_{max} \qquad \begin{matrix}[\%] \\ \text{(A13)}\end{matrix}$$

When the photosensor signal is in the dead-band no action occurs. Finally, every time the signal is higher than S_{off}, luminaires can be turned off. Indeed, even though the luminaires were on at the maximum level and the switching off action determined a signal reduction equal to $S_{el,\delta max}$, thanks to the dead-band presence, the resulting signal would be higher than S_{up}. Given these premises, $\delta(t)$ is:

$$\delta(t) = \begin{cases} \delta_{t-1} + \min \delta_i : \delta_i > \left(1 - \frac{S_t}{S_{up}}\right) \cdot \delta_{max} & if\ S(t) \le S_{up} \\ 0 & if\ S(t) \ge S_{off} \\ \delta_{t-1} & if\ S_{up} < S(t) < S_{off} \end{cases} \qquad \begin{matrix}[\%] \\ \text{(A14)}\end{matrix}$$

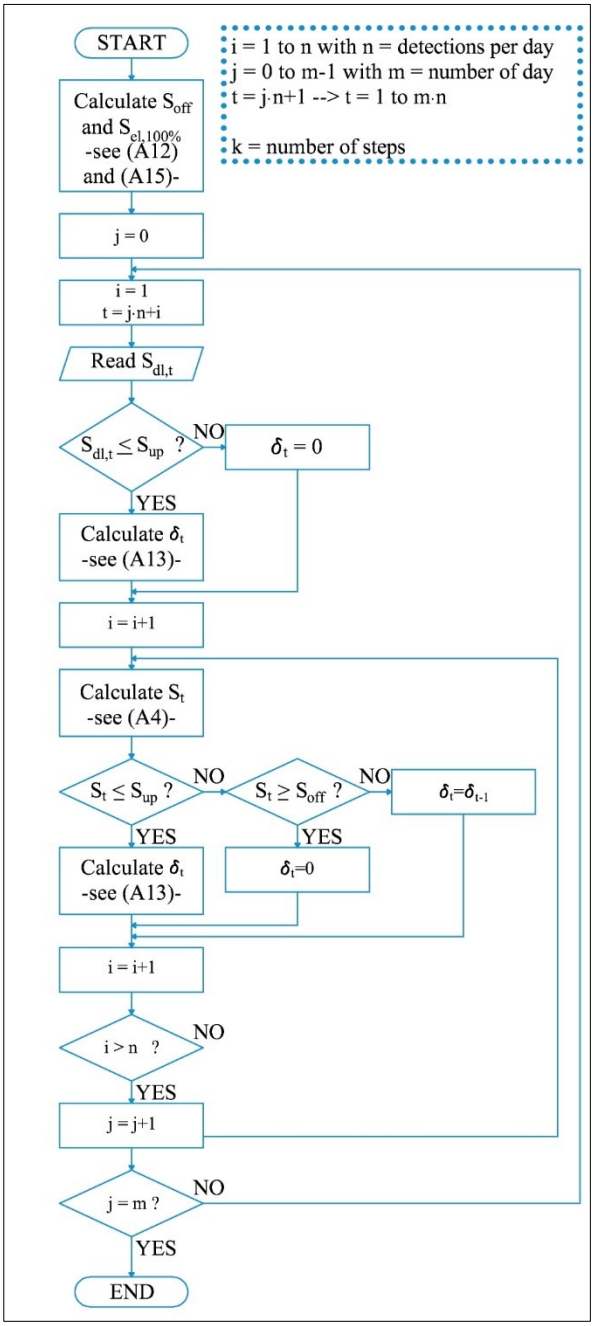

Figure A 8: Open-loop stepped systems simulation workflow in DET

To simulate closed-loop stepped systems users have to insert in DET $S_{el,\delta max}$, δ_{max}, the partial dead-band and the number of steps. Based on

these data the tool evaluates S_{off} according to the (A12). Also in this case, for $\delta(t)$ calculation a daily cycle is considered. From the second detection of the day on, as it was already said about closed-loop switching systems, it is necessary to evaluate S_t according to the (A4), since the photosensor detects both daylight and electric light. For this purpose, at the beginning of the calculation workflow, $S_{el,100\%}$ is calculated as:

$$S_{el,100\%} = \frac{S_{el,\delta max}}{\delta_{max}} \quad \text{(A15)}$$

A.5. Open-loop dimming

Open-loop dimming systems continuously regulate luminous flux emitted by luminaires depending on photosensor signal. The light output varies from a maximum value, δ_{max}, to a minimum one, δ_{min}. The typical control function of these systems is represented in Figure A9.

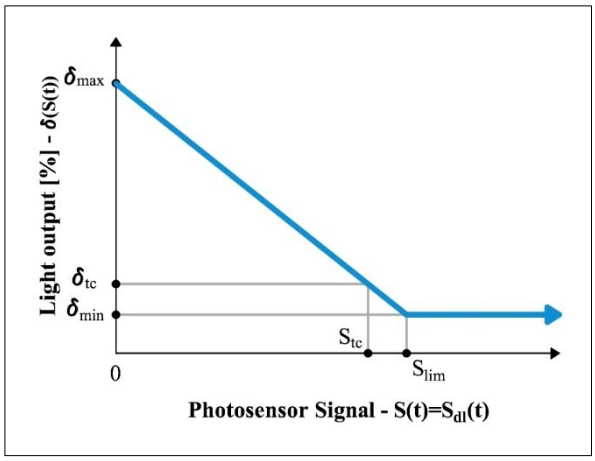

Figure A 9: Open-loop dimming control algorithm

The calibration consists in setting two set points. The former is defined during night, when daylight is absent and luminaires are turned on at the maximum light output. In this situation, since the photosensor is an open-loop one, the corresponding signal is 0. The latter set point is defined during day, when daylight contribution is significant. Specifically, it is recommended that, during the calibration, the work-plane daylight illuminance is such that the corresponding light output (δ_{tc}) is slightly higher than δ_{min} [11]. Finally, once these two set points are found and the control straight line is defined, by knowing δ_{min} (which depends on luminaires characteristics), it is possible to calculate S_{lim} according to the slope of the control function. S_{lim} is a limit signal: if photosensor detections are lower than S_{lim}, the controller properly varies the light output between the maximum and the minimum value, else, it maintains luminaires on at δ_{min} light output.

Rubinstein et al. [44] gave the equations to calculate $\delta(t)$ as a function of the daylight component of the photosensor signal $S_{dl}(t)$. For open-loop systems, considering that the electric light component of the photosensor signal is 0, $\delta(t)$ is calculated as:

$$\delta(t) = \begin{cases} m \cdot S(t) + 1 & if\ S(t) \le S_{lim} \\ \delta_{min} & if\ S(t) > S_{lim} \end{cases} \quad [\%] \quad \text{(A16)}$$

with:

$$m = \frac{\delta_{tc} - 1}{S_{tc}} \quad \text{(A17)}$$

and

$$S_{lim} = \frac{\delta_{min} - 1}{m} \quad \text{(A18)}$$

Considering that δ_{tc} can be calculated as the percentage difference between the electric light illuminance when luminaires are on at 100% light output $\overline{E}_{el,100\%}$ and the daylight illuminance at the calibration, $\overline{E}_{dl,tc}$:

$$\delta_{tc} = \frac{\overline{E}_{el,100\%} - \overline{E}_{dl,tc}}{\overline{E}_{el,100\%}} \quad [\%] \quad \text{(A19)}$$

so m can be written as:

$$m = -\frac{\overline{E}_{dl,tc}}{\overline{E}_{el,\delta 100\%} \cdot S_{tc}} \quad \text{(A20)}$$

The equations are based on the assumption that the maximum luminaires light output is necessarily 1. However, as it was reported in the previous paragraphs, it is possible to associate

daylight-based control strategy and luminance maintenance control strategy to increment energy savings. Considering that the maximum light output is not equal to 1, but equal to a generic δ_{max} value, the (A16) becomes:

$$\delta(t) = \begin{cases} m \cdot S(t) + \delta_{max} \; if \; S(t) \leq S_{lim} \\ \delta_{min} \qquad\qquad if \; S(t) > S_{lim} \end{cases} \quad [\%] \quad \text{(A21)}$$

with:

$$m = \frac{\delta_{tc} - \delta_{max}}{S_{tc}} \quad \text{(A22)}$$

and:

$$S_{lim} = \frac{\delta_{min} - \delta_{max}}{m} \quad \text{(A23)}$$

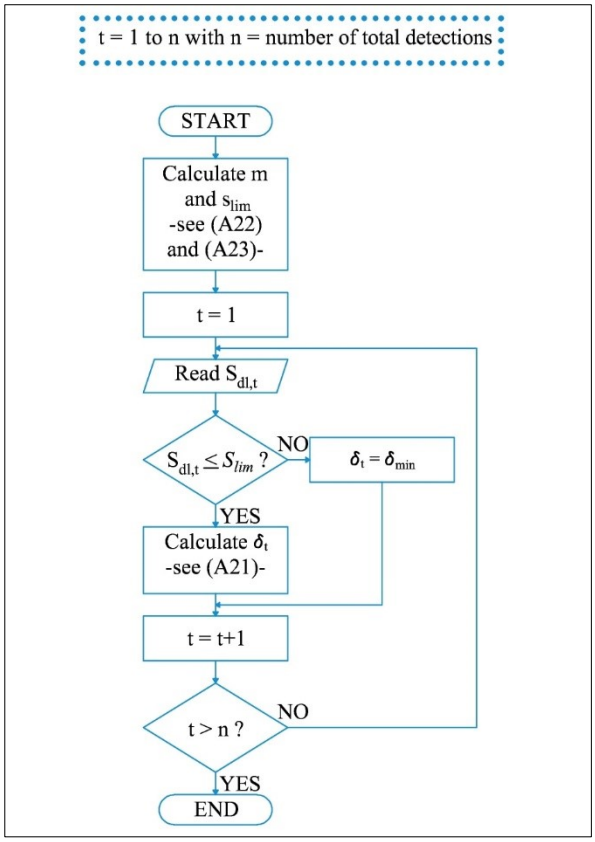

Figure A 10: Open-loop dimming systems simulation workflow in DET

Parameters users must insert in DET to simulate open-loop dimming systems are: δ_{max}, δ_{min}, δ_{tc}, and S_{tc} (i.e. the signal detected by the photosensor at the daytime calibration). Starting from these input data DET calculates m and S_{lim} according to (A22) and (A23) and then it evaluates δ_t for each photosensor detection t, as it is reported in Figure A10.

A.6. Closed-loop integral reset

The closed-loop integral reset control operates so that, given the electric light component of the photosensor signal when luminaires are on at the maximum light output ($S_{el,\delta max}$), light system must be continuously regulated in order to maintain the photosensor signal constant and equal to the very value of $S_{el,\delta max}$. The light output varies from a maximum value (δ_{max}) to a minimum one (δ_{min}). This control typology can be calibrated by setting the following parameters, that allow defining the control function reported in Figure A11: δ_{max}, δ_{min} and $S_{el,\delta max}$. So, the calibration is performed without considering daylight.

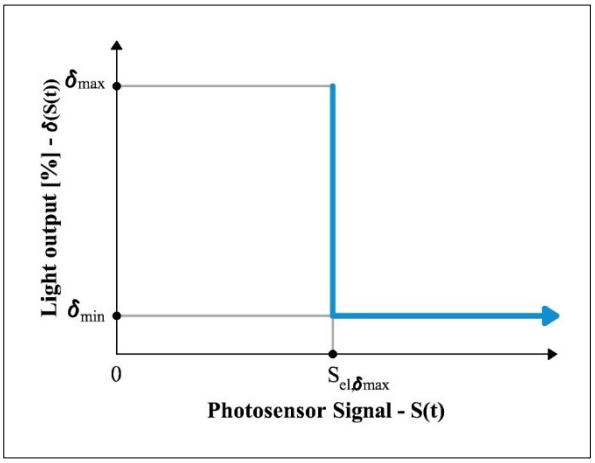

Figure A 11: Closed-loop integral reset control algorithm

Control equations to calculate $\delta(t)$ were given in [44]. It is considered that δ_{max}=1. So, the control must operate such that the photosensor signal is always equal to the electric light component of the photosensor when luminaires are turned on at 100%, $S_{el,100\%}$. The system is closed-loop and then each photosensor detection S_t is the sum of a daylight component, $S_{dl,t}$, and an electric light one, $S_{el,t}$. So:

$$S_t = S_{dl,t} + S_{el,t} = S_{el,100\%} \quad \text{(A24)}$$

Considering that $S_{el,t}$ can be evaluated as the product of δ_t and $S_{el,100\%}$:

$$S_{dl,t} + \delta_t \cdot S_{el,100\%} = S_{el,100\%} \quad \text{(A25)}$$

So, the equation to evaluate $\delta(t)$ is:

$$\delta(t) = \begin{cases} 1 - \dfrac{S_{dl}(t)}{S_{el,\delta 100\%}} & if\ S_{dl}(t) \le S_{dl,lim} \\ \delta_{min} & if\ S_{dl}(t) > S_{dl,lim} \end{cases} \quad [\%] \quad \text{(A26)}$$

with:

$$S_{dl,lim} = S_{el,\delta 100\%} - \delta_{\min} \cdot S_{el,\delta 100\%} = \\ = S_{el,\delta 100\%} \cdot (1 - \delta_{\min}) \quad \text{(A27)}$$

Also in this case, it is considered that δ_{max} certainly corresponds to 100% of the luminaires light output (δ_{max}=1). Associating daylight-based control and luminance maintenance control, the (A26) becomes:

$$\delta(t) = \begin{cases} \dfrac{S_{el,\delta max} - S_{dl}(t)}{S_{el,\delta 100\%}} & if\ S_{dl}(t) \le S_{dl,lim} \\ \delta_{min} & if\ S_{dl}(t) > S_{dl,lim} \end{cases} \quad [\%] \quad \text{(A28)}$$

with:

$$S_{dl,lim} = S_{el,\delta max} - \delta_{\min} \cdot S_{el,\delta 100\%} \quad \text{(A29)}$$

If δ_{max} is equal to 1, the (A26) and the (A27) coincides with the (A28) and the (A29) respectively.

Parameters needed in DET to simulate such a control system are: δ_{max}, δ_{min} and $S_{el,\delta max}$. Based on these data the tool calculates the electric component of the photosensor signal when luminaires are on at 100%, $S_{el,100\%}$, according to the (A15) and $S_{dl,lim}$ according to the (A29). Finally, it calculates δ_t values for each $S_{dl,t}$ value provided by the users. The DET workflow to simulate closed-loop integral reset systems is represented in Figure A12.

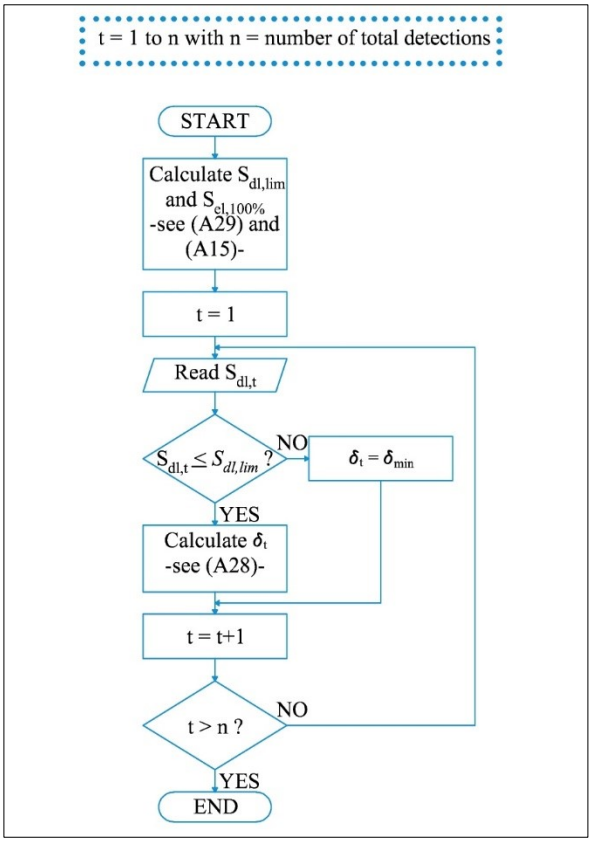

Figure A 12: Closed-loop integral reset systems simulation workflow in DET

A.7. Closed-loop proportional dimming

Closed-loop proportional dimming is a dimming system as well as the integral reset one, but it considers the fact that the ratio of the work-plane daylight illuminance to the photosensor signal is different from the ratio of the work-plane electric light illuminance to the photosensor signal. So, it is calibrated accounting for daylight contribution.

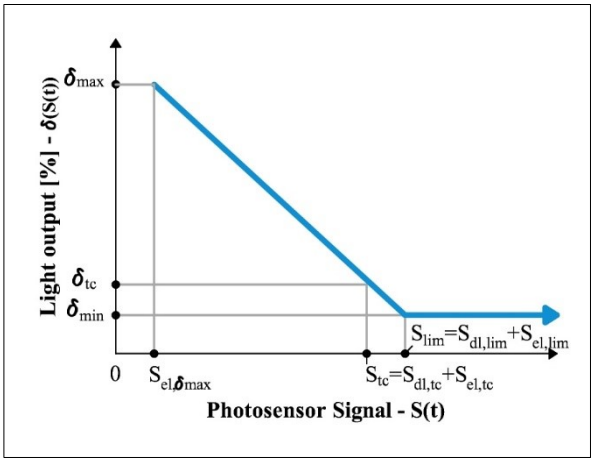

Figure A 13: Closed-loop proportional dimming control algorithm

As it was already observed about open-loop dimming systems, closed-loop ones can be calibrated by setting two points that define the slope of the control straight line. Also in this case the former point is defined during night, but, when daylight is absent and luminaires are on at δ_{max}, the photosensor detects the corresponding electric light amount, $S_{el,\delta max}$, since it is a closed-loop one. The latter point is set in presence of daylight. Also in this case it is recommended that the work-plane daylight illuminance is such that the light output at the calibration, δ_{tc}, is slightly higher than δ_{min} [11]. Setting δ_{min}, S_{lim}, that is composed by a daylight and an electric light component ($S_{dl,lim}$ and $S_{el,lim}$), can be calculated according to the slope of the function.

According to [44], considering that δ_{max}=1, $\delta(t)$ can be evaluated as:

$$\delta(t) = \begin{cases} \dfrac{1 + m \cdot (S_{dl}(t) - S_{el,100\%})}{1 - m \cdot S_{el,100\%}} & if\ S_{dl}(t) \le S_{dl,} \\ \delta_{min} & if\ S_{dl}(t) > S_{dl,} \end{cases} \quad [\%] \quad (A30)$$

with m defined as a function of daylight work-plane illuminances at the calibration $\overline{E}_{dl,tc}$, the corresponding photosensor signal $S_{dl,tc}$, the electric light illuminance when luminaires are on at 100% light output $\overline{E}_{el,100\%}$ and the corresponding photosensor signal $S_{el,100\%}$:

$$m = \frac{\overline{E}_{dl,tc}}{\overline{E}_{dl,tc} \cdot S_{el,100\%} - \overline{E}_{el,\delta 100\%} \cdot S_{dl,tc}} \quad (A31)$$

and:

$$S_{dl,lim} = \frac{\delta_{min}(1 - m \cdot S_{el,100\%}) - 1}{m} + S_{el,100\%} \quad (A32)$$

If we consider that the maximum light output is a generic δ_{max}, $\delta(t)$ is:

$$\delta(t) = \begin{cases} S(t) \cdot m + q\ if\ S(t) \le S_{lim} \\ \delta_{min} \quad if\ S(t) > S_{lim} \end{cases} \quad [\%] \quad (A33)$$

with:

$$m = \frac{\delta_{tc} - \delta_{max}}{S_{tc} - S_{el,\delta max}} \quad (A34)$$

and:

$$q = \frac{S_{tc} \cdot \delta_{max} - S_{el,\delta max} \cdot \delta_{tc}}{S_{tc} - S_{el,\delta max}} \quad (A35)$$

The (A33) can be written as a function of $S_{dl}(t)$. Since $S(t)$ is composed of a daylight component, $S_{dl}(t)$, and an electric light one, $S_{el}(t)$, if $S(t) \le S_{lim}$:

$$\delta(t) = (S_{dl}(t) + S_{el}(t)) \cdot m + q \quad [\%] \quad (A36)$$

$S_{el}(t)$ can be evaluated as the product of the light output $\delta(t)$ and the electric light photosensor signal when luminaires are on at 100%, $S_{el,100\%}$. So:

$$\delta(t) = (S_{dl}(t) + \delta(t) \cdot S_{el,100\%}) \cdot m + q \quad [\%] \quad (A37)$$

The (A33) becomes:

$$\delta(t) = \begin{cases} \dfrac{m \cdot S_{dl}(t) + q}{1 - m \cdot S_{el,100\%}} & if\ S_{dl}(t) \le S_{dl,lim} \\ \delta_{min} \quad if\ S_{dl}(t) > S_{dl,lim} \end{cases} \quad [\%] \quad (A38)$$

From (A37) we can find $S_{dl,lim}$, i.e. the limit daylight component of the photosensor signal corresponding to δ_{min}. It is:

$$S_{dl,lim} = \frac{\delta_{min}(1 - m \cdot S_{el,100\%}) - q}{m} \quad (A39)$$

DET input data to calibrate closed-loop proportional dimming are: δ_{max}, $S_{el,\delta max}$, δ_{tc} and the daylight component of S_{tc}, i.e. $S_{dl,tc}$. Starting from this data it calculates $S_{el,100\%}$, m, q and $S_{dl,lim}$ according to the (A15), (A34), (A35) and (A38) respectively. Then it infers S_{tc}:

$$S_{tc} = S_{dl,tc} + \delta_{tc} \cdot S_{el,100\%} \quad (A40)$$

Finally, knowing these data, it can calculate $\delta(t)$ values as it is reported in Figure A14.

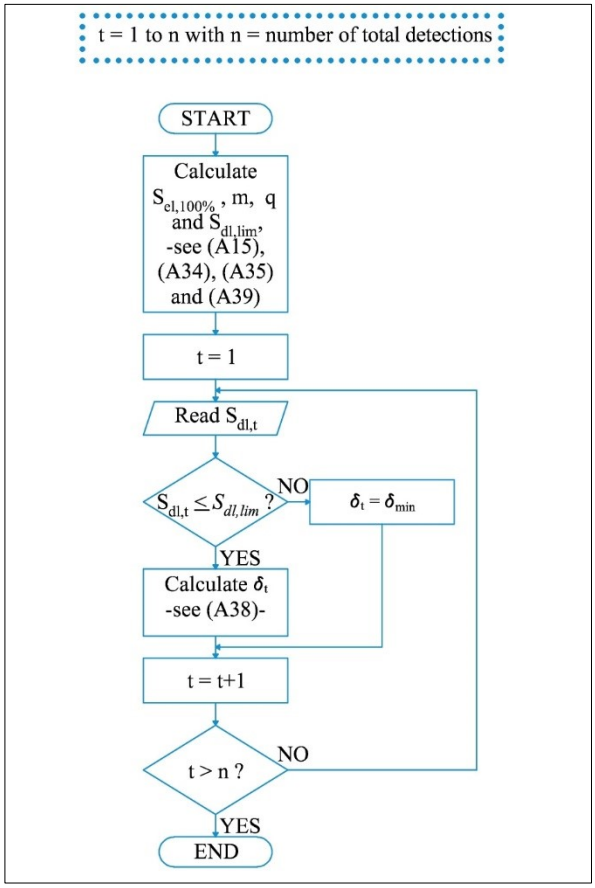

Figure A 14: Closed-loop proportional dimming systems simulation workflow in DET

Nomenclature

DIA	Daylight Integration Adequacy	[%]
$\overline{E}_{dl}(t)$	Average daylight illuminance at the work-plane	[lx]
$\overline{E}_{dl,tc}$	Average daylight illuminance at the work-plane at the calibration	[lx]
$\overline{E}_{el}(t)$	Average electric light illuminance provided by the lighting system to the work-plane	[lx]
$\overline{E}_{el,id}(t)$	Average electric light illuminance a system should ideally provide to the work-plane, in order to perfectly integrate daylight and achieve $\overline{E}_{task}$	[lx]
$\bar{E}_{el,ref}(t)$	Average electric light illuminance at the work-plane provided by the reference system	[lx]
$\bar{E}_{el,tc}$	Average electric light illuminance at the work-plane when luminaires are turned on at δ_{tc}	[lx]
$\bar{E}_{el,100\%}$	Average electric light illuminance at the work-plane when luminaires are on at 100%	[lx]
$\overline{E}_{task}$	Average maintained illuminance at the work-plane according to standard prescriptions	[lx]
$\overline{E}_{tot}(t)$	$\overline{E}_{dl}(t) + \overline{E}_{el}(t)$	[lx]
ILE	Intrinsic Light Excess	[lx·h]
$ILE_{\%}$	Percentage Intrinsic Light Excess	[%]
LD	Light Deficit	[lx·h]
$LD_{\%}$	Percentage Light Deficit	[%]
LR	Light Requirement	[lx·h]
LR_{dl}	Light Requirement fulfilled by daylight	[lx·h]
LW	Light Waste	[lx·h]
$LW_{\%}$	Percentage Light Waste	[%]
S(t)	Photosensor signal, sum of $S_{dl}(t)$ and $S_{el}(t)$	[lx]
$S_{dl}(t)$	Daylight component of the photosensor signal	[lx]
$S_{dl,lim}$	Daylight component of the S_{lim} photosensor signal	[lx]
$S_{dl,tc}$	Daylight component of the photosensor signal at the calibration	[lx]
$S_{el}(t)$	Electric light component of the photosensor signal	[lx]
$S_{el,lim}$	Electric light component of the S_{lim} photosensor signal	[lx]
$S_{el,tc}$	Electric light component of the photosensor signal at the calibration	[lx]
$S_{el,100\%}$	Electric light component of the photosensor signal when luminaires are turned on at 100%	[lx]
$S_{el,\delta max}$	Electric light component of the photosensor signal when luminaires are turned on at δ_{max}	[lx]
S_{lim}	Signal corresponding to δ_{min} according to the slope of the algorithm curve in dimming systems	[lx]

S_{off}	Photosensor signal corresponding to switch-off action in switching and stepped systems	[lx]
S_{on}	Photosensor signal corresponding to switch-on action in switching systems	[lx]
S_{tc}	Photosensor signal at the calibration in dimming systems	[lx]
S_{up}	Photosensor signal corresponding to switch-on action in stepped systems	[lx]
T	Defined time period	[h]
$\Delta E(t)$	$\overline{\mathrm{E}}_{\mathrm{A,el}}(\mathrm{t}) - \overline{\mathrm{E}}_{\mathrm{A,el,id}}(\mathrm{t})$	[lx]
$\delta(t)$	Luminaires light output set by the control system	[%]
δ_{max}	Luminaires maximum light output	[%]
δ_{min}	Luminaires minimum light output in dimming systems	[%]
$\delta_{ref}(t)$	Luminaires light output of the reference system	[%]
δ_{tc}	Luminaires light output necessary to integrate $\overline{\mathrm{E}}_{\mathrm{A,dl,tc}}$	[%]

References

[1] K. Papamichael et al., "IES RP-5-13 Recommended Practice for Daylighting Buildings", IES-Illuminating Engineering Society, 2013.

[2] M. Bodart and A. De Herde, "Global energy savings in offices buildings by the use of daylighting", Energy and Buildings, vol. 34, no. 5, pp. 421-429, 2002.

[3] P. Ihm, A. Nemri, and M. Krarti, "Estimation of lighting energy savings from daylighting", Building and Environment, vol. 44, no. 3, pp. 509-514, 2009.

[4] X. Yu and Y. Su, "Daylight availability assessment and its potential energy saving estimation–A literature review", Renewable and Sustainable Energy Reviews, no. 52, pp. 494-503, 2015.

[5] M. C. Dubois and Å. Blomsterberg, "Energy saving potential and strategies for electric lighting in future North European, low energy office buildings: A literature review", Energy and Buildings, vol. 43, no. 10, pp. 2572-2582, 2011.

[6] S. Cammarano, A. Pellegrino, V. R. M. L. Verso, and C. Aghemo, "Daylighting design for energy saving in a building global energy simulation context", Energy Procedia, vol. 78, pp. 364-369, 2015.

[7] P. Boyce, C. Hunter, and O. Howlett, "The benefits of daylight through windows", Troy, New York: Rensselaer Polytechnic Institute, 2003.

[8] J. F. Duffy and C. A. Czeisler, "Effect of light on human circadian physiology", Sleep medicine clinics, vol. 4, no. 2, pp. 165-177, 2009.

[9] K. M. J. Farley and J. A. Veitch, “A room with a view: A review of the effects of windows on work and well-being”, Citeseer, 2001.

[10] M. S. Mayhoub, "Innovative daylighting systems’ challenges: A critical study", Energy and Buildings, vol. 80, pp. 394-405, 2014.

[11] D. L. Di Laura, K. H. Houser, R. G. Mistrick, and G. R. Steffy, “Lighting controls” in "The Lighting Handbook, 10th Edition", Illuminating Engineering Society, 2011.

[12] "Market Data: Intelligent Lighting Controls", Navigant Research, 2017.

[13] L. Bellia, F. Fragliasso, and A. Pedace, "Lighting control systems: factors affecting energy savings’ evaluation", Energy Procedia, vol. 78, pp. 2645-2650, 2015.

[14] M. Bonomolo, M. Beccali, V. L. Brano, and G. Zizzo, "A set of indices to assess the real performance of daylight-linked control system", Energy and Buildings, no. 149, pp. 235-245, 2017.

[15] S. Escuyer and M. Fontoynont, "Lighting controls: a field study of office workers’ reactions", Transactions of the Illuminating Engineering Society, vol. 33, no. 2, pp. 77-94, 2001.

[16] P. J. Littlefair, "Photoelectric control: the effectiveness of techniques to reduce switching frequency", Lighting Research and Technology, vol. 33, no. 1, pp. 43-55, 2001.

[17] G. Newsham, J. Veitch, C. Arsenault, and C. Duval, "Effect of dimming control on office worker satisfaction and performance", in Proceedings of the IESNA annual conference, July 2004, pp. 19-41.

[18] N. Gentile, T. Laike, and M.-C. Dubois, "Lighting control systems in individual offices rooms at high latitude: Measurements of electricity savings and occupants’ satisfaction", Solar Energy, vol. 127, pp. 113-123, 2016.

[19] T. Moore, D. J. Carter, and A. I. Slater, "User attitudes toward occupant controlled office lighting", Lighting Research and Technology, vol. 34, no. 3, pp. 207-216, 2002.

[20] A. Slater, "Occupant use of lighting controls-A review of current practice, problems and how to avoid them", Fuel and Energy Abstracts, Vol. 3, No. 37, p. 237.

[21] A. Slater, "Lighting controls in offices: How to improve occupant comfort and energy efficiency", In Proceedings of the CIBSE national lighting conference, Bath, London, UK, 1996. p. 178-184.

[22] L. Bellia, F. Fragliasso, and E. Stefanizzi, "Why are daylight-linked controls (DLCs) not so spread? A literature review", Building and Environment, vol. 106, pp. 301-312, 2016.

[23] L. Doulos, A. Tsangrassoulis, and F. V. Topalis, "A critical review of simulation techniques for daylight responsive systems", In Proceedings of the European Conference on Dynamic Analysis, Simulation and Testing applied to the Energy and Environmental performance of Buildings DYNASTEE. 2005.

[24] A. Pellegrino, V. R. M. L. Verso, L. Blaso, A. Acquaviva, E. Patti, and A. Osello, "Lighting control and monitoring for energy efficiency: a case study focused on the interoperability of building management systems", IEEE Transactions on Industry Applications, vol. 52, no. 3, pp. 2627-2637, 2016.

[25] L. Bellia and F. Fragliasso, "New parameters to evaluate the capability of a daylight-linked control system in complementing daylight", Building and Environment, vol. 123, pp. 223-242, 2017.

[26] L. Bellia, F. Fragliasso, and G. Riccio, "Daylight fluctuations effect on the functioning of different daylight-linked control systems", Building and Environment, vol. 135, pp. 162-193, 2018.

[27] L. Bellia and F. Fragliasso, "Evaluating performance of daylight-linked building controls during preliminary design", Automation in Construction, vol. 93, pp. 293-314, 2018.

[28] B. Roisin, M. Bodart, A. Deneyer, and P. D'herdt, "Lighting energy savings in offices using different control systems and their real consumption", Energy and Buildings, vol. 40, no. 4, pp. 514-523, 2008.

[29] S. Onaygıl and Ö. Güler, "Determination of the energy saving by daylight responsive lighting control systems with an example from Istanbul", Building and Environment, vol. 38, no. 7, pp. 973-977, 2003.

[30] A. D. Galasiu, G. R. Newsham, C. Suvagau, and D. M. Sander, "Energy saving lighting control systems for open-plan offices: a field study", Leukos, vol. 4, no. 1, pp. 7-29, 2007.

[31] E. S. Lee, D. L. DiBartolomeo, and S. E. Selkowitz, "The effect of Venetian blinds on daylight photoelectric control performance", Journal of the Illuminating Engineering Society, vol. 28, no. 1, pp. 3-23, 1999.

[32] A. D. Galasiu, M. R. Atif, and R. A. MacDonald, "Impact of window blinds on daylight-linked dimming and automatic on/off lighting controls", Solar Energy, vol. 76, no. 5, pp. 523-544, 2004.

[33] H. Shen and A. Tzempelikos, "Daylighting and energy analysis of private offices with automated interior roller shades", Solar energy, vol. 86, no. 2, pp. 681-704, 2012.

[34] H. Shen and A. Tzempelikos, "Sensitivity analysis on daylighting and energy performance of perimeter offices with automated shading", Building and environment, vol. 59, pp. 303-314, 2013.

[35] E. Shen, J. Hu, and M. Patel, "Energy and visual comfort analysis of lighting and daylight control strategies", Building and Environment, vol. 78, pp. 155-170, 2014.

[36] M. R. Atif and A. D. Galasiu, "Energy performance of daylight-linked automatic lighting control systems in large atrium spaces: report on two field-monitored case studies", Energy and Buildings, vol. 35, no. 5, pp. 441-461, 2003.

[37] M. Chiogna, A. Mahdavi, R. Albatici, and A. Frattari, "Energy efficiency of alternative lighting control systems", Lighting Research & Technology, vol. 44, no. 4, pp. 397-415, 2012.

[38] D. H. W. Li, K. L. Cheung, S. L. Wong, and T. N. T. Lam, "An analysis of energy-efficient light fittings and lighting controls", Applied Energy, vol. 87, no. 2, pp. 558-567, 2010.

[39] D. H. W. Li, T. N. T. Lam, and S. L. Wong, "Lighting and energy performance for an office using high frequency dimming controls", Energy Conversion and Management, vol. 47, no. 9-10, pp. 1133-1145, 2006.

[40] R. Mistrick, C.-H. Chen, A. Bierman, and D. Felts, "A comparison of photosensor-controlled electronic dimming systems in a small office", Journal of the Illuminating Engineering Society, vol. 29, no. 1, pp. 66-80, 2000.

[41] L. Doulos, A. Tsangrassoulis, and F. Topalis, "Quantifying energy savings in daylight responsive systems: The role of dimming electronic ballasts", Energy and Buildings, vol. 40, no. 1, pp. 36-50, 2008.

[42] L. Doulos, A. Tsangrassoulis, and F. V. Topalis, "The role of spectral response of photosensors in daylight responsive systems", Energy and Buildings, vol. 40, no. 4, pp. 588-599, 2008.

[43] L. Doulos, A. Tsangrassoulis, and F. Topalis, "The impact of colored glazing and spectral response of photosensors in the estimation of daylighting energy savings", In Proceedings of the 2nd PALENC Conference and the 28th AIVC Conference. 2007.

[44] F. Rubinstein, G. Ward, and R. Verderber, "Improving the performance of photo-electrically controlled lighting systems", Journal of the Illuminating Engineering Society, vol. 18, no. 1, pp. 70-94, 1989.

[45] S. Ranasinghe and R. Mistrick, "A study of photosensor configuration and performance in a daylighted classroom space", Journal of the Illuminating Engineering Society, vol. 32, no. 2, pp. 3-20, 2003.

[46] M. Rossi, A. Pandharipande, D. Caicedo, L. Schenato, and A. Cenedese, "Personal lighting control with occupancy and daylight adaptation", Energy and Buildings, vol. 105, pp. 263-272, 2015.

[47] D. Caicedo and A. Pandharipande, "Distributed illumination control with local sensing and actuation in networked lighting systems", IEEE Sensors Journal, vol. 13, no. 3, pp. 1092-1104, 2013.

[48] D. Caicedo, A. Pandharipande, and M. Vissenberg, "Smart modular lighting control system with dual-beam luminaires", Lighting Research & Technology, vol. 47, no. 4, pp. 389-404, 2015.

[49] A. Pandharipande and D. Caicedo, "Daylight integrated illumination control of LED systems based on enhanced presence sensing", Energy and Buildings, vol. 43, no. 4, pp. 944-950, 2011.

[50] J. Snyder, "Energy-saving strategies for luminaire-level lighting controls", Building and Environment, 2018, doi: 10.1016/j.buildenv.2018.10.026

[51] P. R. Boyce, "Editorial: Advancing lighting controls", Lighting Research and Technology, no. 47, p. 131, 2015.

[52] A. Sarkar and R. G. Mistrick, "A novel lighting control system integrating high dynamic range imaging and DALI", Leukos, vol. 2, no. 4, pp. 307-322, 2006.

[53] A. Sarkar, M. Fairchild, and C. Salvaggio, "Integrated daylight harvesting and occupancy detection using digital imaging", International Society for Optics and Photonics, vol. 6816, p. 68160F.

[54] G. R. Newsham and C. Arsenault, "A camera as a sensor for lighting and shading control", Lighting Research & Technology, vol. 41, no. 2, pp. 143-163, 2009.

[55] "Photosensors - Dimming and Switching Systems for Daylight Harvesting", NLPIP - National Lighting Product Information Program, 2007, vol. 11.

[56] E. Tetri, "Daylight linked dimming: effect on fluorescent lamp performance", Lighting Research & Technology, vol. 34, no. 1, pp. 3-9, 2002.

[57] Y. Gu, N. Narendran, T. Dong, and H. Wu, "Spectral and luminous efficacy change of high-power LEDs under different dimming methods", International Society for Optics and Photonics, vol. 6337, p. 63370J.

[58] M. Dyble, N. Narendran, A. Bierman, and T. Klein, "Impact of dimming white LEDs: chromaticity shifts due to different dimming methods", International Society for Optics and Photonics, vol. 5941, p. 59411H.

[59] I. PAR1789, "Recommending practices for modulating current in High Brightness LEDs for mitigating health risks to viewers", 2010.

[60] A. Wilkins, J. Veitch, and B. Lehman, "LED lighting flicker and potential health concerns: IEEE standard PAR1789 update", In Proceedings of Energy Conversion Congress and Exposition (ECCE), 2010, p. 171-178.

[61] N. Gentile and M.-C. Dubois, "Field data and simulations to estimate the role of standby energy use of lighting control systems in individual offices", Energy and Buildings, vol. 155, pp. 390-403, 2017.

[62] R. Delvaeye, W. Ryckaert, L. Stroobant, P. Hanselaer, R. Klein, and H. Breesch, "Analysis of energy savings of three daylight control systems in a school building by means of monitoring", Energy and Buildings, vol. 127, pp. 969-979, 2016.

[63] R. G. Mistrick and J. Thongtipaya, "Analysis of daylight photocell placement and view in a small office", Journal of the Illuminating Engineering Society, vol. 26, no. 2, pp. 150-160, 1997.

[64] A.-S. Choi, K.-D. Song, and Y.-S. Kim, "The characteristics of photosensors and electronic dimming ballasts in daylight responsive dimming systems", Building and Environment, vol. 40, no. 1, pp. 39-50, 2005.

[65] M. Chiogna, R. Albatici, and A. Frattari, "Electric lighting at the workplace in offices: Efficiency improvement margins of automation systems", Lighting Research & Technology, vol. 45, no. 5, pp. 550-567, 2013.

[66] M. Beccali, M. Bonomolo, G. Ciulla, and V. L. Brano, "Assessment of indoor illuminance and study on best photosensors' position for design and commissioning of Daylight Linked Control systems. A new method based on artificial neural networks", Energy, vol. 154, pp. 466-476, 2018.

[67] D. H. W. Li, A. C. K. Cheung, S. K. H. Chow, and J. C. Lam, "Switching frequency and energy analysis for photoelectric controls", Building and Environment, vol. 85, pp. 205-210, 2015.

[68] J. Mardaljevic, "Simulation of annual daylighting profiles for internal illuminance", International Journal of Lighting Research and Technology, vol. 32, no. 3, pp. 111-118, 2000.

[69] C. F. Reinhart, "Tutorial on the use of daysim simulations for sustainable design", Institute for Research in Construction, National Research Council Canada. Ottawa (Ont.), 2006.

[70] Z. Rogers, "Daylighting Metric Development Using Daylight Autonomy Calculations. Sensor Placement Optimization Tool". Boulder, Colorado, USA: Architectural Energy Corporation, 2006.

[71] A. Nabil and J. Mardaljevic, "Useful daylight illuminance: a new paradigm for assessing daylight in buildings", Lighting Research & Technology, vol. 37, no. 1, pp. 41-57, 2005.

[72] A. Nabil and J. Mardaljevic, "Useful daylight illuminances: A replacement for daylight factors", Energy and buildings, vol. 38, no. 7, pp. 905-913, 2006.

[73] EN 12464-1: Light and lighting - Lighting of work places - Part 1: Indoor work places, 2011.

[74] M. David, M. Donn, F. Garde, and A. Lenoir, "Assessment of the thermal and visual efficiency of solar shades", Building and Environment, vol. 46, no. 7, pp. 1489-1496, 2011.

[75] J. Mardaljevic, L. Heschong, and E. Lee, "Daylight metrics and energy savings", Lighting Research & Technology, vol. 41, no. 3, pp. 261-283, 2009.

[76] J. Mardaljevic, M. Andersen, N. Roy, and J. Christoffersen, "Daylighting metrics for residential buildings", in 27th Session of the CIE, Sun City, South Africa, 9-16 July 2011.

[77] Daysim Web Page, Available: https://daysim.ning.com/, Last access: 9th December 2018.

[78] DIVA Web Page, Available: http://diva4rhino.com/, Last access: 9th December 2018.

[79] L. Doulos, A. Tsangrassoulis, and F. V. Topalis, "Multi-criteria decision analysis to select the optimum position and proper field of view of a photosensor", Energy Conversion and Management, vol. 86, pp. 1069-1077, 2014.

[80] C. E. Ochoa, M. B. C. Aries, and J. L. M. Hensen, "State of the art in lighting simulation for building science: a literature review", Journal of Building Performance Simulation, vol. 5, no. 4, pp. 209-233, 2012.

[81] Radiance Web Page, Available: https://www.radiance-online.org/, Last access: 9th December 2018.

[82] SPOT Web Page, Available: https://www.manula.com/manuals/zrogers/spot-pro-v-5/1/en/topic/1-0-introduction, Last access: 9th December 2018.

[83] A. Williams, B. Atkinson, K. Garbesi, E. Page, and F. Rubinstein, "Lighting controls in commercial buildings", Leukos, vol. 8, no. 3, pp. 161-180, 2012.

[84] M. Krarti, P. M. Erickson, and T. C. Hillman, "A simplified method to estimate energy savings of artificial lighting use from daylighting", Building and Environment, vol. 40, no. 6, pp. 747-754, 2005.

[85] V. R. M. L. Verso, A. Pellegrino, and F. Pellerey, "A multivariate non-linear regression model to predict the energy demand for lighting in rooms with different architectural features and lighting control systems", Energy and Buildings, vol. 76, pp. 151-163, 2014.

[86] EN15193-1: Energy performance of buildings - Energy requirements for lighting, 2017.

[87] V. R. M. L. Verso, A. Pellegrino, and C. Aghemo, "The Energy Performance for Lighting in Buildings According to the New EN 15193-1: Potential Energy Saving due to Different Photodimming Controls", In: 2018 IEEE International Conference on Environment and Electrical Engineering and 2018 IEEE Industrial and Commercial Power Systems Europe (EEEIC/I&CPS Europe). IEEE, 2018. p. 1-6.

[88] S. L. Wong, K. K. W. Wan, and T. N. T. Lam, "Artificial neural networks for energy analysis of office buildings with daylighting", Applied Energy, vol. 87, no. 2, pp. 551-557, 2010.

[89] R. W. da Fonseca, E. L. Didoné, and F. O. R. Pereira, "Using artificial neural networks to predict the impact of daylighting on building final electric energy requirements", Energy and Buildings, vol. 61, pp. 31-38, 2013.

[90] N. K. Kandasamy, G. Karunagaran, C. Spanos, K. J. Tseng, and B.-H. Soong, "Smart lighting system using ANN-IMC for personalized lighting control and daylight harvesting", Building and Environment, vol. 139, pp. 170-180, 2018.

[91] C. Ehrlich, K. Papamichael, J. Lai, and K. Revzan, "Simulating the operation of photosensor-based lighting controls", In Proceedings of Building Simulation 7h International Building Performance Simulation Association Conference, Rio de Janeiro, Brazil, August 13-15, 2001.

[92] C. Ehrlich, K. Papamichael, J. Lai, and K. Revzan, "A method for simulating the performance of photosensor-based lighting controls", Energy and buildings, vol. 34, no. 9, pp. 883-889, 2002.

[93] Y. Yoon, J.-H. Lee, and S. Kim, "Development of computational algorithm for prediction of photosensor signals in daylight conditions", Building and Environment, vol. 89, pp. 229-243, 2015.

[94] H. Choi, S. Hong, A. Choi, and M. Sung, "Toward the accuracy of prediction for energy savings potential and system performance using the daylight responsive dimming system", Energy and Buildings, vol. 133, pp. 271-280, 2016.

[95] DIALux web page, Available: https://www.dial.de/it/dialux/, Last access: 9th December 2018.

[96] nesa web page - Pyranometer data sheet, Available: http://www.nesasrl.eu/media/PDF/RSG1.pdf., Last access: 9th December 2018.

[97] Delta OHM web page - Pyranometer data sheet, Available: http://www.deltaohm.com/ver2012/download/LP_PYRA02_03_12_it.pdf. , Last access: 9th December 2018.

[98] nesa web page - Luxmeter data sheet, Available: http://www.nesasrl.eu/media/PDF/Lux.pdf. , Last access: 9th December 2018.

[99] D. L. Di Laura, K. H. Houser, R. G. Mistrick, and G. R. Steffy, The Lighting Handbook, 10th Edition. Illuminating Engineering Society, 2011.